MINING TREATMENT EFFLUENT POND MODELING:
A RISK-BASED APPROACH

ROUZBEH ABBASSI

Mining Treatment Effluent Pond Modeling: A Risk-based Approach

by

Rouzbeh Abbassi

A thesis submitted to the

School of Graduate Studies

in partial fulfillment of the

requirements for the degree of

Doctor of Philosophy in Civil Engineering

Faculty of Engineering and Applied Science

Memorial University of Newfoundland

January, 2010

St. John's Newfoundland Canada

Abstract:

Acid Mine Drainage (AMD) discharged to the surrounding environment may cause serious environmental problems. Sulphidic mine wastes are oxidized resulting in the consequent release of AMD. Different metals such as cadmium, cobalt, copper, iron, lead, nickel, zinc, etc. are released to the environment when sulfides of these metals are exposed to the air. AMD affects the surface water as well as groundwater nearby and limits the reuse of the mine water for processing purposes. Because of differences in mine sites and ambient conditions, the prediction of AMD water composition is very complicated and remains a great concern for scientists. The determination of the minerals involved in producing AMD, as well as the oxidation reactions and chemical components produced in these reactions, are essential prior to choosing the appropriate treatment technology. The oxidation reactions of the minerals and chemical components produced by these reactions are discussed in this thesis. A methodology for predicting the minerals involved in the production of AMD is presented and may be used in conjunction with analytical techniques to reduce the cost of using sophisticated techniques.

The determination of the possible chemical components included in AMD may aid in finding a suitable treatment system for treating mine water. Waste Stabilization Pond (WSP) technology is one of the natural treatment methods that use chemical and biological processes for AMD treatment. The design of the WSP is based on many assumptions, one of which is that the pond is well mixed. That is, there are no concentration gradients within the pond or the pond is modeled as a Continuously Stirred Tank Reactor (CSTR). However, in reality due to the heterogeneity of the constituents of the wastewater and influence of controlling parameters (i.e., temperature & concentration), these assumptions are over simplified. The concentration, wind shear, and temperature stratification within the pond significantly impact the flow pattern within the system. Instead of using ideal reactor models, dispersed flow model covers the non-idealities within the pond. This model is highly related to the hydraulic conditions of the pond. This non-ideal model is rarely used for determining the concentration gradient within the pond, because the main parameters of the model (i.e. actual retention time and dispersion coefficient) are not easy to obtain. Computational Fluid Dynamic (CFD) codes are one of the options presented for defining these two parameters. A methodology discussed in this thesis is using CFD as a suitable option for determining the main parameters of the dispersed flow model. A dispersion model is tested and validated for modeling the concentration gradient within the pond, and CFD is used for determining the dispersion coefficient and actual retention time via case studies in this thesis.

Following the determination of the chemical concentrations in the effluent, assessment of the effect of these concentrations on human health and the ecosystem is required. Environmental risk assessment is a systematic process for describing and quantifying the hazardous effect of chemical contaminants to human health and ecosystems. The USEPA framework is used for identifying and quantifying the risk of chemical contaminants to ecological entities. The four steps of the USEPA framework are hazard identification, exposure assessment, dose-response modeling, and risk characterization. The estimated risk of the effluent of treatment systems may be used to assess the performance of the treatment process. Furthermore, the risk value is associated with different uncertainties and therefore uncertainty assessment may not be neglected in any risk assessment process. The ecological risk assessment methodology and quantification of risk associated with effluent contaminants from the tailing pond to the ecosystem is demonstrated in this thesis via a case study.

DEDICATION

To my grandmother

Although she is no longer with us, she is forever remembered. I am sure she shares my joy and happiness in the heaven.

Acknowledgements

I am heartily thankful to my supervisor, Professor Faisal Khan whose encouragement, guidance and support from the initial to the final level enabled me to develop an understanding of the subject as well as giving me extraordinary experiences through out the work with him. I was extraordinarily fortunate in having him as a great friend and supervisor throughout this research and I hope to have his guidance in my whole life.

I am deeply grateful to my supervisor, Dr. Kelly Hawboldt, for her detailed and constructive comments, and for her important support throughout this work. She taught me how to write academic papers, made me a better researcher, had confidence in me when I doubted myself, and brought out the good ideas in me. Thank you very much for your encouragement and help. I will never forget what you have done for me during my PhD research.

Deepest gratitude is also due to the member of the supervisory committee, Dr. Majid Abdi for his assistance during different stages of my PhD research.

I am grateful to Professors Manuel Rodriguez, Bing Chen and Yanjun Chang for their helpful discussions and comments during my oral defense.

I would like to thank my family for their support. My father has been a great inspiration for me in life. I am indebted to my father for his care and love. He spared no effort to provide the best possible environment for me to grow up and attend school. He had never complained in spite of all the hardships in his life. You are always my hero. My mother is the one who sincerely raised me with her caring and gently love. I remember her constant support when I encountered difficulties. Mother, I love you. I feel proud of my sister for her talents. She had been a role model for me to follow unconsciously and has always been one of my best counselors.

Words fail me to express my appreciation to my wife, whose dedication, love and persistent confidence in me, has taken the load off my shoulder. I owe her for being unselfishly let her intelligence, passions, and ambitions collide with mine. I would also thank her family for letting me take her hand in marriage, and accepting me as a member of the family, warmly.

My special gratitude is due to my uncles, Dr. Dariush Abbassi and Dr. Syrus Abbassi for their loving support.

I also wish to thank Mr. Simon Dadishoo for revising the English of my manuscript, Mr. Ashkan Arefi, Mr. Mehdi Fatemi and Mr. Mohammad Haghighi for their valuable advices during this research. Moreover, I appreciate Dr. John Hawboldt for his valuable support during my life in St.John's.

I would like to take the opportunity to thank my officemate, Ms. Maryam Kalantarnia, and all my lovely friends in INCO building, 63 PindBud (Eilnaz, Ashkan, Moe, Mohammad, Amin, Milad and Nima) and especially Alireza Noroozi and Omid Zadakbar who are always helpful.

Lastly, I offer my regards and blessings to all of those who supported me in any respect during the completion of this research.

Table of Contents

List of Tables

List of Figures

List of Symbols[*]

Chapter 2

a	Measured heat output (μw)
BW	Body Weight: The average body weight in kilograms for an individual's age group
C_0	Influent concentration
C	Effluent concentration
C_{e1}	Effluent BOD_5 concentration of reactor 1
CF	Concentration in food groups (mg of contaminant / gr of food)
C_{i1}	Influent BOD_5 concentration of reactor 1
C_{max}	Maximum concentration
CR	Consumption rate: The amount of food from the food group eaten (mg/day)
D	Total pond depth
D'	Depth of active zone
ED_a	Estimated dose through air inhalation (mg/kg/day)
ED_f	Estimated dose from food: It is expressed as milligrams of the contaminant eaten per kilogram of body weight per day (mg/kg/day)
ED_s	The amount taken eating soil (mg/kg/day)
ED_{ss}	The amount absorbed through skin contact with the soil
ED_w	Estimated dose through drinking water (mg/l/day)
ED_{ws}	The amount absorbed through skin contact with water
EF	Exposure factor: It shows how often a person has been exposed to the contaminant over a lifetime

---

[*] If the above illustration of any symbol conflicts with the illustration of that symbol given in the following text then preference should be given to the illustration, which is provided in the following chapters.

IR	Inhalation Rate: The amount of air that a person breathes normally in the day (m^3/day)
k	Von karman's constant
K_s	First order anaerobic reaction rate constant
L	Total pond length
L'	Length of plug-flow reactor in active zone
N	Number of reactors in series
Q	Flow rate
R_h	Hydraulic radius
r_{ox}	Oxidation rate (molL^{-1}S^{-1})
r_{pp}	Precipitation rate (molL^{-1}S^{-1})
S_p	fraction of anaerobic fermentation products that do not leave the pond as a gas
t	Mean pond residence time
t_1	Residence time in reactor 1
TS	Toxicity score
V_R	Volume of the element
W	Sample weight (gr)
X_A	Fraction of C_A which is converted
$\Delta_f H$	Reaction energy (Kjmol^{-1})
θ	Retention time

Chapter 4

a	Refers to fore-section
A	Pond cross section (m^2)

b	Refers to reaction section
c	Refers to after-section
CSTR	Continuously Stirred Tank Reactor
C_A	Chemical concentration of the element “A”
C_D	Drag coefficient
C_i	Concentration at ith measurement
D	Axial dispersion coefficient (m^2/hr)
D_{AB}	Diffusivity coefficient
D_p	Particle diameter
f	Fraction of reactant remaining
$f(0^-)$	Composition at upstream side of fore-section-reactor boundary
$f(0^+)$	Composition at downstream side of fore-section-reactor boundary
$f(1^-)$	Composition at upstream side of reactor after section boundary
$f(1^+)$	Composition at downstream side of reactor after section boundary
F_D	Drag force
F_x	Additional acceleration (force/unit particle mass) term
k	First order reaction rate constant
L	Length of the pond
M	Mass of tracer injected
N	Constant in general solution for differential equation
Pe	Peclet number
PFR	Plug Flow Reactor

R	Reaction group, kl/u
Re	Reynolds number
r_A	Reaction rate
t	Actual retention time
t_i	Time at i^{th} measurement
T	Theoretical retention time
u*	Shear Velocity
U	Flow velocity
u_p	Particle velocity
u_x	Velocity in x direction
u_y	Velocity in y direction
u_z	Velocity in z direction
W	Width of the pond
z	Longitudinal distance (m)
Z	Height of the pond
ρ_A	Density of the element A
ρ_p	Density of the particle
μ	Dynamic viscosity
τ	Residence time of the pond (S)
ν	Kinematic viscosity (m^2/S)
σ_i	Variance based on discrete time measurement
ω_A	Mass fraction ($\omega_i = \frac{m_i}{m}$)

Chapter 5

BCF	Bio-Concentration Factor
BW	Body Weight
bw_t	Body weight of test animals
bw_w	Body weight of wildlife animals
C_t	Total metal concentration in the overflow
C_s	Concentration in ingested soil
C_w	Concentration in drinking water
C_{aa}	Concentration in ingested aquatic animals
C_{ap}	Concentration in ingested aquatic plants
C_{ta}	Concentration in ingested terrestrial animals
C_{tp}	Concentration in ingested terrestrial plants
D_{exp}	Expected dose
FI	Food ingestion
F_{ing}	Ingested transfer factor
HI	Hazard Index
HQ	Hazard Quotient
I_s	Soil ingestion rate
I_w	Water intake rate
I_{aa}	Aquatic animal ingestion rate
I_{ap}	Aquatic plants ingestion rate
I_{ta}	Terrestrial animals ingestion rate
I_{tp}	Terrestrial plants ingestion rate

K_{aa}	Fraction of animal's annual intake from the metal sources
K_{ap}	Fraction of animal's annual aquatic plant intake from the metal sources
K_s	Fraction of animal's annual soil intake from the metal sources
K_{ta}	Fraction of animal's annual terrestrial animals intake from the metal sources
K_{tp}	Fraction of animal's annual terrestrial plants intake from the metal sources
K_w	Fraction of animal's annual water intake from the metal sources
$NOAEL_t$	Non-Observed Adverse Effect Level in test animals
$NOAEL_w$	Non-Observed Adverse Effect Level in wildlife animals
WI	Water Intake
It_a	Terrestrial animals ingestion rate
Z_r	Root zone depth

CHAPTER 1

Introduction

1.1 Overview

Mining processes may cause environmental problems that can adversely affect human health and the ecosystem. The impacts of mining on the environment are based on the nature of the ore body, the type of mining and the size of operation. Acid generation and metal dissolution are examples of issues related to mining activities. AMD can affect mine water quality and limit the recycling capability of mine water for processing purposes and also for usage as secondary water. It may also adversely affect the plant and animal communities along downstream channels and ground water quality.

In light of various sources that produce AMD and the problems caused by AMD, researchers have begun research in the quality of mine water. Different static and kinetic tests on the sulfide wastes have presented the information on the ability of waste to generate acid. The prediction of mine water composition is very complicated and remains a great challenge for scientists. Therefore, having knowledge of different possible chemical components of specific AMD is necessary prior to selecting a treatment process.

Different treatment methods of AMD have been developed, which are divided into traditional and innovative categories (Costello, 2003). After the completion of the treatment process, tailing waste enters the pond in order to be stabilized and released into the environment. Tailing ponds are commonly observed in every country, which contain "the residue (tailing) of the milling process to extract metals from mined ores" (Ginige, 2002). Stabilization the tailing wastes in a pond is one of the cheap and effective methods of treatment.

A series of chemical reactions occurs in tailing ponds, depending on the geology and the hydrology of the specific mine site. There are a variety of different approaches available to design the ponds; however, the majority of them are based on the design of the chemical reactors. The chemical reactors are intricate vessels designed to convert the feedstock to the desired product. There has been a lot of effort put into the modeling, simulation and analysis of chemical reactors. Designing methods of the pond as reactor is based on the chemical reactions that occur in the pond and physical nature of the wastewater.

There are two types of ideal chemical reactors, Continuously Stirred Tank Reactor (CSTR) and Plug Flow Reactor (PFR). The designs of them are based on the particle transportation. Researchers used these two types of ideal reactors for modeling the WSPs (Arceivala, 1981; Pearson et al., 1995), in some cases the results of using these ideal models may not fit with the actual effluent of the systems.

In reality, the flow in the ponds is rarely ideal and the assumptions of CSTRs and PFRs often do not hold true. The majority of the ponds that do not have mechanical mixing mechanisms do not reach a CSTR conditions (Polprasert et al., 1985). Wind and temperature are the most important factors that affect the degree of mixing (James, 1987). It is important to mention that the effect of short circuiting and stagnant region does exist to a certain degree in WSPs (Belzile et al., 2004). The stratification of temperature and mass, which is usual in the ponds as described in the subsequent chapters, is the main reason to reject the assumptions of ideality.

As a result, designing the pond based on the ideal models is unable to predict the effluent of the pond (Lee, 2006). The hybrid models which are the combinations of CSTRs and PFRs are recommended by many researchers (Ferrara, 1981; Juanico, 1991), but many parameters used in these models (e.g. the place of thermocline) are not easy to determine without testing at the field and they are really case sensitive.

The dispersion model is another option of non-ideal model that may cover the gap between PFRs and CSTRs. Many researchers have mentioned that a dispersed flow model better represents the conditions of non-ideal flow in WSPs. This model is highly related to two different parameters, the actual retention time and the dispersion index. Finding the actual amount of these parameters of dispersed flow model remains a great challenge for scientists (Wood et al., 1998; Shilton, 2001).

The prediction of the effluent from contaminant ponds is important as it must meet the local and regional water and sewage regulations. At the same time, surface and groundwater in the area should comply with the guidelines.

Environmental risk analysis is a tool that may assess the risk of effluent contaminants of the pond to ecological entities and human health. The risk assessment process is divided into different components according to different organizations such as Environmental Protection Agency (EPA) and Canadian Council of Ministers of the Environment (CCME). Finding the risk of effluent contaminants of the pond to the ecosystem and comparing the results with the existing guidelines may help to discover the actual performance of the treatment system, and the level of treatment required to meet the guidelines.

1.2 Problem statement

The existence of different minerals in the specific mine site, the oxidation reactions of these minerals and different chemical components producing by theses oxidation reactions cause complexity in the composition of AMD and are the basis of determining which treatment system is appropriate. Therefore, the need of the methodology to discover the chemical composition of AMD is apparent.

There have been significant researches conducted in modeling the contaminant transport in the tailing pond. These models are based on many assumptions, one of which is that the pond is perfectly mixed. That means there are no concentration gradients within the pond or the pond is modeled as a CSTR. In reality, the assumptions of ideal reactors do not exist in a majority of the ponds. Therefore, the existence of the model to predict the chemicals concentration gradient within the ponds is required.

Moreover, the effluent concentration of the WSP can affect the human health and ecosystem. Consequently, the existence of the process to determine the hazardous effect of the effluent contaminants on the surrounding environment is essential.

Conversely, by taking into account the above problems, significant limitations still exist in the AMD characterization and pond modeling. These limitations are:

✓ Lack of characterization of the minerals producing AMD
✓ Lack of published information of different categories of chemical components in AMD
✓ Lack of information of different chemical reactions occurring in the tailing ponds
✓ Shortcomings of transport model in the tailing ponds

- ✓ Under use of risk assessment approaches and risk-based decision making for evaluating pond disposal

This research aims to overcome these limitations.

1.3 Objectives and scope of the proposed research

1.3.1 Objectives

The objectives of this research are as follows:

- ✓ To obtain better understanding about the minerals producing AMD
- ✓ To obtain more comprehensive understanding of different categories of AMD chemical components
- ✓ To develop the non-ideal reactor model for tailing pond
- ✓ To develop/revise a model to determine the fate of contaminant within the tailing pond
- ✓ To develop a risk model (Considering ecology and human health) to evaluate different AMD treatment strategies
- ✓ To develop risk-based design methodologies for AMD treatment design

1.3.2 Scope

In order to achieve the objectives of the research to be carried out, the following areas should be considered:

- ✓ Literature review for better understanding of different chemical components of AMD and the reactions occurring in the tailing pond
- ✓ Developing a methodology for AMD characterization

✓ Tailing pond modeling using advance approaches

✓ Evaluating the guidelines for better understanding the environmental risk assessment processes

✓ Risk assessment of AMD and tailing pond system

✓ Development of risk-based waste management strategies

It is noteworthy that the following objects are not evaluated in this research:

✓ Different methods for extracting the ore from the mine site

✓ Different ways the AMD get produced

✓ Different treatment methods of AMD

✓ Final disposal methods of sludge which is produced in the tailing pond

The extent of this PhD research has been outlined in the figure below:

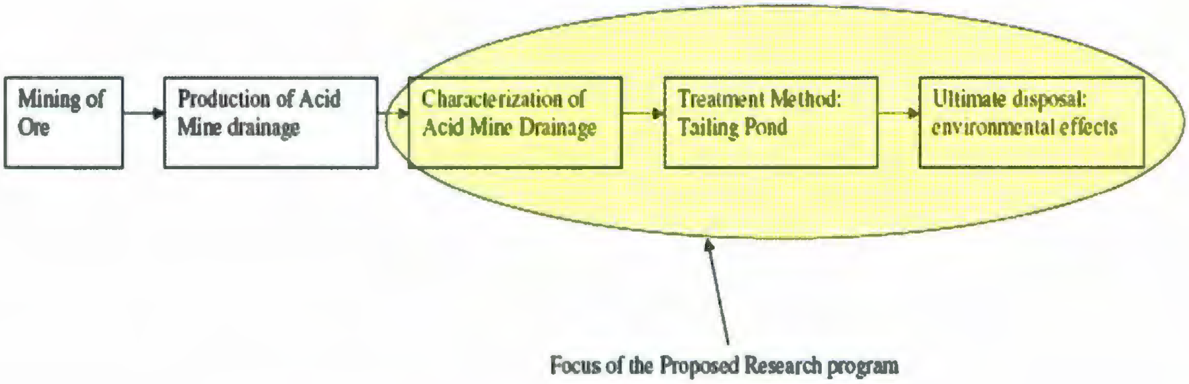

Figure 1.1. Focus of the proposed PhD research

The scope of this research may be seen in the following flowchart:

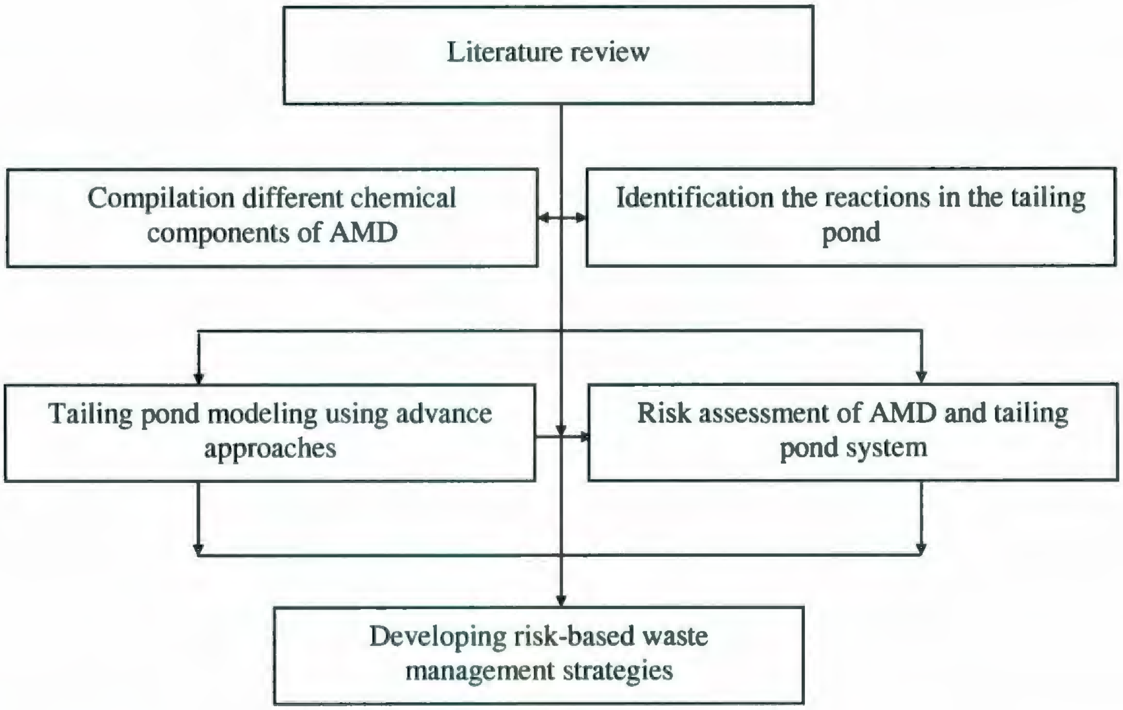

Figure 1.2. The scope of this PhD research

1.4 Organization of the thesis

The thesis is divided into six chapters. Chapter 1 introduces the problem, objectives and scope of doing this research. Chapter 2 reviews the literatures about research conducted to the state in three fields: i) AMD characterization, ii) WSP modeling, and, iii) Environmental risk assessment. Chapter 3 develops a methodology for AMD characterization. The evaluation of this methodology is also discussed using a case study from the Wolverine coal mine in northeastern BC, Canada.

In Chapter 4, the non-ideal dispersed flow model is presented. Furthermore, different methods to determine the actual retention time and dispersion index as the main parameters of dispersion model are explored. The methodology to determine these parameters using Computational Fluid Dynamics (CFD) is demonstrated with a case study for its validation. Dispersed flow model is also validated using two different case studies in this chapter.

In Chapter 5, the USEPA (1998) ecological risk assessment (ERA) framework is discussed. A case study of effluent contaminants of the tailing pond is used in assessing and characterizing ecological risk assessment.

Chapter 6 provides the conclusions of the present research. Recommendations are also made for the future research work related to the risk-based decision making of AMD characterization and WSP modeling.

Finally, Chapter 7 summarizes the novelty and contribution of the present work. Figure 1.3 demonstrates sequence of the thesis to achieve the objectives outlined above.

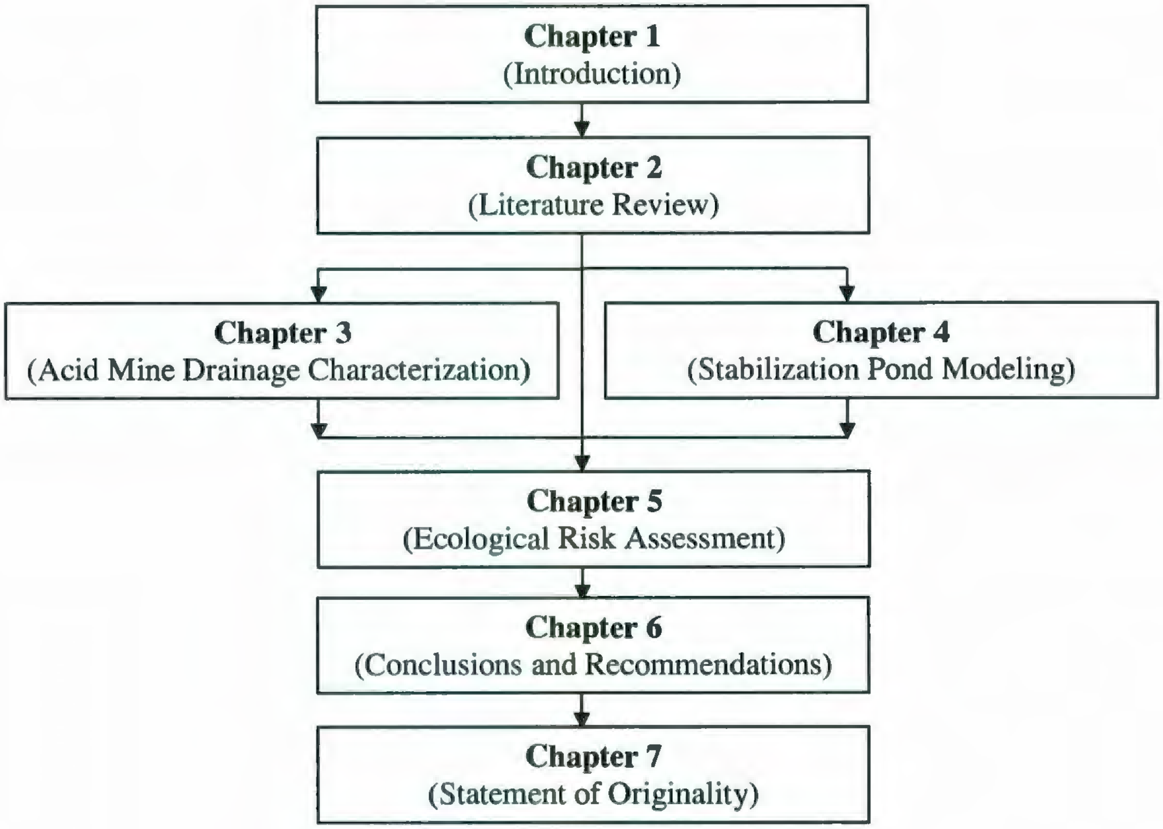

Figure 1.3. Organization of the thesis

CHAPTER 2

Literature Review

2.1 Mine water quality

The prediction of mine water quality is important during mining and mineral processing activities. AMD is one of the environmental issues in sulfide ore mining (Nieto et al, 2007). Sources of producing AMD can be grouped into primary and secondary.

Table 2.1. Different sources for producing AMD (Akcil et al., 2006)

Primary Sources	**Secondary Sources**
Mine rock dumps	Treatment sludge pounds
Tailings impoundment	Rock cuts
Underground and open pit mine workings	Concentrated load-out
Pumped/nature discharged underground water	Stockpiles
Diffuse seeps from replaced overburden in rehabilitated areas	Concentration spills along roads
Construction rock used in roads, dams, etc.	Emergency ponds

Considering these different sources in the mine sites, AMD is produced and released into the environment, creating many environmental hazards.

Sulfides wastes are characterized by elevated acidity, high concentration of sulfides and metals such as cobalt, copper, iron, lead, nickel, zinc, etc. (Nieto et al., 2007). The release of AMD reduces the value of pH and it has high specific conductivity and high concentrations of iron and toxic metals. Thus, the effluent from the metal mining industry can have serious impact on human and ecological health (Akcil et al., 2006).

In short, the problems of producing AMD include the following (Lupankwa et al., 2006):

- Limits the reuse of mine water and processing water by its effect on mine water quality
- Corrosion
- Negative impacts on flora and fauna communities
- Impacts on the groundwater quality
- Impacts on downstream water used for fishing or irrigation purposes

The prediction of tailing water composition is complicated and remains a challenge for scientists.

2.1.1 Chemical components of AMD

Many types of sulfide minerals produce AMD, some of which can be seen in Table 2.2. Among them iron sulfides are the most common. The reactions of acid generation are best declared by examining the oxidation of pyrite (FeS_2), which is one of the most typical sulfide minerals (Akcil et al., 2006).

Pyrite is one of the dominant minerals in AMD, and is commonly associated with coal and metal ore deposits (Elberling et al., 1994; Lottermroser et al., 2003). As a matter of fact, the chemical processes producing AMD can be exemplified by oxidation of pyrite. Therefore, the oxidation mechanism and the rate of oxidation of pyrite can be chosen to represent the process of AMD generation by the sulfide minerals.

Table 2.2. AMD producing sulfide minerals (Akcil et al., 2006)

Mineral	Composition
Pyrite	FeS_2
Marcasite	FeS_2
Chalcopyrite	$CuFeS_2$
Chalcocite	Cu_2S
Sphalerite	ZnS
Galena	PbS
Millerite	NiS
Pyrrhotite	$Fe_{1-x}S$
Arsenopyrite	FeAsS
Cinnabar	HgS

Metals such as cadmium, cobalt, copper, iron, lead, nickel, zinc, etc. are released into the environment when sulfides of these metals are exposed to the air (Garcia et al., 2005). The oxidation process of pyrite begins as follows (Revengai et al., 2004; Sherriff et al., 2007):

$$2FeS_{2\,(s)} + 7O_2 + 2H_2O \rightarrow 2Fe^{+2} + 4SO_4^{-2} + 4H^+ \qquad (2\text{-}1)$$

There are several chemical and biological processes related to the oxidation of pyrite (Lonesiy, 2006).

When sufficient oxygen is dissolved in the water, the oxidation of ferrous iron to ferric iron occurs as follows:

$$2Fe^{+2} + 1/2O_2 + 2H^+ \rightarrow 2Fe^{+3} + H_2O \qquad (2\text{-}2)$$

The oxidation of ferrous to ferric iron is very slow in acidic solutions and this is the rate determining step in pyrite oxidation. The reaction constant (K) is $2.8*10^{-6}$ L/mol.Atm at $T = 30.5\,^{o}C$ (Nordstrom, 1985). The reaction rate can be seen below:

$$-\frac{dFe^{2+}}{dt} = K\,[Fe^{2+}]^2[O_2]$$

Both chemical and bacterial oxidants participate in ferrous iron oxidation. The pH, temperature and dissolved oxygen affect the bacterial oxidation of ferrous iron as well as ferrous iron oxidation kinetics. In another step, the ferric iron precipitates as ochre as stated by the following reaction:

$$2Fe^{+3} + 6H_2O \leftrightarrow 2Fe(OH)_{3\,(s)} + 6H^+ \qquad (2\text{-}3)$$

In this process, more hydrogen ions are released into the environment and this may lead to pH reduction. Iron hydroxide ($Fe(OH)_3$) may produce an orange and yellow sludge at the bottom, which is harmful for aquatic life (Lonesiy, 2006). $Fe(OH)_3$ is not stable at a pH below 3.5, where ferric iron remains in solution (Dold, 2005). Finally, the ferric iron may react with pyrite to produce more ferrous iron and acidity:

$$14Fe^{+3} + FeS_2 + 8H_2O \rightarrow 2SO_4^{-2} + 15Fe^{+2} + 16H^+ \qquad (2\text{-}4)$$

Ferric iron is a strong oxidant of pyrite in low pH conditions where oxidation of ferrous iron to ferric iron is catalyzed by bacteria (Lonesiy, 2006). As pH increases, the oxidation of pyrite is via oxygen and oxidation of pyrite with ferric iron is less significant.

By integrating the above reactions, the final reaction for the oxidation of pyrite is as follows:

$$FeS_{2(S)} + \frac{15}{4} O_{2\,(g)} + \frac{7}{2} H_2O \rightarrow Fe(OH)_{3\,(S)} + 2\,SO_4^{-2} + 4H^+ \qquad (2\text{-}5)$$

This reaction shows that for each unit of pyrite that is oxidized, four units of haydrogen ions (H^+) will be produced and this will increase acidity in the system (Lonesiy, 2006).

Espana et al. (2006) evaluated the amount of ferrous iron oxidation and ferric iron precipitation and calculated the rate of the reactions considering inflow and outflow concentrations. The resulting rate equations are as follows:

$$r_{0x} = \frac{\Delta[Fe(\mathrm{II})]}{\Delta t} = ([\mathrm{Fe(\,II\,)}]_{in} - [\mathrm{Fe(\,II\,)}]_{out})/t \qquad (2\text{-}1)$$

$$r_{pp} = \frac{\Delta[Fe_t]}{\Delta t} = ([\mathrm{Fe}_t]_{in} - [\mathrm{Fe}_t]_{out})/t \qquad (2\text{-}2)$$

r_{0x} = oxidation rate ($molL^{-1}s^{-1}$)

r_{pp} = precipitation rate ($molL^{-1}s^{-1}$)

$[Fe(\,II\,)]_{In}$ = ferrous iron concentration (in mol/L) at the inflow station

$[Fe(\,II\,)]_{In}$ = ferrous iron concentration (in mol/L) at the outflow station

t = travel time between station (s)

The amount of ferrous iron, ferric iron and total iron at the Lomero mine portal in hourly evaluation can be seen in Figure 2.1.

The amount of ferrous iron is reduced from inlet to outlet (due to ferrous iron oxidation) and the amount of ferric iron increases, respectively, but both completely dependent on the temperature which changes daily and seasonally.

The oxidation rate for this mine site varies between $4*10^{-7}$ and $7*10^{-7}$ mol $L^{-1}s^{-1}$ for temperatures between 20 and 35 ^{o}C. This reaction rate is 10^5 to 10^6 times faster than the abiotic (in the absence of microorganisms) reaction rate. The rate of ferrous iron oxidation is strongly catalyzed by acidophilic iron oxidizing bacteria. Studies show that the bacterial activity dependent on temperature, pH and dissolved oxygen is more effective on ferrous iron oxidation than ferrous iron concentration itself.

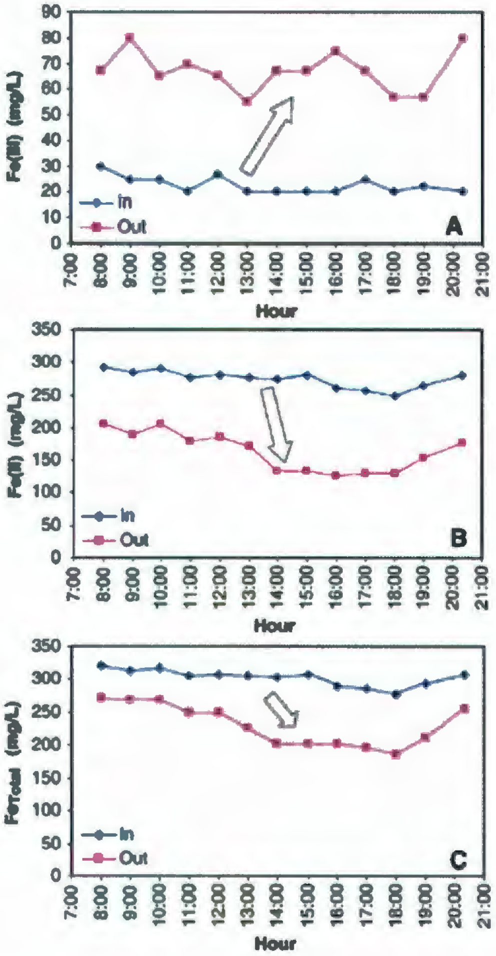

Figure 2.1. The amount of ferrous oxidation and ferric precipitation (Espana et al., 2006)

The investigations show that the rate of the reactions is not constant at different hours of the day and it depends on daily temperatures. A decrease in the rate will be observed during the evening. At sunset and sunrise when the temperature is lowest, the lowest oxidation rate is observed. Bacterial cell concentration and temperature are two factors that affect the rate of oxidation.

At the pH ranged between 2.7 and 3.1, the precipitation rate of ferric iron is between $1.7*10^{-6}$ and 10^{-7} mol $L^{-1}s^{-1}$. In an AMD where the pH is too far below this range, no precipitation takes place (Espana et al., 2006).

By taking temperature into account, the precipitation rate of ferric iron demonstrates a condition similar to the oxidation rate of ferrous iron, and the precipitation shows a strong removal of iron from the acidic solution. However, the relation (correlation factor) between bacterial cell concentration and oxidation rate has been unknown until now (Espana et al., 2006).

The rate of ferrous iron oxidation in the field is 5 to 8 times faster in magnitude than the oxidation rate in the laboratory tests, which are in the abiotic condition (Kirby, 1998). In another investigation, pyrite oxidation rate was calculated by the following equation:

$$r = \Delta H_f^{-1} * \text{the molecular mass of } FeS_2 * a * W^{-1} \quad (2\text{-}3)$$

It should be mentioned that pyrite and pyrhotite are chemically and biologically oxidized and this is obvious in microcalorimetric data in several studies (Kirby, 1998). The different rates for pyrite and pyrhotite oxidation found in different mine sites are related to "molecular oxygen diffusion, temperature, metal sulfide reactivity and abundance of metal sulfide oxidizing bacteria" (Kock et al., 2006).

There are many physical, chemical and biological factors that affect the rate of AMD generation. These factors can be seen below (Akcil et al., 2006):

- ✓ pH
- ✓ Temperature
- ✓ Oxygen content of the gas phase, if saturation is less than 100%
- ✓ Oxygen concentration in water phase
- ✓ Degree of saturation with water
- ✓ Bacterial activity and
- ✓ Chemical activity of ferric iron

Therefore, chemical and biochemical reactions take place when sulfide minerals are associated with water and oxygen (the process was mentioned for pyrite oxidation), which leads to produce acidity. This acidity and the metals that are released in the sulfide minerals oxidation processes have hazardous effects on human health and the environment. To choose the best way for treating AMD, one should have complete information about the oxidation process and the rate of the reactions in different stages. However, scientists remain concerned about the prediction of AMD composition, although such a prediction is very complicated.

2.1.2 Chemical reactions in the tailing pond

A series of chemical reactions happens in the pond, which are related to the particular geology and hydrology of the specific mine site. The reaction between mineral pyrite, water and oxygen is the major problem of AMD (Lonesiy, 2006). The chemical oxidation of a mineral can be classified as acid producing or consuming (the reactions which generate or consume H^+) or non-acid producing or consuming (Lottermroser, 2003). These types of reactions are described in the following sections.

2.1.2.1 Non-acid producing sulfide minerals

There are many metal sulfides that can participate in the reaction with oxygen and release metal ion into a solution but may not produce acidity. Examples of such reactions may be seen below (Costello, 2003; Da Silva et al., 2003):

Sphalerite: $ZnS_{(S)} + 2O_{2(aq)} \rightarrow Zn^{+2} + SO_4^{-2}$ (2-6)

Galena: $PbS_{(S)} + 2O_{2(aq)} \rightarrow Pb^{+2} + SO_4^{-2}$ (2-7)

Millerite: $NiS_{(S)} + 2O_{2(aq)} \rightarrow Ni^{+2} + SO_4^{-2}$ (2-8)

Greenockite: $CdS_{(S)} + 2O_{2(aq)} \rightarrow Cd^{+2} + SO_4^{-2}$ (2-9)

Chalcopyrite: $CuFeS_{2(S)} + 4O_{2(aq)} \rightarrow Cu^{+2} + Fe^{+2} + SO_4^{-2}$ (2-10)

Covellite: $CuS_{(s)} + 2O_{2(aq)} \rightarrow Cu^{2+} + SO_4^{-2}$ (2-11)

Some metal sulfides can participate in the reaction with oxygen and not produce acidity. However, if a different oxidant such as ferric iron is present, these reactions may produce acidity as well. For example, the process of oxidation of sphalerite by ferric iron may be seen below:

$ZnS + 2\ Fe^{3+} \rightarrow Zn^{2+} + S^0_{(ppt)} + 2\ Fe^{2+}$ (2-12)

$2\ Fe^{2+} + 0.5\ O_2 + 2\ H^+ \xrightarrow{Bacteria} 2\ Fe^{3+} + H_2O$ (2-13)

$S^0 + 1.5\ O_2 + H_2O \xrightarrow{Bacteria} SO_4^{2-} + 2\ H^+$ (2-14)

2.1.2.2 Acid producing sulfide minerals

Metal sulfides may react with oxygen and produce acidity. In addition to pyrite, the details on acid producing minerals are outlined below:

Pyrrhotite ($Fe_{(1-x)}$ S)

Pyrrhotite is the most common iron sulphide in nature after pyrite (Belzile et al., 2004). The x in the pyrrhotite formula can be varied from 0.125 (Fe_7S_8) to 0 (FeS, troilite) (Dold, 2005). The oxidation of pyrrhotite is as follows (Brookfield et al., 2006):

$Fe_{(1-x)}\ S + (2 - \frac{x}{2})\ O_2 + x\ H_2O \rightarrow (1 - x)\ Fe^{2+} + SO_4^{2-} + 2\ xH^+$ (2-15)

The stiochiometery of the pyrrhotite effects on the production of acid. When x = 0, no acid will be produced and when x = 0.125 (Fe_7S_8), the maximum amount of acid will be produced (Dold, 2005). Raising the temperature increases pyrrhotite oxidation (Belzile et al., 2004).

Chalcopyrite ($CuFeS_2$)

The complete oxidation of chalcopyrite or copper pyrite as mentioned above does not produce any acidity. However, "the combination of ferrous iron oxidation and ferrihydrate hydrolysis" will lead to acid production as follows (Dold, 2005):

$$CuFeS_2 + \frac{17}{2} O_2 + 5\ H_2O \rightarrow 2\ Cu^{2+} + 2\ Fe(OH)_3 + 4\ SO_4^{2-} + 4\ H^+ \qquad (2\text{-}16)$$

This reaction illustrates that for the oxidation of each unit of chalcopyrite, 4 units of H^+ will be produced.

Arsenopyrite (FeAsS)

The chemical reaction for the oxidation of arsenopyrite is as follows (Belzile et al., 2004):

$$4\ FeAsS + 13\ O_2 + 6\ H_2O \rightarrow 4\ Fe^{2+} + 4\ SO_4^{2-} + 4\ H_2AsO_4^- + 4\ H^+ \qquad (2\text{-}17)$$

The oxidation rate of arsenopyrite is the same as that of pyrite when the oxidant is ferric iron but if the oxidation is carried out by oxygen, the oxidation rate of arsenopyrite is lower than that of pyrite (Dold, 2005).

The oxidation of pyrite, sphalerite and arsenopyrite is the main source for producing SO_4^{-2} in the oxidized tailing wastewater (Romero et al., 2007).

Some other sulphide minerals may produce acidity as well and are discussed in the following paragraphs. These minerals may be oxidized by oxygen or by ferric iron.

Enargite (Cu_3AsS_4):

Enargite is a copper arsenic sulfosalt mineral with the chemical formula Cu_3AsS_4, which is mostly found in the copper mines. The oxidation may be caused by oxygen (Smith et al., 2003):

$$Cu_3AsS_4 + 8.75\ O_2 + 2.5\ H_2O \rightarrow 3\ Cu^{2+} + HAsO_4^{2-} + 4\ SO_4^{2-} + 4\ H^+ \quad (2\text{-}18)$$

Or it may be caused by ferric iron:

$$CuAsS_4 + 35\ Fe^{3+} + 20\ H_2O \rightarrow 3\ Cu^{2+} + 35\ Fe^{2+} + HAsO_4^{2-} + 4SO_4^{2-} + 39\ H^+ \quad (2\text{-}19)$$

Marcasite (FeS_2):

Marcasite has the same structure but different symmetry and crystal shapes compared to pyrite. It is rare but it may be locally abundant in some types of ore deposits. The oxidation of marcasite by oxygen and ferric iron may be seen below (Rinker et al., 1997).

$$FeS_2 + 3.5\ O_2 + H_2O \rightarrow Fe^{2+} + 2\ SO_4^{2-} + 2\ H^+ \quad (2\text{-}20)$$

$$FeS_2 + 14\ Fe^{3+} + 8\ H_2O \rightarrow 15\ Fe^{2+} + 2SO_4^{2-} + 16\ H^+ \quad (2\text{-}21)$$

In addition, ferrous iron in the reaction above may be oxidized by reaction 2-2 and recycled as an oxidant in the reaction above.

Tennantite ($Cu_{12}As_4S_{13}$):

Tennantite is one of the common sulfosalts. The oxidation of tennantite is as follows (Lin, 2006):

$$Cu_{12}As_4S_{13} + 12\ H_2O \rightarrow 12\ Cu^{2+} + 4\ H_3AsO_3 + 13\ S + 12\ H^+ + 36e^- \quad (2\text{-}22)$$

The oxidation of intermediate products may produce more acidity as follows:

$S + 4\,H_2O \rightarrow SO_4^{2-} + 8\,H^+ + 6\,e^-$ (2-23)

$H_3AsO_3 + H_2O \rightarrow H_3AsO_4 + 2\,H^+ + 2e^-$ (2-24)

2.1.2.3 Oxidation mechanism of acid insoluble compounds

Various intermediate inorganic sulfur compounds are formed in the course of the multi-step oxidation process (Moses et al., 1987).

The three acid insoluble metal sulfides are FeS_2 (pyrite), MoS_2 (molybdenite) and WS_2 (tungstenite). Luther (1987) described why ferric iron rather than oxygen reacts with the pyrite surface. By the initial attack of ferric iron as an oxidant, "the sulfur moiety of pyrite is oxidized to soluble sulfur intermediate (Luther, 1987)." Thiosulfate is the first soluble sulfur intermediate in the dissolution of pyrite by ferric iron.

In the next step, tetrathionate is the main product of thiosulfate degradation in the course of pyrite oxidation. The degradation of tetrathionate strongly depends on pH and on the availability of catalysts (bacteria). Due to the specific pH of the mine water and oxygen availability, tetrathionate may degrade again to disulfane-monosulfonic acid and trithionate respectively. Finally, trithionate can be hydrolyzed to thiosulfate and sulfate.

As a result, the series of reactions occurs in a cyclic degradation of thiosulfate via polythionates to sulfate, shown in the Figure 2.2. Since thiosulfate is a key compound in the reaction series, the pyrite oxidation mechanism has been named the thiosulfate mechanism (Schippers, 2004). Therefore, various intermediate reactions occur in AMD according to pH, bacterial and oxygen availability, which should be defined to determine the chemical compounds in the specific AMD.

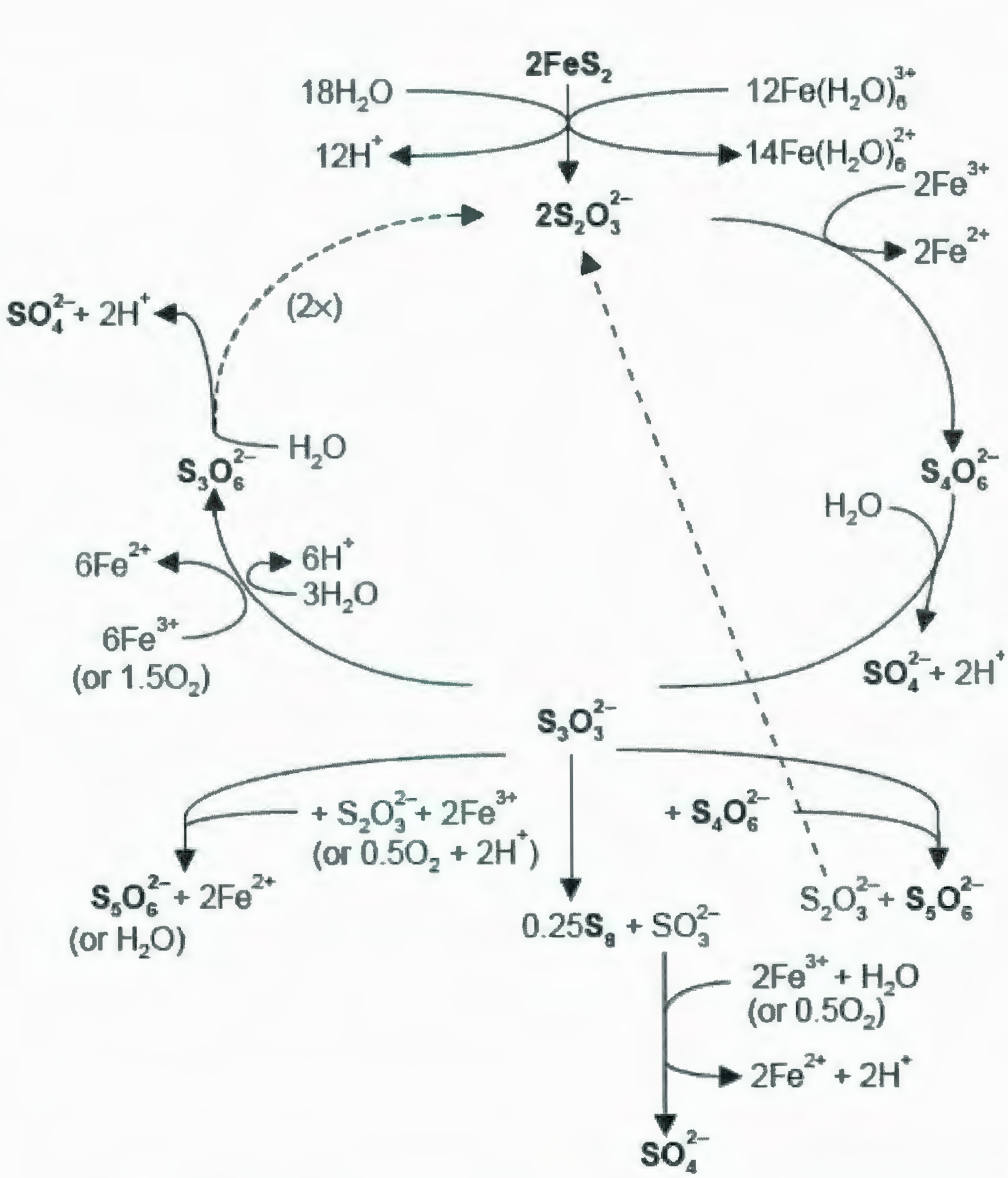

Figure 2.2. A cyclic degradation of thiosulfate via polythionates to sulfate (Schippers, 2004)

2.1.2.4 Oxidation mechanism of acid soluble compounds

As described above, FeS_2, MoS_2 and WS_2, which are known as acid insoluble sulfides can be degraded by oxidation in the environment, but other metal sulfides, such as $CuFeS_2$ (chalcopyrite), FeS (troilite), ZnS (sphalerite) and As_2S_3 (orpiment), can be dissolved by protons.

Due to the acid solubility of metal sulfides (MS) and to the proton attack, the first reaction occurs as follows:

$MS + 2H^+ \rightarrow M^{2+} + H_2S$ (2-25)

Unlike pyrite oxidation, "the M-S bonds in acid soluble metal sulfides may be cleaved before the sulfur is oxidized" (Schippers, 2004). H_2S is oxidized by ferric iron according to reaction 2-26.

$H_2S + Fe^{3+} \rightarrow H_2S^{*+} + Fe^{2+}$ (2-26)

Because ferric iron breaks metal sulfide bonds more effectively than protons, the H_2S^{*+} radical may be formed in one reaction without intermediately occurring H_2S as follows:

$MS + Fe^{3+} + 2H^+ \rightarrow M^{2+} + H_2S^{*+} + Fe^{2+}$ (2-27)

By dissociation of the strong acid (H_2S^{*+}), a HS^* radical may lead to the polysulfide formation as follows:

$H_2S^{*+} + H_2O \rightarrow H_3O^+ + HS^*$ (2-28)

The reaction of two radicals of HS^* leads to a disulfide ion in the following reaction:

$2\ HS^* \rightarrow HS^{2-} + H^+$ (2-29)

The oxidation of a disulfide ion is done by a ferric iron or a HS* radical. This oxidation by HS^* is shown in reaction 2-30.

$HS_2^- + HS^* \rightarrow HS_2^* + HS^-$ (2-30)

Polysulfides decompose to rings of elemental sulfur, mainly S_8 rings (>99%) in acidic solution, by the following reaction.

$HS_9^- \rightarrow HS^- + S_8$ (2-31)

The formation of thiosulfate (polythionates and sulfate) happens as indicated by the following reactions:

$$H_2S_n + \frac{3}{2}O_2 \rightarrow H_2S_2O_3 + [\frac{(n-2)}{8}]S_8 \tag{2-32}$$

$$H_2S_n + 6Fe^{3+} + 3H_2O \rightarrow H_2S_2O_3 + [\frac{(n-2)}{8}]S_8 + 6Fe^{2+} + 6H^+ \tag{2-33}$$

The mechanism of metal sulfide (MS) oxidation via polysulfides is shown in Figure 2.3.

Table 2.3. Main sulfur compound products from the oxidation (biological and chemical) of acid soluble and insoluble compounds (Schippers, 2004)

	Chemical oxidation	**Biological oxidation**
FeS_2, pH 2, oxic, O_2 as an oxidant	sulfuric acid, elemental sulfur	Sulfuric acid; aerobic strongly acidophilic Fe^{2+} (and S) oxidizer; e.g., Acidithiobacillus ferrooxidants
MS, pH 2, oxic, O_2 as an oxidant	Elemental sulfur	Sulfate; aerobic, strongly acidophilic Fe^{2+} and S oxidizer; e.g.,Acidithiobacillus ferrooxidants
FeS_2, pH 7-8, oxic, O_2 as an oxidant	Trithionate, tetrathionate, sulfuric acid, thiosulfate	Sulfuric acid; {aerobic moderately acidophilic S oxidizer; e.g., Thiomonas intermedia}, microaerophilic Fe^{2+} oxidizer
MS, pH 7-8, oxic, O_2 as an oxidant	Elemental sulfur, thiosulfate	Sulfate; aerobic moderately acidophilic S oxidizer; e.g., Thiomicrospira frista, and microaerophilic Fe^{2+} oxidizer
FeS_2, pH 2, anoxic, Fe^{3+} ions as oxidant	Sulfuric acid, elemental sulfur	Sulfuric acid; {anaerobic strongly acidophilic S oxidizer and Fe^{3+} reducer; e.g., Acidithiobacillus ferrooxidants}
MS, pH 2, anoxic, Fe^{3+} ions as oxidant	Elemental sulfur, sulfate	Sulfuric acid; {anaerobic, strongly acidophilic S oxidizer and Fe^{3+} reducer; e.g., Acidithiobacillus ferrooxidants}
FeS_2, pH 7-8, anoxic, Mn^{4+} oxide as oxidant	Sulfate, tetrathionate, trithionate, thiosulfate	No oxidation
MS, pH 7-8, anoxic, Mn^{4+} oxide as oxidant	Elemental sulfur, sulfate	Sulfate; {Sulfur disproportionating bacterium; e.g., Desulfocapsa sulfoexigens}
MS, pH 7-8, anoxic, Nitrate as oxidant	No oxidation	Sulfate; moderately acidophilic S [or Fe^{2+}] oxidizer; e.g., Thiobacillus denitrificans, and anaerobic Fe^{2+} oxidizer
MS, pH 7-8, anoxic, CO_2 as oxidant, light	No oxidation	Sulfate; anaerobic, phototrophic Fe^{2+} oxidizer; e.g., Rhodovulum iodosum

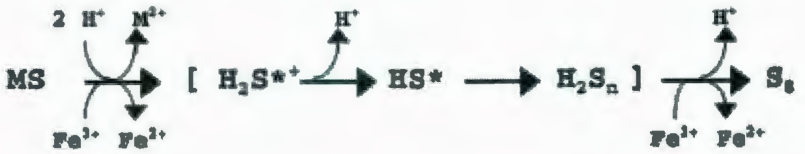

Figure 2.3. Scheme for metal sulfide (MS) oxidation via polysulfides (Schippers, 2004)

Based on the oxidation reactions discussed previously, metals such as cadmium, cobalt, copper, iron, lead, nickel, zinc etc. and different sulfur compounds such as thiosulfate, thrithionate, tetrathionate, pentathionate, sulfate and elemental sulfur are present in the tailing waste. The existence of the metal sulfides in the AMD is related to the specific conditions of the site, such as pH and Eh (the voltage potential with respect to the standard hydrogen electrode) of the mine water. Moreover, the role of microorganisms in the oxidation reactions can not be neglected and should be considered when obtaining the rate of the oxidation reactions.

2.1.3 The role of microorganisms in the oxidation process

Microorganisms play an important role in the oxidation process and one of the critical factors that control the generation of acidic waters (Komnitsas et al., 1995). Oxidation that occurs in the presence of microorganisms is known as biotic; while, oxidation in the absence of microorganisms is abiotic (Lottermroser, 2003).Generally, oxidation of minerals can be grouped accordingly:

1) Biotic direct oxidation, with oxygen in the presence of microorganisms.
2) Abiotic direct oxidation, with oxygen in the absence of microorganisms.
3) Biotic indirect oxidation, with oxygen and iron in the presence of microorganisms.

4) Biotic indirect oxidation, with oxygen and iron in the absence of microorganisms.

Bacteria are adsorbed on the mineral's surface "physically," considering the forces of molecular interaction, or "chemically", due to the formation of a chemical bond between the cell and the elements. The bacteria absorbed on the minerals tend to change the electrode potential, depolarizing the mineral surface through oxidation of sulfur and ferrous iron. This leads to an increase in the Eh of the mine water, producing highly oxidized conditions (Komnitsas et al., 1995).

Oxidation of sulphur or sulphides for energy production is restricted to the bacteria, such as Thiobacillus, Thiomicrospira, and Sulfolobus. These bacteria all produce sulphuric acid (i.e. H^+ and sulphate ions (SO_4^{-2})) as metabolic product. These bacteria are identified to accelerate the generation of AMD from the minerals in the mine site, where sulphide oxidation catalyzed by bacteria may produce over 1000 times more acid in comparison with the chemical reactions alone (Rawat et al., 1982; Egiebor et al., 2007).

The biological oxidation rate is highly dependent on the pH of the mine water, being most rapid at pH between 3 and 3.5. The biological oxidation of ferrous iron, as the slowest reaction of sulphide minerals oxidation, is 1 million times greater in compare with abiotic conditions. As a result, consideration of the biological condition of the specific AMD to determine the reactions kinetic should not be neglected.

2.1.4 Different methods for finding the minerals producing the AMD in the mine site

Due to the complex nature of AMD, no specific methodology is standard for qualitative and quantitative characterization of AMD formation. Optical and electron microscopy are some of the common methods used for mineral matter characterization.

Although these techniques are widely used for identifying and characterizing different minerals, the low resolution of optical microscopes for a particle size less than 5-10 μm is a major problem. Many minerals, particularly clay and accessory minerals, with a grain size less than 5-10 μm (typically between 0.01-10 μm) can not be identified and characterized. A similar disadvantage is encountered in EM (electron microscopy), where detection of grain size below the 0.5-1 μm is not possible. This limits detection of many accessory minerals in coal (Vassilev et al., 2003).

Table 2.4. Advantageous and disadvantageous of mineral identification techniques (Vassilev et al., 2003)

Identification Techniques	Advantageous	Disadvantageous
Optical microscopy	- Valuable information about optical characteristics and properties, such as size, composition & morphology provided by this method	- Particle size less than 5-10 μm can not be detected - Minerals with low reflectance or intimately associated with coal macerals may not be recognized
Electron microscopy	- The distribution of elements ("elemental map") in phases may be conducted and photographed	- Particle size less than 0.5-1 μm can not be detected - Elements with the atomic weights below that of Na cannot be detected - Detailed characterization of samples is a time consuming process
X-Ray diffraction	- The detection of occurrence and degree of crystallinity forming, major, and some minor crystalline phases independently from their size	- The relatively low sensitivity of the XRD technique requires significant preliminary physical and chemical separations - This technique should be used together with the other techniques, due to the detection limits and peak overlapping

One of the most common and useful methods for identifying minerals is X-Ray diffraction (XRD) (Yaman et al., 2001). This technique is useful for the detection of different minerals (Pollack, 1979), although factors such as different absorption characteristics and crystallite size may reduce the degree of accuracy. This method is costly too; needs a degree of interpretation and consequently and highly trained personnel. However, identification of many minerals by only XRD is not possible, and so this technique is used in conjunction with other techniques such as separation procedures, optical, and scanning electron microscopy.

2.2 Stabilization pond model

WSPs are one of the treatment systems that take advantage of naturally occurring chemical and biological processes to cleanse contaminated mine waters and are used for treating AMD. Although chemical oxidation is the predominant reaction taking place in the pond, the existence of sulphate reducing bacteria in the sludge of the pond bottom leaves open the possibility of their use in the reduction of the metals and sulphite ion presented in the influent AMD (Garcia et al., 2005).

The simplicity of construction and operation are the main advantage of this treatment system (Shilton, 2006). While WSP technology has been developed in past 50 years for treating a wide range of wastewater; little attention has focused on using of this system for treating AMD (Rose et al., 1998).

Different models exist to represent the contaminants' transportation along the pond. The standard reactor theory derived from the process engineering field may be applied to model the complexity of the chemical transport within the WSP. Integrating the rate of chemicals' oxidation reactions with an appropriate mass balance equation may help to design the pond based on chemical reactor design (Shilton, 2006).

2.2.1. Ideal models

Designing methods of the pond vary by the chemical reactions that happen in the pond and the physical nature of the wastewater. These methods are based on various reactor assumptions (Metcalf et al., 1979). "Ideal reactors are model systems for which the transport and mixing processes are exactly defined" (Gujer, 2008). Two ideal reactor models, CSTR and PFR, are widely used for the WSP design. The assumptions of ideal reactors are the basis of the WSP designed, as stated by many researchers (Gloyna, 1976; Moreno et al., 1990). The properties of the ideal reactors are identified in Table 2.5.

Table 2.5. Overview of the characteristics of the ideal reactors (Gujer, 2008)

Type of reactor	Influent and effluent	Volume	Internal mixing
Batch reactor	No	Constant	∞ large in x, y, z
CSTR	Yes, equal	Constant	∞ large in x, y, z
PFR	Yes, equal	Constant	∞ large in y, z Advection in x
Stirred tank reactor with variable volume	Yes, different amount	Variable	∞ large in x, y, z

The properties of ideal reactors, frequently used to model the WSP, are introduced and discussed in the following paragraphs.

2.2.1.1 Continuously Stirred Tank Reactor (CSTR)

In CSTR models, one or more fluids enter the reactor and are assumed to be perfectly mixed (Metcalf et al., 1979). Some assumptions in this type of reactor include:

1) In steady-state condition, the influent flow rate is equal to the effluent flow rate; otherwise the tank will overflow or go empty.
2) All of the calculations related to these reactors assume perfect mixing, which means a concentration gradient does not exist in the reactor.
3) If an infinite number of CSTRs are operated in series, they would be equivalent to PFR. This assumption may help to design a PFR by N series CSTRs (N = number of reactors in series).
4) A constant temperature is assumed within the reactor, which means any heat stratification does not exist.

These assumptions are for an ideal CSTR, but in reality, this model is difficult to achieve. For designing the CSTR, it should be noted that the reactor's design is based on the following general word statement (Levenspiel, 1972; Chow et al., 1979):

Rate of accumulation of reactant within the system boundary = rate of flow of reactant into the system boundary – rate of flow of reactant out of the system boundary + rate of disappearance (utilization) of reactant within the system boundary.

And in simple mathematical terms:

$$V\left(\frac{dC}{dt}\right) = QC_0 - QC + V(-KC) \tag{2-4}$$

By considering the assumptions of CSTR and solving the above equation by applying the boundary conditions of a specific situation (specific influent concentration and the retention time), the concentration gradient within the reactor may be evaluated.

The effluent concentration calculated from the materials' mass balance for a tracer is as follows (the tracer does not disappear through its transportation within the reactor and the reaction term is eliminated):

$$V\frac{dC}{dt} = QC_0 - QC \tag{2-5}$$

Solving this equation will lead to the following result:

$$C = C_0\,(1 - e^{-t/t_0}) \tag{2-6}$$

If N CSTRs are assumed in series, the equation changes to the following:

$$V/n\,(dC_2/dt) = QC_1 - QC_2 \tag{2-7}$$

$$C_1 = C_0\,e^{-N\theta} \tag{2-8}$$

By considering the above equations:

$$C_2 = C_0 N\theta e^{-N\theta} \tag{2-9}$$

Integrating these equations for finding the effluent of N reactors in series will lead to:

$$C_e = (C_0/ (N-1)!)\, (N\theta)^{N-1}\, e^{-N\theta} \qquad (2\text{-}10)$$

The series CSTRs can be used for modeling treatment plants. For example, Wilson et al. (1984) used CSTRs in series for modeling the pond. The pond was divided into CSTRs with equal volumes, and the model allowed mixing between CSTRs. This model had a good prediction of the observed effluent (Wilson et al., 1984).

2.2.1.2 Plug Flow Reactor (PFR)

This type of reactor, which is also called piston flow (Arceivala, 1981), is divided into different plugs, with each plug assumed to be uniform in temperature, pressure and composition. However, once a plug moves in the longitudinal direction, there may be variation in these terms.

In the PFR, the general balance equation is not simplified to a simple algebraic relationship as it can be simplified in CSTR, but it involves the evaluation of an integral as shown in equation 2-13.

The element within the reactor is assumed and the mass balance equation for this element is written as follows (Hill, 1977; Froment et al., 1979):

(Rate of flow of the reactant into volume element) = (Rate of flow of reactant out of volume element) + (Rate of disappearance of reactant by chemical reactions within the volume element)

$$C_A = (C_A + dC_A) + (-r_A)dV_R \qquad (2\text{-}11)$$

$C_A + dC_A$ = the molal flow rate of reactant exiting from the element

And $dC_A = r_A dV_R$

Assuming X_A as a fraction of C_A which is converted:

$$C_A = C_{A0}\,(1-X_A) \qquad (2\text{-}12)$$

$$\rightarrow dC_A = -C_{A0}\, dX_A$$

By combing the equations above:

$$\frac{dV_R}{C_{A0}} = \frac{dX_A}{(-r_A)} \quad \rightarrow \quad \frac{V_R}{C_{A0}} = \int_{x_{Ain}}^{x_{Aout}} \frac{dX_A}{(-r_A)} \qquad (2\text{-}13)$$

2.2.2 Non-ideal models

In reality, the flow in the reactors is rarely ideal and the assumptions of CSTRs and PFRs may not exist. Most of the ponds that do not have mechanical mixing do not reach CSTR conditions (Polprasert et al., 1985). Wind and temperature are the most important factors that affect the degree of mixing. (James, 1987; Torres et al., 1997). The effects of short circuiting and stagnant region cannot be neglected in WSPs (Banda, 2003). The results of designing the reactors based on the ideal flow do not accurately predict effluent of the ponds (Lee, 2007). The stratification of temperature and mass are the main reasons for rejecting the ideality assumptions.

Therefore, the two ideal models for designing the reactor, CSTR and PFR, may not accurately predict the effluent of the ponds in the non-ideal conditions where the temperature and concentration stratify. The temperature stratification is the main reason for the concentration gradient within the pond.

The reason for these kinds of stratification, which are the main causes of non-idealities in the pond, will be described in the following (Torres et al., 1999; Abis et al., 2006; Banda et al., 2006; Lovanh et al., 2007):

- Daily variation of temperature

- Seasonal variation of temperature
- Difference between the inlet flow temperature and the temperature within the pond
- Effects of wind, which leads to the mixing of contaminants in the surface layer
- Difference between the flow velocities in the pond
- Effects of shear stress of walls on the return flow velocities which affect the back-mixing velocity
- Existence of the dead region (usually in the corners of the pond) which prevents the advantageous use of the whole volume of the pond

An energy balance can be used to estimate the average pond water temperature as a function of thermal energy stored in the pond. Increasing the temperature of the wastewater affects physical, chemical and biological processes. The energy balance is based on the conservation of energy and mass within the control volume (Karteris et al., 2005; Van Buren et al., 2000).

Circulation patterns and flow velocities impact temperature stratification within the pond. Van Buren et al. (2000) evaluated the temperatures in the pond by a stationary temperature probe. This evaluation showed that the average temperature at the surface was 3.6^{o}C warmer than the average temperature recorded at the bottom of the pond. On top of this, cool inflow water travel in the main advective zone was 2^{o}C cooler than return flow in the recirculation zone. The temperature stratification (vertically and horizontally) results in density stratification in the pond. In addition, the sedimentation of mass by the gravity forces affects the homogeneity along the pond. As a result, the mass is distributed within the pond in different layers (corresponding to densities), leading to mass stratification within the pond.

2.2.2.1 Hybrid models

Researchers have studied the impact of stratification on the treatment efficiency of the WSPs. Lorens et al. (1992) found that if there is no thermal stratification in the pond, the WSP has approximately CSTR conditions. When the thermal stratification starts, a well defined thermocline is produced in the pond. The upper layer, which is aerobic, is called the epilimnion and the bottom which is anaerobic is the hypolimnion. The temperature, dissolved oxygen and pH are affected by this stratification.

The hydraulic routing through the pond is affected by "wind mixing, thermal stratification, pond geometry and other basic design parameters"(Preul et al., 1987). The resulting model is based on the CSTR and PFR reactors. They separated the pond into active and return zones. The return zone is evaluated as a CSTR and active zone as PFR. The schematic of the model can be seen below (Preul et al., 1987):

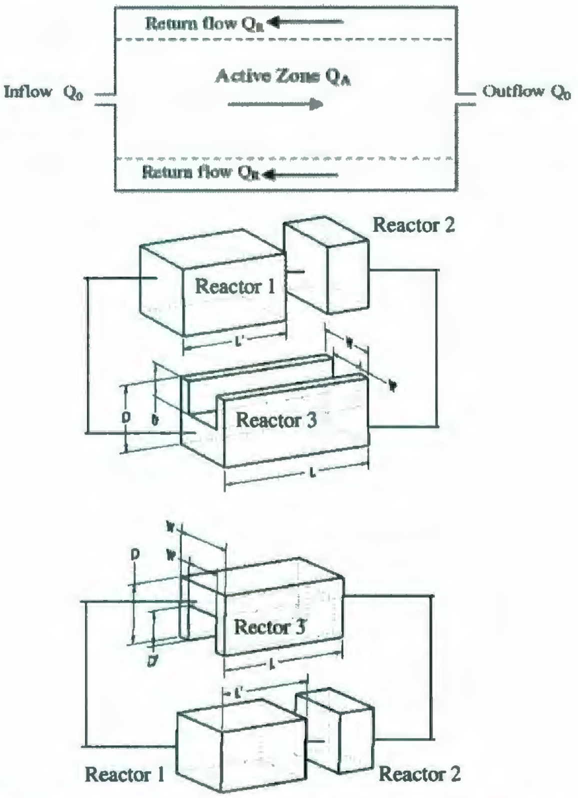

Figure 2.4. Hydraulic pattern in the pond (Preul et al., 1987)

In warmer periods, the inflow is directed to the bottom, and in colder periods, it is directed to the top, as can be seen in Figure 2.4. As a result, the equation that is applicable for predicting the effluent contaminants of the pond during winter is not the same as the one that is used during warmer climate in the summer.

Ruochuan et al. (1996) studied water quality stratification considering some water variations such as pH, water temperature and dissolved oxygen in the vertical profiles. The researchers found that, cooling at night resulted in a completely or partially mixed condition. In the winter, there is no mixing with wind and a weak stratification with water temperatures from 0 to 4^{o}C may be seen. After the formation of the ice layer, the pond becomes essentially anoxic by early January. The bottom sediments which are heated during summer, release some heat during winter. When the ice thawed out, daily stratification begins when the water warms up to 8^{o}C. In that time, after the production of a sharp thermocline, the surface water temperature rises up to 18^{o}C and the bottom temperature remains at about 8^{o}C. This study also evaluated jet mixing effects (the turbulent mixing which occurs as a result of the inflow velocity of the pond) and demonstrated that the effect of the mixing does not result in complete mixing. Based on their work, three types of pond stratification were proposed: 1) Completely mixed during day and night 2) Stratified during the day and mixed during night 3) Continuously stratified during consecutive days and nights (Ruochuan et al., 1996).

Juanico (1991) suggested a series of ponds instead of a single one. He argued that the PFR model perform much better compared to CSTR for parameters with high removal constant such as bacteria. The series of several ponds are recommended instead of a single big one to reduce the effect of short circuiting. The author concluded that actual rectangular ponds are not perfectly mixed, but have "a central partial mixed area running from inlet to outlet surrounded by dead areas" (Juanico, 1991). The dead areas in the non-ideal flow can be seen in Figure 2.5.

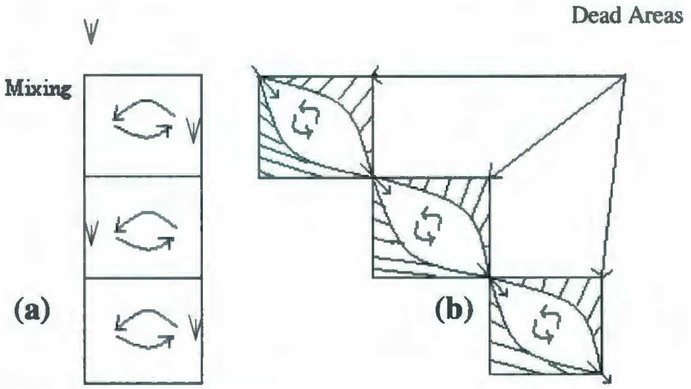

Figure 2.5. Dead area in the pond (Juanico, 1991)

The stratification measurement techniques in various ponds showed that the current models cannot be used in stratified ponds.

In addition to stratification, pond geometry will impact treatment efficiency. Ferrara et al. (1981) used the model simulations to indicate the effects of various pond geometries and inlet and outlet configurations. The pond was divided into active and return zones, as can be seen in Figure 2.6.

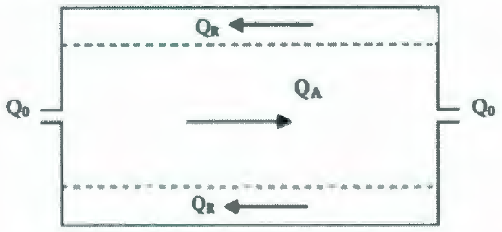

Figure 2.6. Model of hydraulic pattern in Pond (Ferrara et al., 1981)

The effluent concentration of the pond can be evaluated by the following formula:

$$C_e/C_i = 1/[1+KV_T/Q_0((D_sQ_0-KV_T\beta +KV_T\beta^2)/(D_sQ_0-K\beta V_T))] \qquad (2\text{-}14)$$

β = the ratio of the active zone volume (V_A) to the total pond volume (V_T)

The researchers proposed that if D_s is too high and the term in the parentheses is approximately equal to 1, this model is a CSTR. The effluent concentrations may be calculated by the following formula (Ferrara et al., 1981):

$$C_e/C_i = 1/(1+KV_T/Q_0) = 1/(1+Kt) \qquad (2\text{-}15)$$

Hybrid pond models have shown good agreement with experimental data under specific conditions. There are limitations with these models. First, experimental data must exist in order to calculate the parameters of the model. Work has been done to develop predictive equations for the unknown parameters, but not be useful for design purposes (Shilton, 2001). Furthermore, different separation surfaces (e.g. the place of thermocline) used in these models are not easy to find without testing at the field and are case sensitive. The parameters are based on the environmental conditions (e.g. temperature) and are highly variable. Therefore, depending on the conditions of the pond, the use of these models may lead to misleading results.

2.2.2.2 Dispersion model

In PFR model, no intermixing between fluid packets is allowed; however, molecular and turbulent diffusion can skew the profile as may be seen in Figure 2.7. Furthermore, in CSTR, the influent is completely mixed within the tank as soon as it enters the reactor. In the dispersed flow model, each element of incoming flow resides in the reactor for a different length of time. Therefore, it lies between the ideal PFR and CSTR. This non-ideal model can be used to determine the flow conditions in most reactors in which the assumptions of ideal reactors do not exist (Arceivala, 1981).

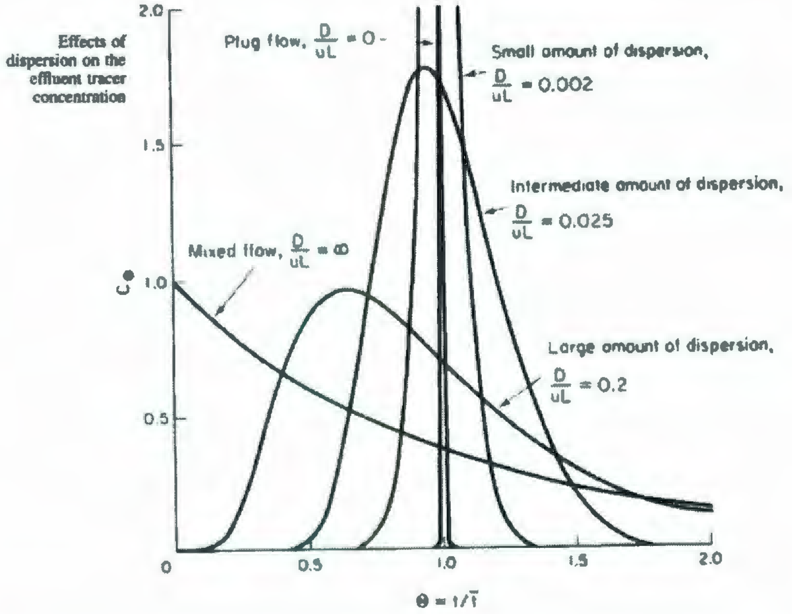

Figure 2.7. Concentration as function of time for different pond models (Arceivala, 1981)

Figure 2.7 is obtained by considering tracer concentrations at different time intervals. This diagram is called C-diagram. The C-diagram gives the "age" distribution at the exit. Different reactors show different trends; therefore, it can be seen how different types of reactors respond to tracer tests in terms of the dimensionless term D/UL or dispersion number. For the CSTR, the tracer is completely mixed with the tank, therefore, concentration C is equal to C_0. Therefore, at t=0, $C/C_0=1$. For the PFR, the tracer flows through the tank uniformly and appears all at once in the effluent at time $t = t_0$; hence, $t/t_0 = 1$.

As can be seen in Figure 2.7, the dispersion model covers the gap between PFRs and CSTRs models (Valsaraj, 1995). Researchers propose a dispersion model more accurately shows the conditions of non-ideal flow in WSP (Arceivala, 1981; Polprasert et al., 1985; Chien et al., 1995).

Some authors propose the short circuiting problem that is usual in the pond because of stratification, can be accounted in the non-ideal dispersed flow model (Banda, 2003).

Hayes (2001) propose a dispersed flow model where the radial mixing is neglected and only the dispersion in the length of the reactor is assumed. The steady state differential equation used is as follows (Ramaswami et al., 2005):

$$\frac{1}{Pe}\frac{d^2 f(z)}{dz^2} - \frac{df(z)}{dz} - \mathrm{Rf}\,(z) = 0 \qquad (2\text{-}16)$$

If no chemical reactions exist within the pond, the one dimensional dispersed flow model may be simplified to:

$$u\frac{\partial C_A}{\partial z} = D_{AB}\frac{\partial^2 C_A}{\partial z^2} \qquad (2\text{-}17)$$

Multiplying both parts of the equation to L and divided to D_{AB}:

$$Pe * \frac{\partial C_A}{\partial z} = L\frac{\partial^2 C_A}{\partial z^2} \qquad (2\text{-}18)$$

In the equations above:

Peclet number (Pe) = (Mass transfer by diffusion)/ (Mass transfer by convection)

$$Pe = \frac{L^2 / D_{AB}}{L / U} \qquad (2\text{-}19)$$

$$Pe = \frac{UL}{D} \quad \text{and} \quad R = \frac{kL}{u}$$

Considering the dispersion equation in different forms (steady state or transient conditions, with or without the presence of the reaction term), the concentration gradient within the pond is modeled. This model may cover the gap between the CSTRs and PFRs (as the ideal models) and be a good option for modeling the concentration gradient within the pond (Polprasert et al. 1985; Chien et al. 1995), as it covers the non-idealities within the pond.

2.2.2.3 Computational Fluid Dynamics (CFDs)

The term CFD includes computer-based methods for solving the linked partial-differential equations that consider the conservation of energy, momentum and mass in fluid flow. In the past few years, commercial CFD software for modeling basins is being widely used (Shilton, 2001). Molnar et al. (2005) explained that because of the lack of a general theory for a prediction of non-idealities in mixing, CFD codes may be used to predict the quality of mixing.

Many researchers used the CFD software to show the hydraulic behavior of the basins, considering different conditions experienced by the specific basin (Wood et al., 1995; Shilton 2001).

Sweeney et al. (2005) concluded stratification affects the flow pattern and subsequently the treatment efficiency. They evaluated the stratification within the pond and it become clear that stratification included short circuiting in the pond. They used the CFD model to predict the mean temperature based on the heat balance between the WSP and the surrounding environment. The results showed that even weak winds may affect stratification and the use of wind shear stress in CFD model leads to better predictions.

Simulating circulation patterns and mass transport in large basins driven by wind and thermocline effects were carried out by Fares (1993) based on the numerical model that he developed. In the next step, Fares et al. (1995) used this model representing the inlet and outlet position, to carry out a study of the flow behavior of a WSP. Their results confirmed the presence of short-circuiting according to wind effects. They continued the work with an objective of using the model to evaluate the effects of different inlet and outlet configurations considering the effect of different wind speeds and directions on the fluid movement in the pond. This investigation showed that wind action across the surface of ponds induces development of a "complex, three-dimensional, helical circulation pattern" (Fares et al., 1995). CFD software may help identify the effect of various parameters such as inlet/outlet configurations or the effect of wind on the pond characteristics and allow for the optimum conditions for the pond performance to be found. But, the CFD software used for modeling the hydraulic patterns of the basins are really case sensitive. An inability to introduce the exact conditions of the basins leads to misleading results.

2.3 Environmental risk assessment

Environmental risk analysis is a systematic process of assessing, managing and communicating risk to human health caused by an event or activity occurring in the environment.

Risk analysis is a detailed examination that consists of risk assessment, risk evaluation and risk management alternatives that are produced to recognize the nature of unwanted, adverse consequences to human life, health, property and environment (Bondad et al., 2008).

The Food and Drug Administration (FDA, 2002) defines "risk analysis as a tool to enhance the scientific basis of regulatory decisions." It includes risk assessment, risk management and risk communication activities. Each component has unique responsibilities. Risk assessment provides information on the extent and characteristics of the risk attributed to a hazard. Risk management includes the activities undertaken to control the hazard. Risk communication involves an exchange of information and opinion concerning risk and risk related factors between the risk assessors, risk managers and other interested parties (Fjeld et al. 2006). In simple terms:

Risk analysis = risk assessment + risk management + risk communication

These three components of risk analysis are dependent on one another for analyzing the magnitude of risk caused by the release of the contaminants, as can be seen in Figure 2.8.

Environmental risk assessment is the characterization of adverse health effects that results from human and ecological exposures to environmental hazards. The field of environmental risk assessment has grown in the last two decades due to the increase in public concern about the adverse effect of chemicals and hazards to the wildlife and ecosystem. Environmental risk assessment uses a set of tools to identify the likelihood and magnitude of adverse effects posed by environmental agents on human health and to natural resources. Conclusively, risk assessment is a systematic process for describing and quantifying the risk related to hazardous substances, processes, actions, or events (Covello et al., 1993).

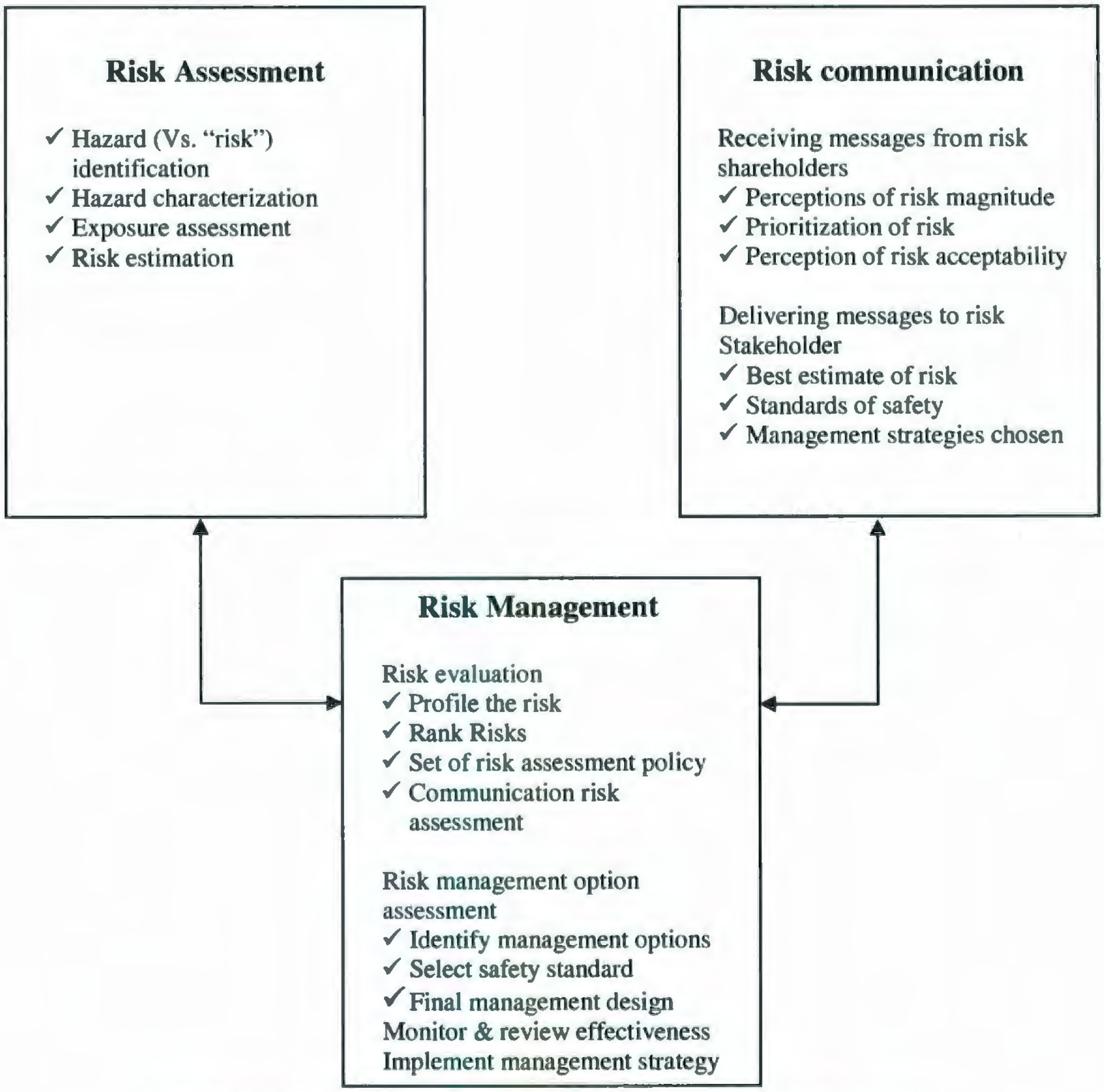

Figure 2.8. Different components of risk analysis (Brunk, 1998)

However, most environmental risk assessments are performed to answer a question or resolve an issue, such as: Is it safe for a proposed chemical plant to operate in this location or is it safe to dispose?

The Canadian Council of Ministers of the Environment (CCME) (1997) has set forth guidelines for a three-tiered system that may be used to derive environmental quality criteria. The following components outlined by CCME are involved in the risk assessment process (CCME, 1997):

Figure 2.9. Different components of risk assessment process (CCME, 1997)

As per Figure 2.9, the receptor is the person or population exposed to the contaminant at the exposure point. One of the important factors in determining exposure includes the characteristics of receptors. For most of the equations used to estimate the exposure, at least two terms (e.g. age, body weight and gender), attempt to define a specific receptor's characteristics or parameters. Some characteristics like body weight, volume of air inhaled per unit, amount of soil consumed inadvertently and time spent indoors and outdoors for human and ecological entities should be evaluated as a part of the environmental risk assessment process. The values for each of the receptors vary significantly and, in this way, which receptors receive the greatest exposure from the contaminant needs to be defined.

Hazard, a measure of harm or the potential of the event to cause harm, is one of the components of the risk assessment process. Different types of hazards exist. Some are natural, while industrial or technological hazards are caused by human beings.

Exposure is one of the components of the analysis phase of a risk assessment. It is a measure of the amount that the likely recipient of a specific hazard takes in. For any special hazard, the greater the exposure, the greater the risk of an adverse effect is on health. Exposure can be simply identified as the amount of the agent that is available to a human or animal. Exposure can occur through different pathways for humans, as shown in Figure 2.10.

The absorption of chemicals is related to the route of exposure. Furthermore, the absorption of a chemical also is affected by its chemical and physical properties. In simple terms, chemicals that are soluble in fat can be absorbed more easily into the body.

These risk assessment processes are divided into different components according to different organizations such as Environmental Protection Agency (EPA) and CCME.

The EPA baseline risk assessment process includes data collection and evaluation, exposure assessment, toxicity assessment and risk characterization (USEPA, 1999), as can be seen in Figure 2.11.

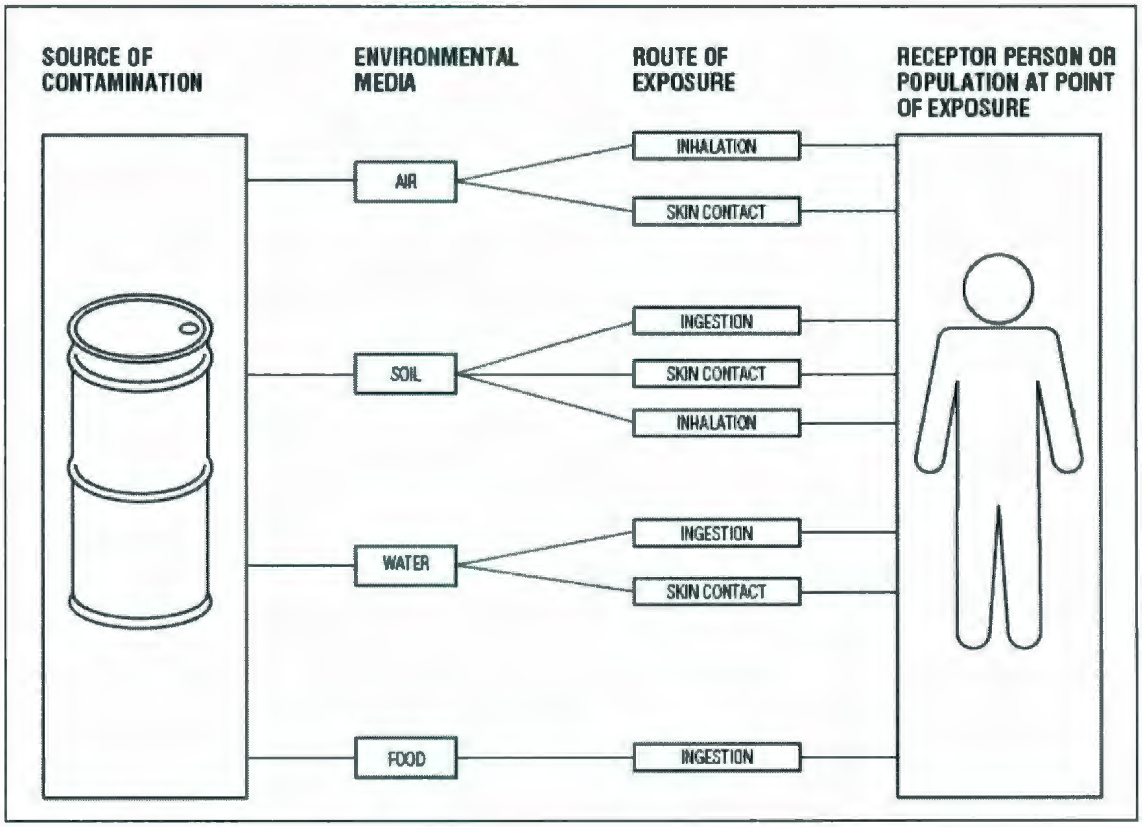

Figure 2.10. Major pathways of human exposure to environmental contaminants (Health Canada, 1995)

There are many different risk assessment approaches proposed by regulations agencies such as EPA and CCME. Most of these approaches are comprised of four steps, which are outlined below:

- ✓ Hazard identification and assessment
- ✓ Exposure assessment
- ✓ Dose-Response assessment
- ✓ Risk characterization

These four steps provide a better understanding of a system's environmental risk assessment. Thus, these steps are described in the following sections.

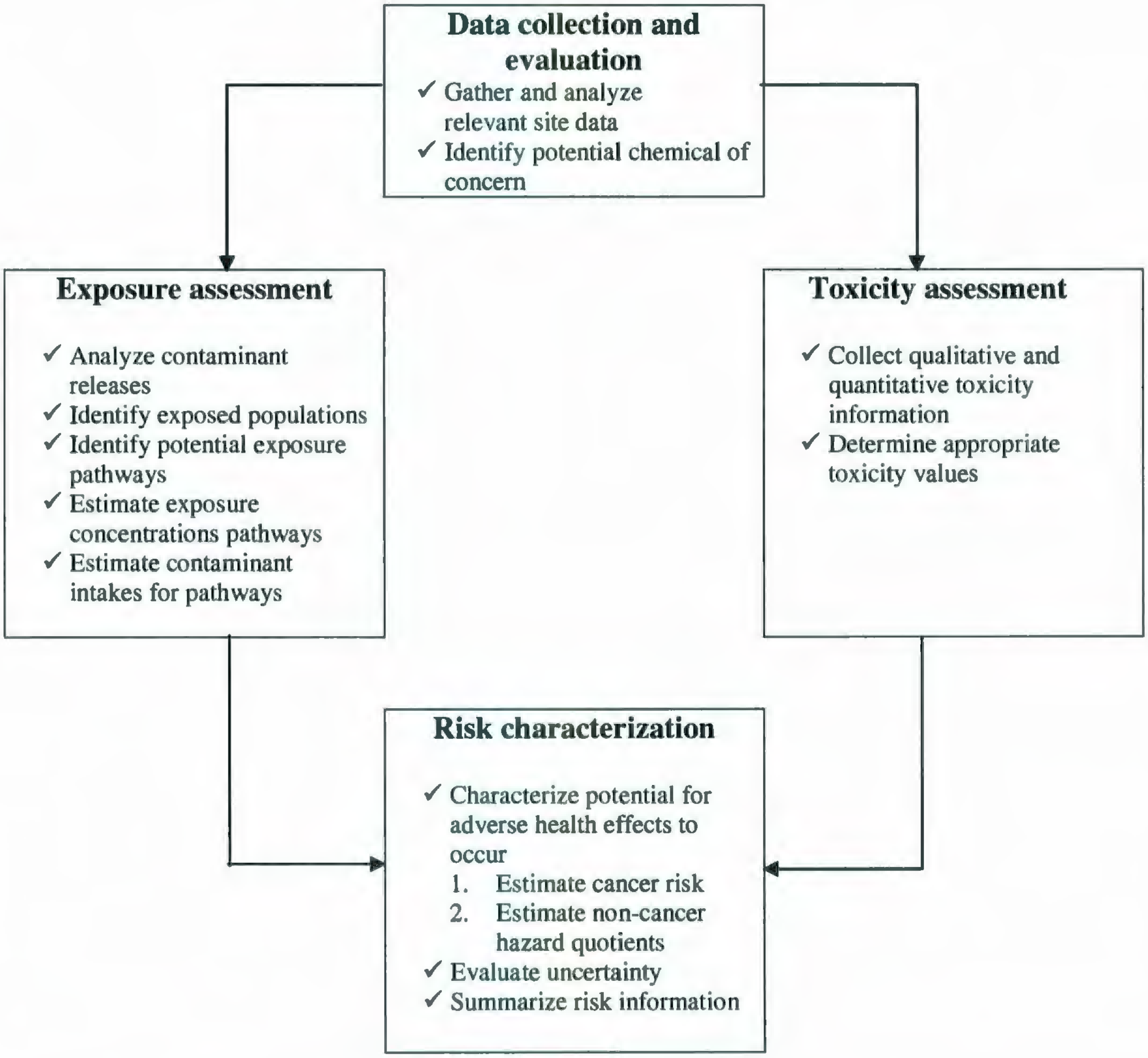

Figure 2.11. Different processes of risk assessment according to EPA (USEPA, 1999)

2.3.1 Hazard identification and assessment

The potential for chemicals to cause adverse effects on the lives of humans, plants and animals can be provided and understood by considering hazard assessment. Hazard identification is the first stage in hazard assessment (Phua et al., 2007). It includes gathering and evaluating toxicity data on the types of health impact or disease that may be produced by a chemical and the conditions under which the impact or the disease is produced. In order to identify the hazard, the data for all contaminants at a site should be examined and the data to stress the chemicals of concern should be consolidated. The following steps show the data needed in hazard identification stages (Khan, 2008):

- Site history
- Land use
- Contaminant levels in media
    - ✓ Air
    - ✓ Ground water
    - ✓ Surface water
    - ✓ Soils and sediments
- Environmental characteristics affecting chemical fate and transport
    - ✓ Geologic
    - ✓ Hydrologic
    - ✓ Atmospheric
    - ✓ Topographic
- Potentially affected population
- Potentially affected biota

Hazard assessment is most commonly used for analyzing the effects of chemicals on the natural environment. The definition of hazard is formulated by Klopffer (1994) as follows:

$$\text{Hazard} = \text{Exposure} * \text{Effect} \tag{2-20}$$

This shows that there is no hazard (bad effect) if there is no exposure. The following steps are involved in hazard assessment:

1) The contaminant data should be sorted by medium (e.g. ground water, soil, etc.) for both carcinogens and non-carcinogens.

2) The average and range of each chemical concentration observed at the site should be demonstrated.

3) The toxicity scores (TS) for each chemical in each medium due to carcinogens and non-carcinogens should be demonstrated as follows:

   For non-carcinogens: Considering exposure duration, the toxicity score is estimated as follows:

   $$TS = \frac{C_{Max}}{RFC} \tag{2-21}$$

   RFC = Chronic reference concentration (an estimate of acceptable daily intake)

   For carcinogens: $TS = SF * C_{Max}$ (2-22)

   SF = Slope factor (slope factor here is considered for daily intake (slope factor * day))

4) Ranking the compounds by toxicity scores for each exposure route.

5) For each exposure route, selecting those chemicals that compose 99 percent of the total score.

2.3.2 Exposure assessment

There has been a significant increase in awareness of environmental issues in recent years and there is a great concern among the people over how their health is affected by environmental factors. Exposure assessment includes estimating the dose or concentration of the contaminant taken in by human and ecological receptors per unit of time. Characterization of the exposure setting, identification of exposure pathways and quantification of exposure are different steps in exposure assessment.

Using the exposure assessment, the following questions can be answered:

1) Who and what is exposed (For example: people, aquatic ecosystems)?
2) How much exposure occurs?
3) How often and how long does the exposure occur and what is its frequency and duration?

Various plausible exposure pathways exist for every valued ecosystem component. Different pathways include direct contact, water ingestion, soil or sediment ingestion, and through the food chains. Indirect contact should be considered as well.

Using the fate and transport model, which is validated through field measurement, the information for input into an exposure model can be provided. Different steps for calculating exposures to chemicals present in the environment can be seen in Figure 2.12.

For calculating people's and ecological entities' expose to environmental contaminants, several assumptions need to be considered.

The average values are generally used for:

- Body weight
- Amount of food and water consumed
- Amount of air breathed, and
- Number of times people and ecological entities are exposed to contaminants over their lifetime

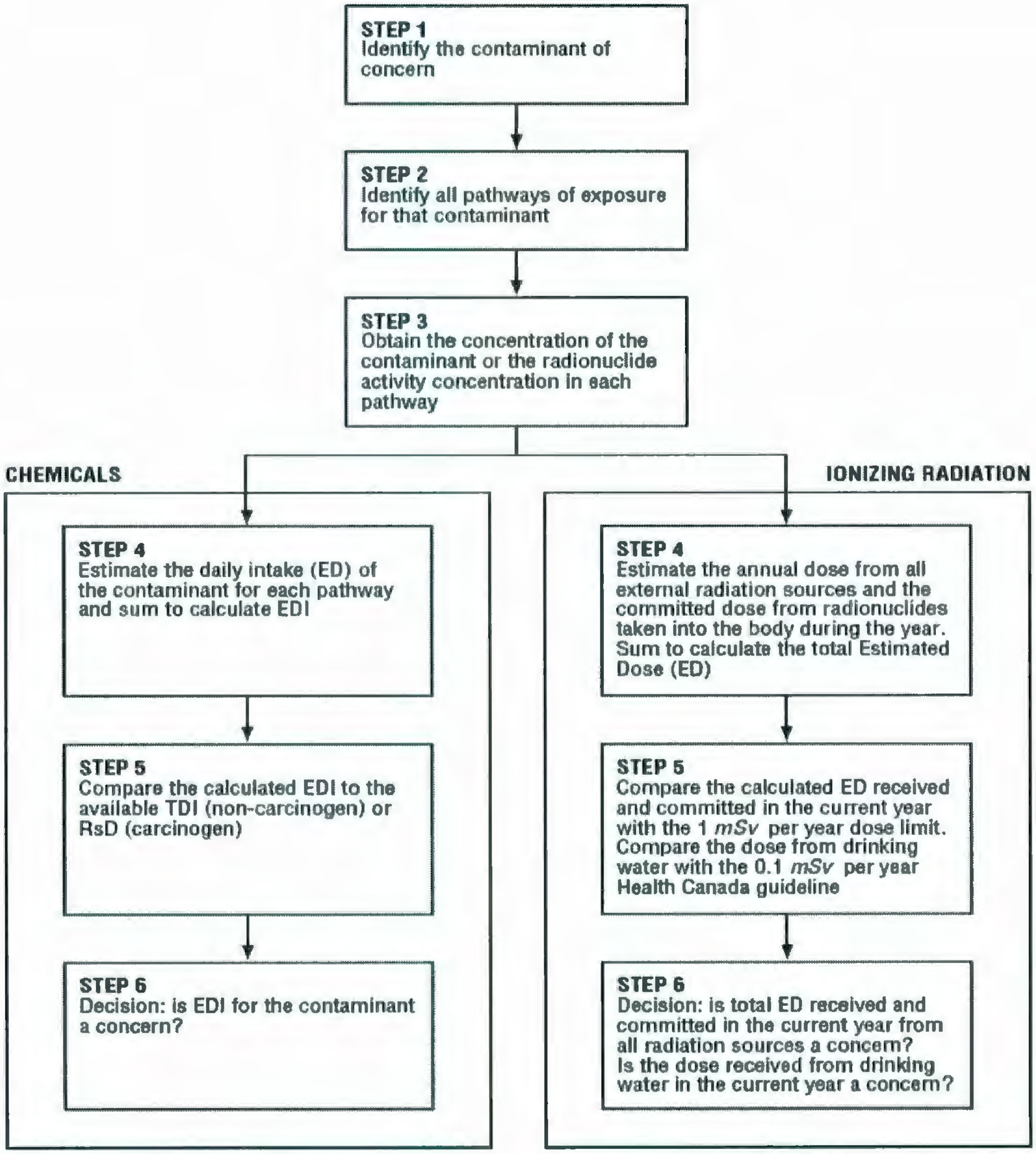

Figure 2.12. Different steps for calculating exposure to chemicals (Health Canada, 1995)

The exposure pathway describes how the contaminants go into the environment from their source to humans or other living organisms.

Exposure pathways include the following steps:

- Source of contamination
- Environmental media

- Point of exposure
- Receptor person or population; and
- Route of exposure

It is noteworthy that the source of environmental contaminants varies from place to place. It can consist of exhaust from cars, wastewater released by factories and mills, waste disposal sites or closed factories or disposal sites. Furthermore, a number of natural sources can release various substances into the environment.

When the contaminants are released from their sources, they can travel over different environmental media to reach the points where human exposures can occur. For humans, the major environmental media are water, air, food and soil. Figure 2.13 shows how contaminants are transported through the food chain and affect human health through exposure and food intake.

The point of exposure is where contact with the contaminants occurs. Different locations that people are exposed during the day and night (e.g. homes, workplaces, lakes, rivers or other bodies of water) can be the point of exposure.

The individual or population that is exposed to the contaminant at the point of exposure is the receptor. For example, people may be exposed to the contaminated air by going outside and breathing. Finally, the route of exposure is the way that the contaminant enters into the human and animal body. Ingestion, inhalation and skin contact are three general routes by which human and animals take the contaminant into their body.

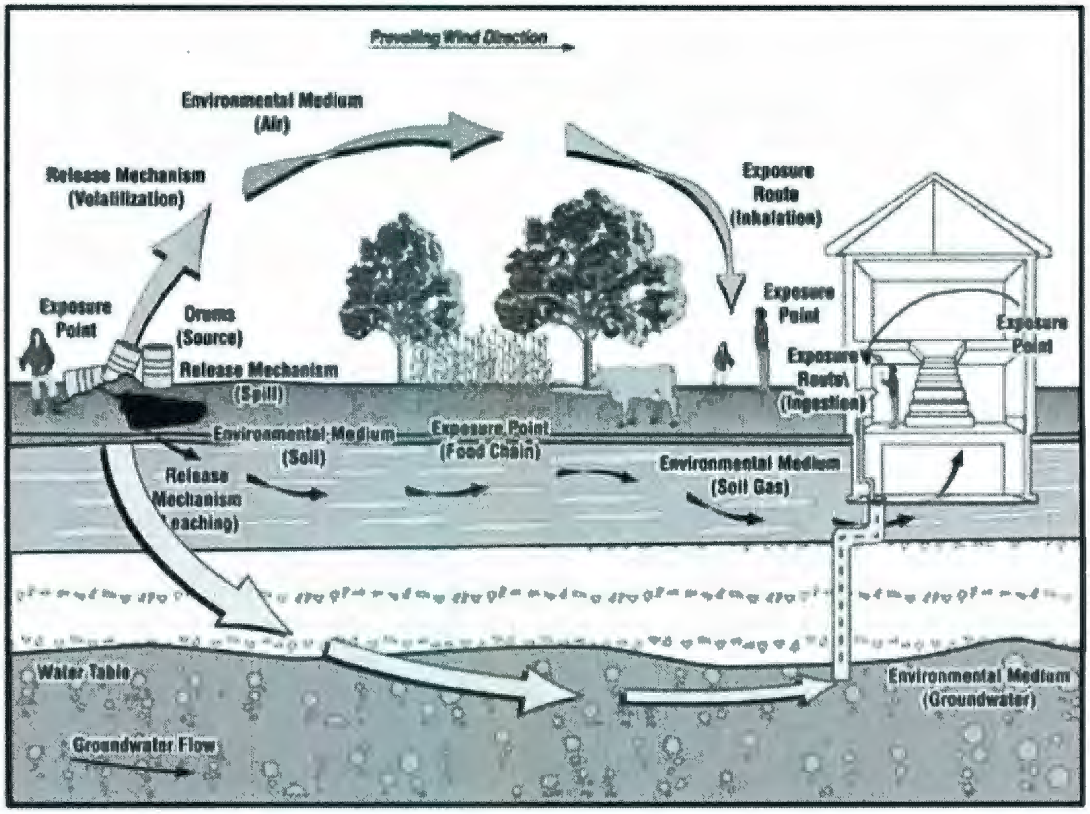

Figure 2.13. Exposure pathways schematic (ATSDR, www.atsdr.cdc.gov)

After determining the different parts of exposure pathways, the exposure factor should be calculated in each pathway of exposure.

As mentioned above, inhalation of the contaminant is one of the pathways of exposure. The amount of a contaminant absorbed into the body by inhalation can be found by the following equation:

$$ED_a = \frac{C * IR * EF}{BW} \tag{2-23}$$

C = Concentration of contaminant in the air (mg/m^3 of air)

The inhalation rate and average body weight for each person according to that person's sex and age can be seen in Table 2.6 and 2.7 (USEPA, 1997).

Table 2.6. Average body weight for each age group according to their sex (USEPA, 1997)

Model Age Group	Body Weight (kg)	
	Male	Female
0-17	34.3	33.0
18-44	78.2	64.3
45-64	79.9	68.0
65+	74.8	66.6

Table 2.7. EPA recommended inhalation values (USEPA, 1997)

Age Group (years)	Sex	Inhalation values (m^3/day)
<1	Both	4.5
1-2	Both	6.8
3-5	Both	8.3
6-8	Both	10
9-11	Male	14
	Female	13
12-14	Male	15
	Female	12
15-18	Male	17
	Female	12
19-65+	Male	11.3
	Female	15.2

Moreover, the amount of a contaminant taken into the body per food is calculated for each individual food by the following equation:

(Food group 1) (Food group 2)

$$ED_f = \frac{CF * CR * EF}{BW} + \frac{CF * CR * EF}{BW} \tag{2-24}$$

Finally, after calculating the amount of exposure for different pathways, the estimated daily intake (EDI) of a chemical can be calculated by adding these amounts of exposure. Estimated Daily Intake of a chemical should be calculated by the following equation:

$$EDI = ED_a + ED_w + ED_s + ED_f + ED_{ws} + ED_{ss} \quad (2\text{-}25)$$

2.3.3 Dose-Response assessment

Dose-Response assessment is the step of the risk assessment process that connects the likelihood and severity of damage on human health from exposures to different levels of risk agents. The quantitative relationship between the level of exposure and the intensity of the resulting adverse health effects is represented by graphs. This graph, which can be seen in Figure 2.14, shows the cumulative exposure or rate of exposure per unit of time.

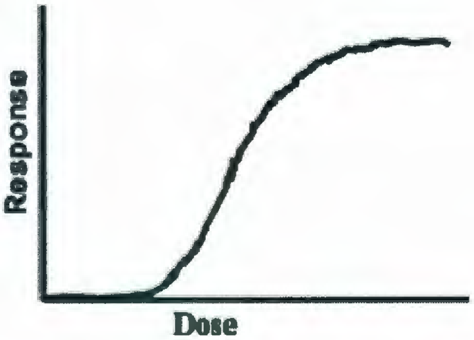

Figure 2.14. Dose-Response curve (USEPA, 1991)

The extrapolation of dose relationships from a specific population to another group or from animal studies to human beings should be conducted according to the following factors:

- ✓ Difference in physical dimensions like body weights

✓Difference in intake

✓Different life span

✓Difference in the absorption rate of chemical, nature, routes.

Regression methods can be used for finding the dose and response relationship if enough data are available. Dose-Response models can be divided into three main categories. These categories are described in the following paragraphs.

Simple Dose-Response models: These models show the single measurement of dose (e.g. cumulative exposure) to a single measure health response (e.g. number of fatalities). These models are used to estimate the number of cases of cancer caused by exposure to low level radiation. For applications of this model, dose-response relationships are usually shown by curves with thresholds.

Tolerance distribution models: These models are based on the fact that each person in the population has an individual threshold tolerance associated with the specific risk agent. In these models, it is assumed that the probability that a particular individual will experience an adverse effect when exposed at the dose level d is the same as the probability for the tolerance level of the individual less than d. The log-probit model is the most commonly used tolerance models. It is popular because the result of toxicity tests often fit the shape assumed in the model. This model is usually used for determining the dose-response of the exposure to toxic gases and estimation of infections from disease caused by organisms.

Mechanistic models: These models usually show the biological processes that lead to an adverse effect as a series of events evolving over time. Although such models can become mathematically complex, they are usually based on very simple biological assumptions. Hit, multistage, and cellular proliferation models are the most well-known in this case (Fjeld, 2006). Mathematical equations of different dose-response models can be seen in Table 2.8.

Table 2.8. Mathematical equations of several dose-response models used in cancer risk assessment (Edler et al., 1998)

Model	Equations for the probability of response (Proportion of population affected at dose d)	Parameter constraints
Probit	$F(d) = \phi(a+b \ln d)$	$b>0$
Logit	$F(d) = [1-\exp(-(a+b \ln d))]^{-1}$	$b>0$
Weibull	$F(d) = 1 - \exp(-bd^k)$	$b>0, K>0$
One hit	$P(d) = [1-\exp(-bd)]$	$b>0$
Multistage	$F(d) = [1-\exp(-\sum_{i=0}^{k} a_i d^i)]$	$a_i \geq 0$

The standard procedure for assessing non-cancer risks related to hazardous components uses a No Observed Adverse Effect Level (NOAEL) approach. NOAEL is the point in which no-effect level is observed. By applying an uncertainty factor to this point, it may be then used to estimate a dose limit for humans. This limit is below a presumed threshold and shows the acceptable exposure level. For establishing a permissible exposure levels for humans for non-carcinogens, the NOAEL is used for finding the RFD (Reference Dose) as follows:

$$\text{RFD} = \frac{NOAEL}{UF} \tag{2-26}$$

UF is the uncertainty factor, which is assumed to be 10 when relevant research based information is missing.

In a new dose-response procedure, the benchmark dose method is used instead of NOAEL. In benchmark modeling, the bench mark (BM), which is the dose related to 10% response, is evaluated. The lower bond of 95% confidence interval for this BM is called LBM (Faustman, 1996).

To determine the best model that can fit the dose and response data, EPA develops the Benchmark Dose Software (BMDS) to facilitate the application of benchmark dose (BMD) methods to the EPA hazardous pollutant risk assessment. This software helps find the Bench Mark (BM) and Lower Bond of 95% of confidence interval (LBM) associated with different doses and responses. After finding BM and LBM, the RFD is calculated as follows:

$$\mathrm{RFD} = \frac{BM, LBM}{UF} \tag{2-27}$$

A different approach is used for carcinogens which are generally assumed to have a non-threshold dose-response. A decision about these chemicals (carcinogens) must be made to determine "how large a risk of cancer can be accepted, in order to set acceptable intake levels" (Health Canada, 1995).

Different acceptable levels of risk are used around the world. These levels vary between one extra cancer death per ten thousand people and one extra cancer death per million people exposed to the contaminants over their entire lifetime.

After establishing the acceptable level of risk, a dose that people can be exposed to on a daily basis over their entire lifetime that will not exceed the accepted level of risk of cancer can be calculated. As the acceptable dose is directly related to the decision about an acceptable level of risk, it is called Risk-specific Dose (RsD). Considering each carcinogen, which has its own slope factor, the RsD is calculated as follows (Health Canada, 1995):

RsD = Acceptable level of risk / Slope factor (2-28)

2.3.4 Risk characterization

By integrating exposure assessment and toxicity assessment, which are discussed earlier, the probability of negative effects is understood. Risk characterization is carried out for individual chemicals and then summed for a mixture of chemicals (Considering that additivity is assumed). Next, the amount of these chemicals can be compared with different guidelines on chemicals concentration. These guidelines suggest different criteria by considering different chemicals and ways of exposure.

Qualitative and quotient methods are suitable for risk characterization. The judgment will be relied on using qualitative methods, such as a ranking system that shows the level of risk in terms of high, moderate or low. If there is sufficient information available about the Expected Environmental Concentration (EEC) in the most important medium or media and where there are adequate studies available in the literature to determine the toxicological benchmark, the quotient method may be used. The quotient is calculated by "taking the ratio of the EEC and a BC (Benchmark Concentration) (CCME, 1996)".

If the quotient is less than 1, it shows that the risk is slight and little or no action is required. If the quotient is near 1, it shows uncertainty in the risk estimate and additional data is required. Finally, if the quotient is more than 1, it shows that the risk is greater and regulatory action may be indicated (CCME, 1996).

CHAPTER 3[2]

Acid Mine Drainage Characterization

Abstract:

It is difficult to predict the quality of AMD due to the diversity of reactions which take place in the mine water. The composition of the mine waste are dependent on the specific mine site and the specific ambient conditions.

Methods such as optical microscopy, electron microscopy, and X-ray diffraction are sometimes used to identify minerals involved in the production of AMD. A simpler method to identify the minerals without losing accuracy would help to decrease costs. This chapter presents an overview of the important oxidation reactions of sulphide minerals and related chemical components produced by these oxidation reactions. A methodology for predicting the minerals producing AMD using MINTEQ is also discussed. This method can be used in conjunction with analytical techniques to characterize AMD for a specific site. While it does not replace analytical tests, it may decrease the number and frequency of these expensive tests. The model has been validated with data from the Wolverine coal mine in northeastern BC, Canada.

---

[2] . A part of this chapter is published and cited as:
Abbassi, R., Khan, F., Hawboldt, K. 2009. Prediction of minerals producing acid mine drainage using a computer-assisted thermodynamic chemical equilibrium model. J. mine water and the environment, 28, pp. 74-78.

3.1 Methodology for AMD characterization

AMD is a highly acidic discharge containing cadmium, cobalt, copper, iron, nickel, and other chemical species that may lead to negative impacts the environment. Due to the complexity of reactions in AMD, it is generally difficult to determine the quality of the mine water. Knowledge of different possible minerals that produce specific AMD, the oxidation reactions related to these minerals and the chemical components produced by these reactions are vital. A variety of techniques for identification and characterization of minerals, different oxidation reactions and different chemical components produced by these chemical reactions are available. Because of the complex character of these constituents, no specific technique is as a universal method for qualitative and quantitative characterization of the mineral matters. Methods such as optical microscopy, electron microscopy and X-Ray diffraction are complex, needing expert analysis and costly to work with. Prior to designing any treatment system, a method for identifying the minerals and reactions which generate AMD is required. The proposed procedure for identifying and characterizing the minerals, their oxidation reactions producing AMD and chemical components in AMD are demonstrated in the Figure 3.1. The procedure begins by measuring metal and non-metal species in the mine water. Based on the conditions experienced by the mine water, Eh-pH diagrams are used to recognize the chemical species that may be thermodynamically favored over others. In the next step, the amount of chemical species are keyed into MINTEQ to obtain the chemical components in the AMD. Finally, based on the oxidation reactions of the minerals and chemical components obtained by MINTEQ, the key minerals and reactions are identified. This procedure is explained in detail in the following sections.

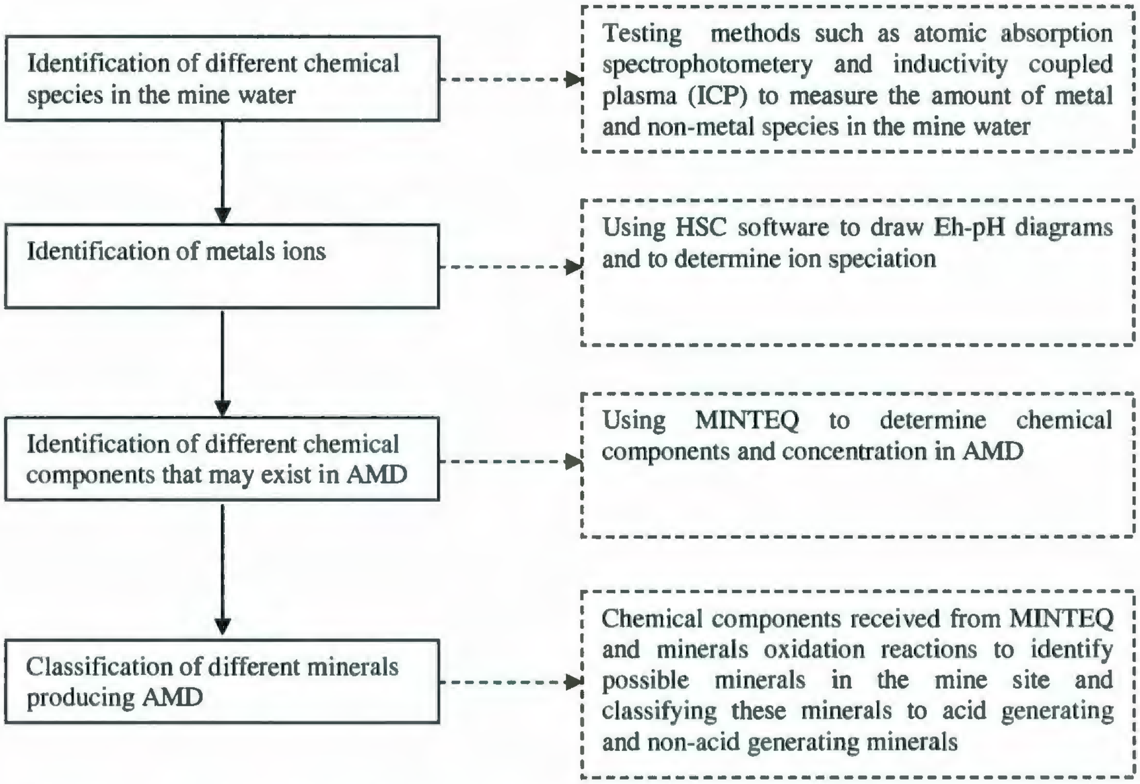

Figure 3.1. Different steps for characterization of AMD and identifying the minerals that produce AMD

3.1.1 Identification of different chemical species in the mine water

Tailings with high sulphide minerals content produce AMD. When mine water contacts with oxygen that exists through ambient air, the reactive sulphides are oxidized and generate an acidic leachate that may act as an agent carrying heavy metals and dissolved salts. As a result, different metal and non-metal species are accumulated in AMD which should be determined using different standard testing methods such as atomic absorption spectrophotometery and inductivity coupled plasma (ICP). Determining some of the characteristics of AMD (e.g. pH, temperature and alkalinity) may help to obtain the existing chemical components in AMD in a specific condition.

3.1.2 Identification of metal ions

Eh-pH diagrams are used for determining the stability areas of metal species in a solution, based on the solution's redox potential (Eh) and pH (Roine, 2002). The horizontal axis in this diagram shows pH for the log function of the H^+ ion concentration, while the vertical axis Eh is for the voltage potential with respect to the standard hydrogen electrode as calculated by the Nernst equation (Pourbaix, 1974).

$$Eh = E^0 + \frac{0.0592}{n} \log \frac{[C]^c [D]^d}{[A]^a [B]^b} \tag{3-1}$$

These diagrams visually present the oxidizing and reducing abilities of the major compounds and are applied commonly in geochemical, environmental and corrosion applications. Any point on the diagram will demonstrate the thermodynamically most stable and theoretically most abundant form of that species at a given potential and pH condition. For instance, due to the Eh-pH diagram for different iron species, at a pH of approximately 7 where the concentration of dissolved ferric iron is too low to measure, all Fe can be assumed to be present as ferrous iron (Ball et al., 2006). Finally, this will lead to selecting and entering the amount of the specific ions (based on the specific condition that the ion experience) in the next step.

3.1.3 Identification of different chemical components in AMD

After detailing different elements that exist in the tailing, different possible chemical components that are produced in AMD need to be evaluated. To this end, computer-assisted thermodynamic chemical equilibrium models are useful tools to predict the behavior of chemical system. MINTEQ is one of the chemical equilibrium models. The data required to predict the equilibrium composition consist of chemical analyses of the

AMD sample to be modeled, total dissolved concentrations for the chemical species and any other applicable invariant measurements for the mine water including pH and temperature. This will also include modeling the solubility of different chemical species according to different conditions that the AMD experiences and finding the possible components and their concentration in the AMD. By entering all of the existing aqueous species and their concentrations, specific pH, specific ionic strength and the amount of alkalinity, and running the model respectively, all of the possible chemical components that may exist in AMD can be evaluated. In the next step, the minerals producing these chemical components according to specific oxidation reactions shown in Table 3.1 are classified through different groups (acid producing or non-acid producing and acid consuming or non-acid consuming) of minerals producing AMD.

Table 3.1. Selected oxidation reactions for mine tailing with oxygen and ferric iron

Mineral	**Oxidation reactions**
(1a) Pyrite (by oxygen)	$FeS_{2\,(s)} + 3.5O_2 + H_2O \rightarrow Fe^{2+} + 2SO_4^{2-} + 2H^+$
(1b) Pyrite (by iron)	$FeS_2 + 14Fe^{3+} + 8H_2O \rightarrow 2SO_4^{-2} + 15Fe^{+2} + 16H^+$
(2a) Marcasite (by oxygen)	Same as pyrite
(2b) Marcasite (by iron)	Same as pyrite
(3a) Chalcopyrite (by oxygen)	$CuFeS_{2(S)} + 4O_{2(aq)} \rightarrow Cu^{2+} + Fe^{2+} + SO_4^{2-}$
(3b) Chalcopyrite (by iron)	$CuFeS_{2(S)} + 16Fe^{3+} + 8H_2O \rightarrow Cu^{2+} + 17Fe^{2+} + 2SO_4^{2-} + 16H^+$
(4a) Pyrrhotite (by oxygen)	$Fe_{(1-x)}\,S + (2 - 0.5x)\,O_2 + x\,H_2O \rightarrow (1-x)\,Fe^{2+} + SO_4^{2-} + 2\,xH^+$
(4b) Pyrrhotite (with iron)	$Fe_{(1-x)}S + (8-2x)\,Fe^{3+} + 2H_2O \rightarrow (9-3x)Fe^{2+} + SO_4^{2-} + 8H^+$
(5a) Arsenopyrite (with oxygen)	$FeAsS + 13/4\,O_2 + 3/2\,H_2O \rightarrow Fe^{2+} + SO_4^{2-} + H_2AsO_4^- + H^+$
(5b) Arsenopyrite (with iron)	$FeAsS_{(S)} + 14Fe^{3+} + 7H_2O \rightarrow 15Fe^{2+} + SO_4^{2-} + H_3AsO_{3(aq)} + 14H^+$
(6a) Sphalerite (with oxygen)	$ZnS_{(s)} + 2O_{2(aq)} \rightarrow Zn^{2+} + SO_4^{2-}$
(6b) Sphalerite (with iron)	$ZnS_{(S)} + 8Fe^{3+} + 4H_2O \rightarrow Zn^{2+} + SO_4^{2-} + 8Fe^{2+} + 8H^+$
(7a) Covellite (with oxygen)	$CuS_{(S)} + 2O_{2(aq)} \rightarrow Cu^{2+} + SO_4^{2-}$
(7b) Covelite (with iron)	$CuS(s) + 8Fe^{3+} + 4H_2O \rightarrow Cu^{2+} + SO_4^{2-} + 8Fe^{2+} + 8H^+$
(8a) Millerite (with oxygen)	$NiS_{(S)} + 2O_{2(aq)} \rightarrow Ni^{2+} + SO_4^{2+}$
(8b) Millerite (with iron)	$NiS(s) + 8Fe^{3+} + 4H_2O \rightarrow Ni^{2+} + SO_4^{2-} + 8Fe^{2+} + 8H^+$
(9a) Greenockite (with oxygen)	$CdS_{(S)} + 2O_{2(aq)} \rightarrow Cd^{2+} + SO_4^{2-}$
(9b) Greenockite (with iron)	$CdS(s) + 8Fe^{3+} + 4H_2O \rightarrow Cd^{2+} + SO_4^{2-} + 8Fe^{2+} + 8H^+$
(10a) Galena (with oxygen)	$PbS_{(S)} + 2O_{2(aq)} \rightarrow Pb^{2+} + SO_4^{2-}$
(10b) Galena (with iron)	$PbS_{(S)} + 8Fe^{3+} + 4H_2O \rightarrow Pb^{2+} + SO_4^{2-} + 8Fe^{2+} + 8H^+$

3.1.4 Classification of different minerals producing AMD

In this step the possible minerals and different reactions related to oxidation of minerals are predicted. These minerals can be classified as acid producing and non-acid producing. Classification helps to determine the oxidizing process of each class according to the multiplicity of this process for each individual component.

3.2 Application of AMD characterization of Wolverine coal mine: A Case study

To verify the proposed methodology, a case study based on the Wolverine (Perry Creek) coal mine located 23km west of Tumbler Ridge in northeastern BC, Canada, (Yukon zinc corporation, 2005) is selected. The water quality at this mine site during operation is shown in the Table 3.2.

Table 3.2. Wolverine AMD parameters and dissolved metals

Parameters		Parameters		Parameters		Parameters	
Cond. (uS/cm)	1860	Thiosalts	452	Cr	0.00125	P	0.08
pH	7.4	Ag	0.0113	Cu	0.0267	Pb	0.0166
TDS	1510	Al	0.07	Fe	0.03	Sb	0.0216
TSS	31	As	0.012	Hg	0.000075	Se	1.825
*. Acidity	365	Ba	0.3485	K	10	Si	0.35
*. Alkalinity	37	Be	0.0038	Li	0.0038	Sn	0.007
*. Hardness	452	B	0.019	Mg	4.97	Sr	0.293
F	0.25	Bi	0.00023	Mn	0.0165	Ti	0.0023
Cl	19	Ca	175	Mo	0.03015	Tl	0.0056
NO_3	0.22	Cd	0.002	Na	201	U	0.0003
SO_4	605	Co	0.0008	Ni	0.014	V	0.0005
CN(T)	0.02	CNO	1.85	CNS	3.7	Zn	0.024

*. The unit of acidity, alkalinity and hardness is mg/l as $CaCO_3$

*. The unit of dissolved metals is mg/l

Treating effluent AMD before releasing to the environment is necessary. Determination of the minerals that produce the specific AMD and different chemical components is required to assign a treatment system.

In this step, the HSC software is used to create Eh-pH diagrams in the specific AMD. The pH of the Wolverine mine water is 7.4 and used in the modeling step (modeling different possible species with MINTEQ). As an example, this Eh-pH diagram for iron is illustrated in Figure 3.2.

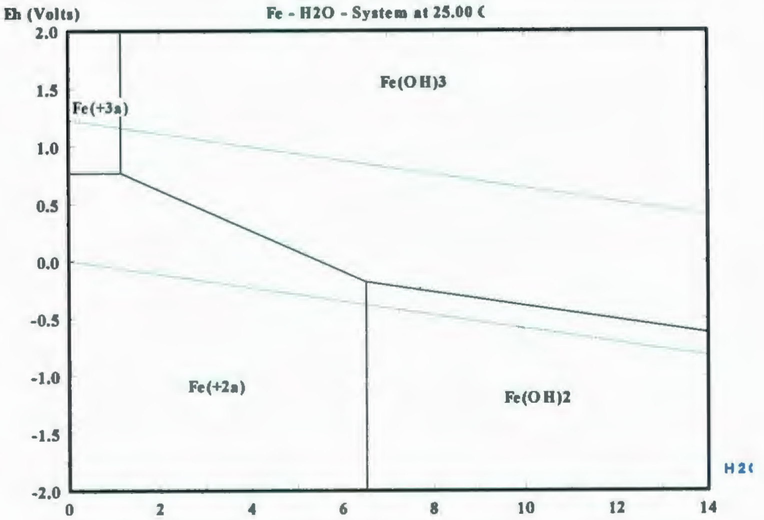

Figure 3.2. Eh-pH diagram for Fe (iron) at 25 ° C

MINTEQ (Version 2.52) is used to model the possible components that exist in Wolverine mine water. The amount of metal and non-metal species that are related to the chemistry of the Wolverine AMD demonstrated in Table 3.2 are entered in the MINTEQ program.

For verification of the chemical components produced by MINTEQ, these chemical components are compared with typical chemical components that are found by oxidation of minerals in different coal AMD. These typical minerals for Wolverine coal mine may be seen in Table 3.3.

The minerals in the mine site can be divided into two groups of acid and non-acid forming sulfide minerals. Hill (1977) explained that most coal bodies are associated with sulphides and/or sulphosalts. Pyrite, pyrrhotite, chalcopyrite, marcasite and sphalerite are the main acid forming minerals in the coal mines. The acidity in AMD stems principally from the formation of free sulphuric acid and hydrolysis of the oxidation products (iron sulphates) of pyrite.

Ferrihydrite ($Fe(OH)_3$) produced in these oxidation processes would not be stable at very low pH, but it is more stable at a pH approximately 8. The existence of $Fe(OH)_3$ amongst the mineral components that are revealed by MINTEQ indicates pyrite in this specific AMD. Moreover, pyrrhotite is an abundant sulfide mineral found in some coal mine environments. The oxidation of pyrrhotite produces $Fe(OH)_3$ and acidity as well. Arsenopyrite is also expected to yield acid according to reactions 5a and 5b in Table 3.1. The existence of AsO_4^{3-} in the output of MINTEQ for this mine site indicates arsenopyrite in the mine site. Acid generation occurs via chalcopyrite oxidation according to reaction 3b in Table 3.1 through the oxidation according to ferric iron path. The $Cu(OH)_2$ exists in AMD at Wolverine coal mine and this may be caused by the oxidation of chalcopyrite. Finally, sphalerite is an acid generating sulfide mineral with an indefinite composition ((Zn, Fe)S). The oxidation of sphalerite may produce acidity due to reaction 6b in Table 3.1. The existence of $Zn(OH)_2$ indicates sphalerite in Wolverine coal mine.

Table 3.3. Minerals identified in Wolverine coal mine

Chemical components	Chemical formula	Acid producing condition
Pyrite	FeS_2	Acid forming sulfide
Pyrrhotite	$Fe_{0.95}S$	Acid forming sulfide
Arsenopyrite	FeAsS	Acid forming sulfide
Sphalerite	ZnS	Acid forming sulfide
Chalcopyrite	$CuFeS_2$	Acid forming sulfide
Chalcocite	Cu_2S	Non-Acid forming sulfide
Galena	PbS	Non-Acid forming sulfide

Some minerals such as chalcocite and galena, which are the usual mineral components in the coal mine, oxidize but do not produce acidity. As an example, the direct oxidation of chalcocite with oxygen does not produce acidity. The existence of $CuSO_4$ can be seen in the output of MINTEQ for this mine water and this can verify the existence of chalcocite in this coal mine. Finally, galena is another sulfide mineral that does not generate acidity and the existence of $PbSO_4$ can be identified in Wolverine AMD. The direct oxidation process of galena led to produce $PbSO_4$ is shown in reaction 10a in Table 3.1. Due to the output of MINTEQ and evaluation of the minerals that exist in the coal mine, the existence of $PbSO_4$ can demonstrate the availability of galena in this mine site.

Summary

AMD may lead to severe environmental problems to adversely affect humans and ecosystems. Predicting the minerals produced AMD, the oxidation reaction of these minerals and the chemical components produced is required prior to selection of specific treatment system. Samples from the mine site are typically tested using methods such as optical microscopy, electron microscopy and X-ray diffraction which are generally costly and complex. A procedure is proposed to identify the chemical components produced in AMD and used to back out the minerals producing these chemical components. In this method, samples from AMD are analyzed and Eh-pH diagrams are used to characterize the specific AMD. Chemical equilibrium models are used then to model the possible chemical components in AMD. By evaluating the chemical components produced by MINTEQ, and going through oxidation processes of these minerals, the minerals having the potential to produce acidity for any specific mine site may be identified. This prediction can be used in conjunction with analytical analysis to optimizing design criteria for treatment. It should be noted this method does not replace analysis but rather supplements it.

CHAPTER 4[3]

Stabilization Pond Modeling

Abstract:

WSP is one of the simple and cost effective methods of treating AMD. The design of the WSP is based on many assumptions, one of which is that the pond is well mixed. That implies that there are no concentration gradients within the pond or the pond may be modeled as a CSTR. However, due to the heterogeneity of the constituents of the wastewater, concentration gradient, temperature gradient, and wind shear, the CSTR assumption is an oversimplification. In reality there are concentration, wind shear, and temperature stratification within the pond, significantly impacting the flow pattern within the system as outlined in chapter 2.

In this chapter, the non-ideal dispersed flow model is used to model the concentration gradient within the pond. A methodology using CFD to determine the main parameters of the model (retention time and dispersion coefficient) based on hydraulic behavior of the basin is also discussed in this chapter. This model is then validated using two case studies.

---

[3] Part of this chapter is submitting to be published and has been presented in the following paper and conferences:
Abbassi, R., Khan, F., Hawboldt, K. 2010. A methodology of finding dispersion coefficient using Computational Fluid Dynamics (CFDs). Journal of environmental sciences, Under process.
Abbassi, R., Khan, F., Hawboldt, K. 2009. Risk based tailing pond water management strategies considering non-idealities in tailing pond modeling. EWRI Conference, Bangkok, Thailand.
Abbassi, R., Khan, F., Hawboldt, K. 2009. Characterization of parameters effect on hydraulic flow pattern of waste stabilization pond. CSCE Conference, St.John's, NL, Canada.

4.1 Dispersion model

In reality, the flow in the reactors is rarely ideal and the assumptions of ideal CSTRs and PFRs may not exist. Most of the ponds, which do not have mechanical mixing, are not able to achieve a completely mixed state and therefore do not satisfy the conditions. Therefore, the dispersion model is suitable to cover these non-idealities. This model may be used in both steady state as well as transient conditions. Furthermore, if the reactions reach equilibrium quickly, the reaction term, can be eliminated. In the following section, the steady state dispersed flow model is solved using Wilhelm-Wehner boundary conditions (Wehner et al., 1956).

4.1.1 Steady-state condition of dispersion model

Considering the mass balance equation for component A (an element selected within the pond volume as shown in Figure 4.1), the advective-diffusive equation may be written as (Clark, 1996):

$$\frac{\partial \rho_A}{\partial t}\Delta x\Delta y\Delta z = (n_{A,x} - n_{A,x+\Delta x})\Delta y\Delta z - (n_{A,y} - n_{A,y+\Delta y})\Delta z\Delta x - (n_{A,Z} - n_{A,Z+\Delta Z})\Delta y\Delta x + r_A\Delta x\Delta y\Delta z \qquad (4\text{-}1)$$

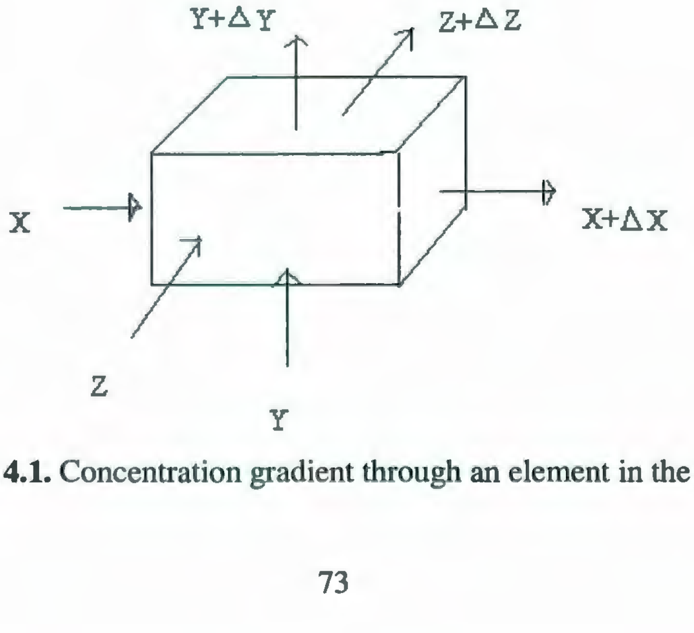

Figure 4.1. Concentration gradient through an element in the pond

If each term of equation 4-1 is divided by $\Delta x \Delta y \Delta z$, equation 4-2 will be received as following:

$$\frac{\partial \rho_A}{\partial t} = \frac{n_{A,x} - n_{A,x+\Delta x}}{\Delta x} + \frac{n_{A,y} - n_{A,y+\Delta y}}{\Delta y} + \frac{n_{A,z} - n_{A,z+\Delta z}}{\Delta z} + r_A \tag{4-2}$$

$$\frac{\partial \rho_A}{\partial t} + \nabla n_A = r_A \tag{4-3}$$

In this equation,

$$n_A = \rho_A \mathrm{u} - \rho_A \mathrm{D_{AB}} \nabla \omega_A \tag{4-4}$$

The equation 4-4 is derived using Fick's first law and general diffusion transport (Amiri, 2003). By substitution of equation 4-4 in to equation 4-3:

$$\frac{\partial \rho_A}{\partial t} + \nabla(\rho_A \mathrm{u} - \rho_A \mathrm{D_{AB}} \nabla \omega_A) = r_A$$

$$\frac{\partial \rho_A}{\partial t} + \rho_A \nabla \mathrm{u} + \mathrm{u} \nabla \rho_A = \mathrm{r_A} + \nabla(\rho \mathrm{D_{AB}} \nabla \omega_A) \tag{4-5}$$

Assuming ρ_A as a constant (incompressible fluid):

$$\frac{\partial \rho_A}{\partial t} = -\nabla(\rho_A \mathrm{u}) \tag{4-6}$$

$$\frac{\partial \rho_A}{\partial t} + \rho_A \nabla \mathrm{u} + \mathrm{u} \nabla \rho_A = 0 \tag{4-7}$$

The differential form of the continuity equation may be written as:

$$\nabla \mathrm{u} = 0 \tag{4-8}$$

Substituting equation 4-8 in to equation 4-5 will lead to the following result:

$$\frac{\partial \rho_A}{\partial t} + \mathrm{u} \nabla \rho_A = r_A + \mathrm{D_{AB}} \nabla^2 \rho_A \tag{4-9}$$

Dividing each term of equation 4-9 by the molar mass of the component:

$$\frac{\partial C_A}{\partial t} + \mathrm{u}\nabla C_A = \mathrm{D_{AB}}\nabla^2 C_A + R_A \tag{4-10}$$

$$\frac{\partial C_A}{\partial t} + (\mathrm{u_x}\frac{\partial C_A}{\partial x} + \mathrm{u_y}\frac{\partial C_A}{\partial y} + \mathrm{u_z}\frac{\partial C_A}{\partial z}) = D_{AB}(\frac{\partial^2 C_A}{\partial x^2} + \frac{\partial^2 C_A}{\partial y^2} + \frac{\partial^2 C_A}{\partial z^2}) + R_A \tag{4-11}$$

In steady state condition where $\frac{\partial C_A}{\partial t} = 0$, a one dimensional form of the dispersion equation may be written as:

$$\mathrm{u}\,\frac{\partial C_A}{\partial z} = \mathrm{D_{AB}}\,\frac{\partial^2 C_A}{\partial z^2} + R_A \tag{4-12}$$

$$\mathrm{D_{AB}}\,\frac{\partial^2 C_A}{\partial z^2} - \mathrm{u}\,\frac{\partial C_A}{\partial z} + R_A = 0 \tag{4-13}$$

If equation 4-13 is then divided by the term u*l and it is assumed that the component A is consumed through the reaction (not produced) and the first order reaction rate exist:

$$\frac{D_{AB}}{ul}\frac{\partial^2 C_A}{\partial z^2} - \frac{u}{ul}\frac{\partial C_A}{\partial z} - \frac{KC_A}{ul} = 0 \tag{4-14}$$

Assuming ul/D_{AB} is equal to Pe (Peclet number), the following equation will be obtained:

$$\frac{1}{Pe}\frac{\partial^2 C_A}{\partial z^2} - \frac{\partial C_A}{\partial z} - RC_A = 0 \tag{4-15}$$

Equation 4-15 is the dispersion equation in dimensionless form for first order reaction (Wehner et al., 1956). The dispersion equation which is the ordinary second orders differential equation in dimensionless form may be seen below:

$$\frac{1}{Pe}\frac{\partial^2 f(z)}{\partial z^2} - \frac{\partial f(z)}{\partial z} - Rf(z) = 0 \tag{4-16}$$

The following divisions are considered in the modeling scenario:

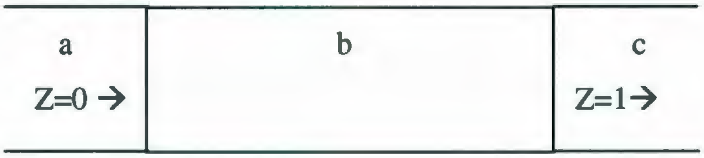

Figure 4.2. Boundary used in dispersion model

Before $Z \leq 0$ and after $Z \geq 1$, no reaction occurs.

$$\frac{1}{Pe_a}\frac{\partial^2 f(z)}{\partial z^2} - \frac{\partial f(z)}{\partial z} = 0 \qquad Z \leq 0 \qquad \text{(i)}$$

$$\frac{1}{Pe_b}\frac{\partial^2 f(z)}{\partial z^2} - \frac{\partial f(z)}{\partial z} - Rf(z) = 0 \qquad 0 \leq Z \leq 1 \qquad \text{(ii)}$$

$$\frac{1}{Pe_c}\frac{\partial^2 f(z)}{\partial z^2} - \frac{\partial f(z)}{\partial z} = 0 \qquad Z \geq 1 \qquad \text{(iii)}$$

Equations 4-17 to 4-22 are six boundary conditions used for solving equations i, ii and iii.

$$f(0^-) - \frac{1}{Pe_a}\frac{\partial f}{\partial z}(0^-) = f(0^+) - \frac{1}{Pe_b}\frac{\partial f}{\partial z}(0^+) \qquad (4\text{-}17)$$

$$f(0^-) = f(0^+) \qquad (4\text{-}18)$$

$$f(1^-) - \frac{1}{Pe_b}\frac{\partial f}{\partial z}(1^-) = f(1^+) - \frac{1}{Pe_c}\frac{\partial f}{\partial z}(1^+) \qquad (4\text{-}19)$$

$$f(1^-) = f(1^+) \qquad (4\text{-}20)$$

$f(\infty)$ is finite (4-21)

$$f(-\infty) = 1 \qquad (4\text{-}22)$$

These boundary conditions are used for solving the following equations:

$$f(z) = N_1 + N_2 \exp(Pe_a z) \qquad Z \leq 0 \qquad (4\text{-}23)$$

$$f\,(\mathrm{z}) = N_3 \exp \frac{Pe_b}{2}(1+a)z + N_4 \exp \frac{Pe_b}{2}(1-a)z \qquad 0 \le Z \le 1 \tag{4-24}$$

$$f\,(\mathrm{z}) = N_5 + N_6 \exp(Pe_c z) \qquad Z \ge 1 \tag{4-25}$$

It may be seen in equation 4-23, 4-24 and 4-25 that six constant values exist in these equations and six boundary conditions are available, that are equations 4-17 to 4-22. Solving the equations 4-23 to 4-25 using the boundary conditions 4-17 to 4-22, will lead to the following results:

$$0 \le Z \le 1 \rightarrow f = g_0 \exp\left(\frac{Pe_b z}{2}\right)\left\{(1+a)\exp\left(\frac{aPe_b(1-z)}{2}\right) - (1-a)\exp\left(\frac{a_n Pe_b(z-1)}{2}\right)\right\} \tag{4-26}$$

In which, $a = \sqrt{1+\frac{4R}{Pe_b}} = \sqrt{1+\frac{4\frac{KL}{u}}{\frac{Lu}{D}}} = \sqrt{1+\frac{4KLD}{Lu^2}} = \sqrt{1+4Kdt}$ (where $d = \frac{D}{uL}$)

And $$g_0 = \frac{2}{(1+a)^2 \exp(\frac{aPe_b}{2}) - (1-a)^2 \exp(-\frac{aPe_b}{2})}$$

Another way to write equation 4-26 is:

$$\frac{C}{C_0} = \frac{4a\exp(\frac{1}{2d})}{(1+a)^2 \exp(\frac{a}{2d}) - (1-a)^2 \exp(\frac{-a}{2d})} \qquad \text{which a} = \sqrt{1+4Kdt} \tag{4-27}$$

$$\frac{C}{C_0} = \frac{4a\exp(\frac{Pe}{2})}{(1+a)^2 \exp(\frac{aPe}{2}) - (1-a)^2 \exp(\frac{-aPe}{2})} \tag{4-28}$$

4.1.2 Transient condition of dispersion model

All of the equations mentioned above are in steady state. Considering time parameter in the dispersed flow equation will result in transient form of the dispersion equation.

The transient one dimensional dispersed flow model is (Nameche et al., 1998; Garcia et al., 2005):

$$\frac{dc}{dt} + U\ \frac{dc}{dz} - \mathrm{D}\ \frac{d^2c}{dz^2} = 0 \qquad (4\text{-}29)$$

Solving equation 4-29 leads to a Gaussian concentration distribution:

$$C(z,t) = \frac{M}{A * \sqrt{4\pi * D * t}}\ \exp\left[\frac{-(z - U * t)^2}{4 * D * t}\right] \qquad (4\text{-}30)$$

Equation 4-30, similar to other equations written for steady state condition, is dependent on the dispersion coefficient (or Peclet number).

4.2 Determination of dispersion model parameters

Researchers (Arceivala, 1981 Polprasert et al., 1985; Chien et al., 1995) have concluded the dispersed flow model predicts the transport of contaminants more reliably than the CSTR or PFR models. This model is a strong function of retention time and dispersion coefficient, which in turn depend on the hydraulic regime of the basin. The following sections will describe the specific parameters which affect these two factors (retention time & dispersion coefficient). Furthermore, the methods for finding these two factors are also discussed.

4.2.1 Actual retention time of the stabilization pond

The treatment efficiency of the basin is directly correlated to its hydraulic regime. A poor hydraulic design of the pond reduces its treatment efficiency (Shilton et al., 2003; 2006). The hydraulic performance of the ponds is a function of the pond geometry, the location of inlet and outlet, the inlet flow velocity, etc. (Piondexter et al., 1981; Thackston et al., 1987; Marecos et al., 1987; Muttamara et al., 1997; Salter et al., 1999; Torres et al., 1999; Brissaud et al., 2000; Shilton et al., 2003; Aldana et al., 2005; Abbas et al., 2006; Agunwamba, 2006; Fyfe et al., 2007). Poor hydraulic design may cause some parcels of water to exit earlier or later than their optimal residence time or short circuiting and dead regions within the pond.

Typically drogue and tracer studies are performed to determine ponds hydraulic parameters (Marecos et al., 1987; Moreno, 1990; Pedahzur et al., 1993; Salter, 1999; Brissaud et al., 2000; Vorkas et al., 2000). Although useful, these tests are costly and time consuming. As a result, a tool for predicting the hydraulic pattern of the basins and actual retention time could be used to tailor any subsequent tracer studies and supplement any tracer data collected.

Various researchers (Baleo et al., 2001; Shilton, 2001) have used CFD software to model the hydraulic behavior of the basins. It is important to know that most of them are not validated using actual experimental data. The results of CFD software give an indication of the hydraulic behavior of the ponds and make an assumed calculation of the actual retention time.

A final method is to use the empirical approaches to show the relation of actual retention time and theoretical retention time based on hydraulic parameters of the pond such as pond's geometry or inlet/outlet positions.

Pond geometry is one of the important factors that affect the hydraulic performance of the basin (Marecos et al., 1987; Torres et al., 1999). It is proposed by researchers that the L/W ratio is the most important factor in the design of the basins (Poindexter et al., 1981). The relation between hydraulic efficiency (the ratio of actual retention time to theoretical retention time) and L/W is outlined in the following equation (Thackston et al., 1987):

$$\frac{t}{T} = 0.84\left[1 - \exp(-0.59\frac{L}{W})\right] \tag{4-31}$$

This equation shows that L/W has great influence on the hydraulic efficiency of the WSP. The deviation of hydraulic efficiency of the ponds relative to different L/W ratio may be seen in Figure 4.3.

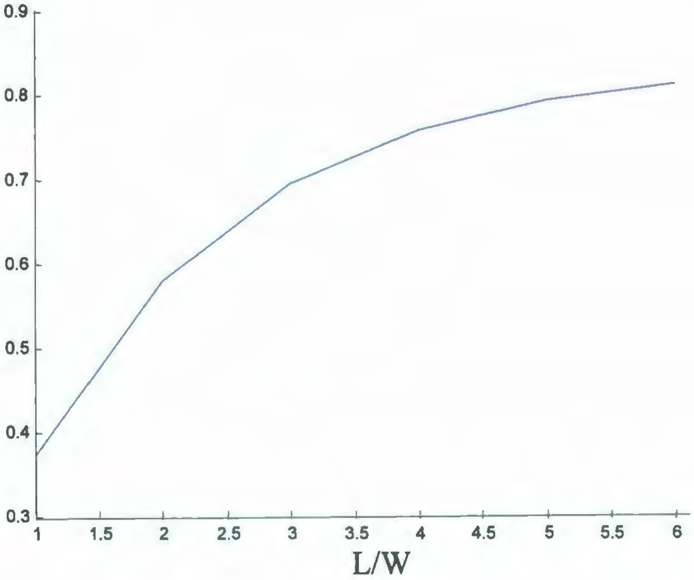

Figure 4.3. Relationship between the effective volume ratio (e) and length to width ratio (Thackston et al., 1987)

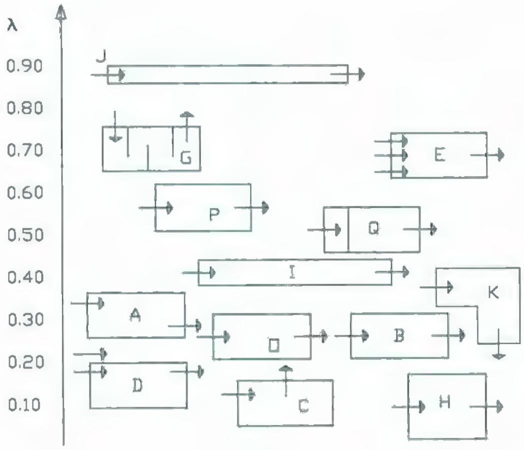

Figure 4.4. Hydraulic efficiency of the ponds based on different geometries and inlet-outlet positions (Persson et al., 2003)

The hydraulic efficiency related to different geometries of the ponds and inlet/outlet configurations is indicated in Figure 4.4 (Persson et al., 2003). This figure shows that the pond with higher length to width ratio (e.g. Pond J) has better hydraulic efficiency in comparison with the others. Abbas et al. (2006) proposed designing the pond with a L/W ratio of 4.

The placement of inlet and outlet impacts the hydraulic efficiency of WSP and the retention time respectively. Wastewater can be discharged at the surface, mid depth, and bottom of ponds. The position of the outlet may also be diverse in the variety of different ponds. The effect of inlet and outlet places on short circuiting was evaluated by Agunwamba (2006). Different inlet/outlet positions showed that short circuiting is highly related to the location of inlet/outlet. Minimum hydraulic efficiency occurs when the inlet and outlet are in front of one another and improves significantly if the inlet and outlet are positioned on the opposite corners of the pond (Persson et al., 2003). The presence of baffles in the pond reduces short circuiting. When baffles are present, shifting the outlet toward the baffles may reduce short circuiting (Safieddine, 2007).

Inflow jet is one of the factors that produces short circuiting within a pond depending on the conditions of the high inlet flow velocity (Fyfe et al., 2007). The influence of the inflow jet reduced as the flow heads to the outlet.

In order to predict the transport of contaminants within the pond accurately, actual retention time of the pond is critical. As tracer studies are costly and time consuming, using a CFD or empirical equations to determine the actual retention time is an alternative option. However, CFD accuracy is only as good as input data; therefore, predictions must be scrutinized carefully.

4.2.2 Dispersion coefficient

The molecular diffusion is described by the Fick's law. According to Fick's law, the dispersion of a tracer (C) may be described by the following equation:

$$\frac{\partial C}{\partial t} = D\frac{\partial^2 C}{\partial^2 x} \tag{4-32}$$

In this equation, D is the axial dispersion coefficient and indicates degree of back-mixing and may be experimentally derived from the results of a tracer study. In actual fact, the dispersion coefficient is a function of the numerous physical parameters that can affect fluid movement in a pond:

- Flow rate and its variation over time
- Inlet size and position
- Outlet position and design
- Wind shear and its variation over time
- Pond geometry (including influences of baffles)
- Temperature/density effects

For designing of new ponds, an accurate method of predicting the dispersion coefficient has been sought in a number of research studies. These methods are described in the following paragraphs.

4.2.2.1 Tracer tests

Tracer tests are widely used for tracking the flow motion in the basins. Finding the hydraulic pattern and dispersion coefficient of the WSP using tracer studies have been evaluated by many researchers (Marecos et al., 1987; Moreno, 1990; Uluatam et al., 1992; Pedahzur et al., 1993; Frederick et al., 1996; Wood, 1997; Salter, 1999; Shilton et al., 2000;

Vorkas et al., 2000). The tracer study is carried out by injection of a tracer in the basins using various techniques such as random, cyclic, step input or pulse input injection. These techniques are displayed in Figure 4.5.

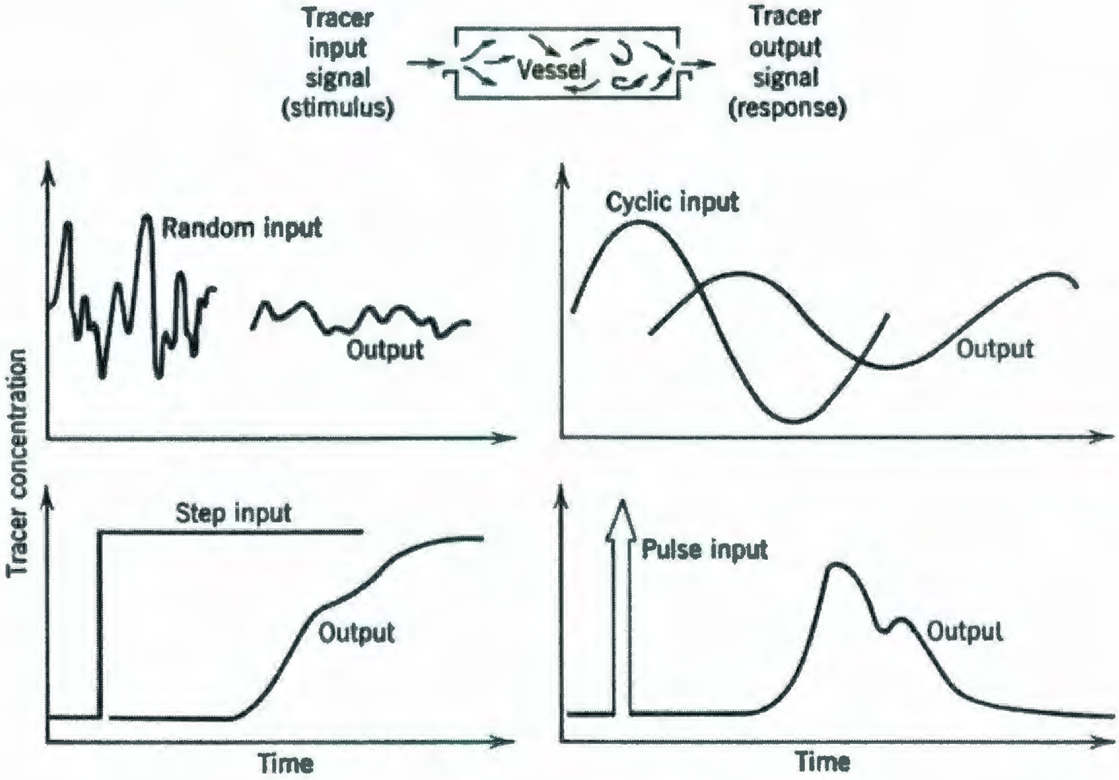

Figure 4.5. Tracer methods (Levenspiel, 1972)

The pulse input is the simplest method where a slug of the tracer enters to the basins and the tracer concentration in the effluent of the basin is measured over time. The amount of the tracer in the effluent in different time step is plotted, known as hydraulic retention time distribution (RTD) curve. An important specification of this curve is the time that the tracer input to the basin (t = 0), until the time that the first tracer is measured leaving the outlet. For CSTR, this time is instantaneous, and for the PFR, this time is the theoretical retention time. But, for the non-ideal flow, this time is something between these two ideal reactors. If the time interval between tracer release within the basin and the first response measured at the outlet is too short, the basin will have significant short circuiting.

It should be noted that tracer tests are costly in time and finances. It also can not be used predicatively for ponds that are to be constructed in the future.

4.2.2.2 Empirical equations for finding dispersion coefficient

Different types of empirical equations are currently being used for predicting the axial dispersion coefficient. The simplest proposed by Arceivala (1981) is based on the pond width. Polprasert et al. (1985) developed an empirical equation based on the pond geometry and retention time. Other researchers used an empirical formula based on the pond geometry and retention time, but with different correlation factors (e.g. Fisher, 1967; Liu 1977). Agunwamba et al. (1992), have stated that the shear stress of the wind also affects the hydraulic behavior of the basin and axial dispersion coefficient.

Nameche et al. (1998) evaluated the number of empirical equations used for predicting the dispersion coefficient. The results of these empirical equations were compared with the actual tracer tests data for more than thirty different basins. Linear and multi-linear regressions were used to develop the empirical equation for predicting the dispersion coefficient.

Empirical equations reduce the cost of actual tracer studies and may be a suitable option for predicting the dispersion coefficient in non-ideal dispersed flow model. The empirical equations, unlike actual tracer studies may solve the problem of predicting the dispersion coefficient for the basins to be constructed in the future.

Table 4.1. Empirical equations for determining the Peclet number (UL/D)

Name	**Condition**	**Formula**
Fisher (1967)	Streams and river	$\frac{1}{Pe} = \frac{0.304 * (w+2z)^{1.5} * \sqrt{\tau.v.w}}{(Lz)^{1.5}}$
Liu (1977)	Large width to depth ratio	$\frac{1}{Pe} = \frac{0.168 * (\tau.v)^{.25} * (W+2Z)^{3.25}}{(LWZ)^{1.25}}$
Polprasert et al., (1985)	Waste stabilization pond	$\frac{1}{Pe} = \frac{0.184 * [\tau.v(W+2Z)]^{0.489} W^{1.511}}{(LZ)^{1.489}}$
Arceivala (1981)	For pond width greater than 30 m	$D = 16.7 W$
Arceivala (1981)	For pond width less than 30 m	$D = 2W^2$
Murphy et al., (1974)	The volume over 300000 m3	$1/Pe = K\tau/L^2$
Nameche et al. (1998)	Stabilization pond and lagoon	$Pe = 0.1(\frac{L}{W}) + 0.01(\frac{L}{Z})$
Agunwamba et al. (1992)	Stabilization pond	$d = 0.102(\frac{u^*}{u})^{-0.8196} (\frac{H}{L}) (\frac{H}{W})^{-(0.981+1.385\frac{H}{W})}$

4.2.2.3 CFD approaches

Using CFD program is another option to find the dispersion coefficient (D). These programs have the ability to model the various conditions that the pond experiences. For the basins that have not been constructed yet, these models give the designer the ability to compare different geometries and find the optimum one according to the surrounding environmental conditions. The parameters affecting the dispersion coefficient, such as different flow rate and its variation over time, the inlet size and position and the wall shear stresses may be considered in CFD modeling.

Using CFD for finding the dispersion coefficient has the following advantages:

- Considers the effect of pond's characteristics such as ponds geometry, inlet size and position
- Considers the parameters such as temperature and viscosity
- Includes surrounding environmental parameters such as wind
- Considers the effect of hydraulic behavior of the basins
- Decreases the cost

The above advantages nominate CFD as one of the favorable options for finding the dispersion coefficient, although these programs are really case sensitive and the lack of complete description of different parameters in the accurate way would cause uncertainty in the results. Furthermore, the user must be aware of the CFD model limitations, assumptions and working knowledge of actual ponds to prevent misinterpretation of results.

4.3 CFD approach: A case study

A methodology for determining the dispersion coefficient is proposed by combining Fluent software (CFD) and Levenspiel's formula. Testing and validation of the method is assessed by field data. The name and the place of the basin used as a case study in this part will not be disclosed herein, due to the confidentiality of the data.

4.3.1 Flow domain and mesh

A two dimensional model was developed for this study. The model created and meshed using Gambit (version 2.4.6). The whole surface was divided to 711819 homogenous quadrilateral cells (30cm*30cm). The parameters related to this model are presented in Table 4.2.

Table 4.2. Geometry and flow parameters of the basin

Parameter	Units	Value
Length (L)	m	512
Width (W)	m	125
Inlet width	m	0.45
Inlet velocity in x-direction	m/s	4.63
Inlet velocity in y-direction	m/s	0
Fluid Density	Kg/m^3	998.2
Fluid viscosity	Kg/(m.s)	0.001

4.3.2 Initial and boundary conditions

The governing equations were solved in combination with the proper initial and boundary constraints. The inlet boundary was specified as an inlet velocity (V=4.63 m/s) and the outlet as an outflow. The no slip boundary condition was chosen for the walls. For discrete phase boundaries, the outflow was chosen as an escape boundary and the walls as reflect boundaries. The boundary conditions that were picked for this case are presented in Table 4.3.

Table 4.3. Inputs to Fluent

Models	Two dimensional Pressure based, Steady state Standard k-epsilon turbulence model
Solution Control	Second order upwind discretization
Materials	Liquid water (H2O), Solid particles
Operating conditions	Operating pressure: 101325 Pa Gravity: Off
Boundary conditions	Inlet: Velocity inlet (V=4.63m/s) Walls: No slip boundaries Outlet: Outflow Discrete phase condition at walls: reflect, normal constant 0.5, tangential constant 0.8 Discrete phase condition at inlet and outlet: escape
Convergence limit	Scaled residuals: 1.0E-04

4.3.3 Particle phase modeling

For a low surface fraction of dispersed second phase (particle), an Eulerian–Lagrangian approach was used. This allows the effects of turbulence modulation (effect of particles on turbulence) to be neglected. The Lagrangian approach divides the particle phase into a representative set of discrete individual particles and tracks these particles separately through the flow domain by solving the equations of particle movement. Assumptions regarding the particle phase included the following: (i) no particle rebounded off the walls/surfaces; (ii) no particle coagulation in the particle deposition process and (iii) all particles are spherical solid shapes. Trajectories of individual particles can be tracked by integrating the force balance equations on the particle (Fluent Inc, 2003):

$$\frac{du_p}{dt} = F_D(u-u_p)+g_x(\rho_p-\rho)/\rho_p+F_x \tag{4-33}$$

Where F_D (Drag force) is calculated according to the following equation:

$$F_D = \frac{18\mu}{\rho_p D^2_p} \frac{C_D \mathrm{Re}}{24} \tag{4-34}$$

And the Reynolds number is defined as:

$$\mathrm{Re} = \frac{\rho D_p \left| u_p - u \right|}{\mu} \tag{4-35}$$

When the flow is turbulent, Fluent uses mean fluid phase velocity in the trajectory equation (Equation 4-33) in order to predict the dispersion of the particles.

4.3.4 Modeling flow and solid phase particles

The Navier-Stokes equation for turbulent flow in a two-dimensional geometry was solved to obtain the water velocity. CFD software sets up and solves fundamental mass, momentum and energy balance equations using numerical techniques. The standard K-ε is a widely used, robust, economical model, which has the advantages of rapid, stable and reasonable results for many flows (Marshall et al., 2003). In this case study, the standard K-ε model is used. After running the model for 5000 iterations and obtaining acceptable convergence, the unsteady particle tracking is used for tracking the solid particles within the basin. For this reason, 5000 spherical particles with the same size are injected at the inlet at the same time. Particle diameters (100 μm) and density (1020 Kg/m^3) is selected based on previous investigation (Gancarski, 2007). This size and density is an acceptable option for modeling the particle as a drogue in the basins. After injection, this model is run for 104 time steps, 1800 seconds each and the amount of the particles escaped from the basin in each time step is calculated. The dispersion number, D/UL may be calculated from the dimensional variance which is defined by Equation 4-36 (Levenspiel, 1972).

$$\sigma^2 = \frac{\sum t_i^{\,2} C_i}{\sum C_i} - \left[\frac{\sum t_i C_i}{\sum C_i}\right]^2 \tag{4-36}$$

The dispersion number (d) (Levenspiel, 1972) was determined using Equation 4-34.

$$\sigma_i^{\,2} = \frac{\sigma^2}{t^2} = 2d - 2d^2(1 - \exp(\frac{-1}{d})) \tag{4-37}$$

The variance and t are used to calculate “d” by a process of trial and error via Excel Solver in Microsoft Excel.

4.3.5 Dispersion coefficient

The data received from actual tracer studies from the field can be seen in Figure 4.6. This is one of the typical RTD for this basin between 12 RTDs that draw during different months of the year. Tracer concentration versus time shows the existence of short circuiting in the basin. The actual retention time using the actual tracer studies is 19.25 hours. Using the actual retention time of the basin from the tracer test and theoretical retention time, the hydraulic efficiency of the basin is calculated to be 37%.

RTD may be determined using unsteady particle injection in Fluent (Figure 4.6). The maximum concentration of the tracer in the exit stream is observed to occur at 1.5 hours. Comparing this peak with the theoretical retention time suggests significant short-circuiting. As mentioned previously, the RTD drawn in Figure 4.6 is one of the RTDs between 12, but the final value of d is calculated based on the concentrations mean value. The existence of short circuiting in the pond was previously reported by other authors as well (Vorkas et al., 2000; Moreno, 1990).

$$t = \frac{\sum C_i t_i}{\sum C_i} \qquad (4\text{-}38)$$

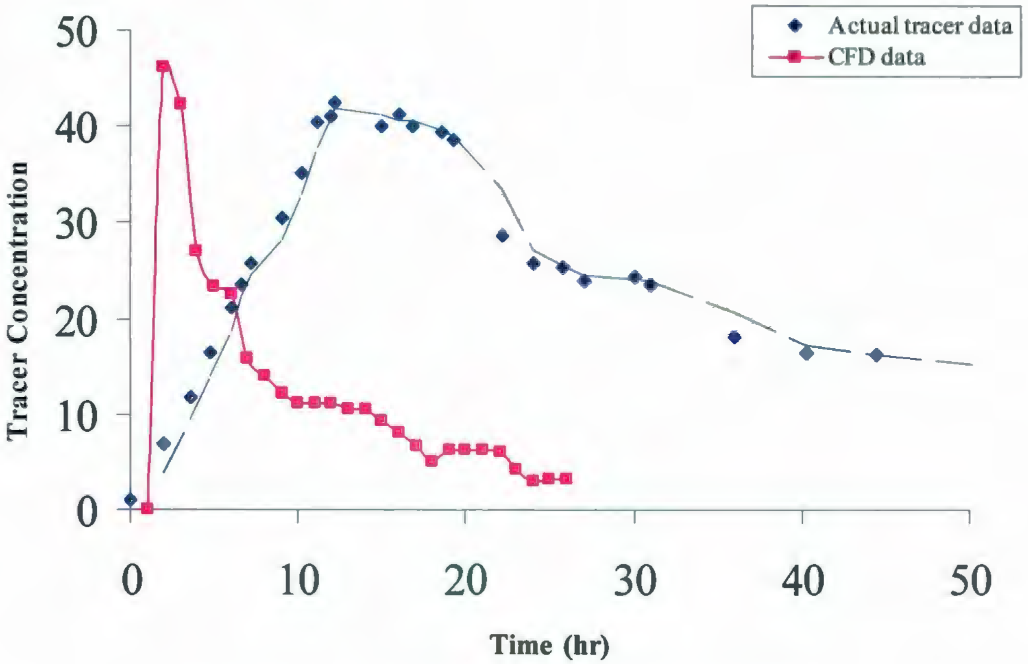

Figure 4.6. RTD using actual tracer and CFD data

Table 4.4. Summary of variables to obtain "d" using Fluent

Function	Value	Function	Value
$\sum C_i$	4457	$\frac{\sum t_i^2 C_i}{\sum C_i} - \left[\frac{\sum t_i C_i}{\sum C_i}\right]^2$	2.6E+10
$\sum C_i t_i$	2.31E+08	σ^2	2.6E+10
$\sum t_i^2 C_i$	1.27E+14	σ_i^2	0.75
$\frac{\sum t_i^2 C_i}{\sum C_i}$	2.84E+10	d	0.5

* i = Different time steps

The amount of actual retention time calculated by data received using CFD modeling and Equation 4-38 is 14.39. Using this value, the hydraulic efficiency (t/T) of the basin is calculated, which is 28%. This compares with the value from Persson et al. (2003) for pond "A" (inlet and outlet in opposite position), which is approximately 30%. Researchers typically run the model with a time span approximately two or three times larger than the theoretical retention time for calculating RTD (Paugatch et al., 2007), as the model assumes a group of particles do not escape from the basin if the actual theoretical residence time is used.

"d" is calculated according to the Levenspiel equations (Levenspiel, 1972). The summary of this calculation is presented in Table 4.4. After determining the variance, the Excel Solver is used and the value of d is calculated by trail and error. "d" was previously calculated as 0.6 by actual tracer test. The calculated value from this study is 0.5. Comparing "d" obtained using actual tracer study and "d" found by CFD, it is confirmed that CFD is a suitable option for calculating "d".

4.4 Application of dispersion model to a case study

Two WSPs with the following characteristics are chosen to test and validate the dispersion model and to compare the results with ideal reactor models. The name and the place of the ponds used as the case studies in this section will not be disclosed herein, due to the confidentiality of the data.

Pond "A" is the WSP in the coal mine area for disposal of the AMD from underground and open pit mining in the region, and pond "B" is the WSP in the Nickel mine site used for co-disposal of tailings and mineralized mine rock during the open pit operations. The hydraulic characteristics of these WSPs are displayed in Table 4.5.

Table 4.5. Characteristics of WSPs used in the case studies

Characteristics	Pond "A"	Pond "B"
Volume	~500,000 m^3	15,755,200 m^3
Area	~163,000 m^2	~1,048,750 m^2
Height	3.06 m	20 m
Flow rate	236.1 $\frac{m^3}{hr}$	900 $\frac{m^3}{hr}$
Retention time	93 days	62 days

The influent and effluent concentrations for chemical species are actual field data. By comparing the concentration of chemical species present in the mine water with CCME, contaminants of concern are selected for modeling the concentration gradient within the pond.

4.4.1 Iron concentration gradient within pond "A"

Based on the chemical components in the pond, obtained by using the methodology outlined in section 3.1.3 of chapter 3, some of the ferrous iron components from MINTEQ are selected for modeling the concentration gradient within the pond (Table 4.6).

Table 4.6. Ferrous iron species at the influent of the pond

Iron species
$Fe(CN)_6^{-4}$
Fe^{+2}
$FeCl^+$
$FeHCO_3^+$
$FeHPO_4$ (aq)
$FeOH^+$
$FeSO_4$ (aq)

Ferrous iron is considered as one of the component in the influent of the pond, as it is one of the most abundant components among the chemical components predicted by MINTEQ.

By comparing the rate of ferrous iron oxidation and precipitation of ferric hydroxide (reactions 2-2 & 2-3), it is evident that the oxidation of ferrous to ferric iron is very slow in acidic solution and thus is the rate determining step in pyrite oxidation. The oxidation rate coefficients for the oxidation of ferrous iron in different months of the year (Diez et al., 2007) may be seen in the following table:

Table 4.7. Ferrous iron oxidation rate coefficients in different months of the year

Month	K (Ferrous iron oxidation rate coefficient)
May	$9*10^{-4}$ (s^{-1})
July	$1*10^{-4}$ (s^{-1})
August	$5*10^{-3}$ (s^{-1})
November	$7*10^{-3}$ (s^{-1})
October	$2*10^{-3}$ (s^{-1})

Another ferrous iron component predicted by MINTEQ is iron sulphate. The oxidation mechanism of iron sulphate is as follows:

$$12FeSO_4 + 3O_2 \rightarrow 2[Fe_2(SO_4)_3]_2 . Fe_2O_3 \quad (4\text{-}3)$$

This is followed by the decomposition of oxidized material to Fe_2O_3:

$$[Fe_2(SO_4)_3]_2 . Fe_2O_3 \rightarrow 3Fe_2O_3 + 6SO_3 \quad (4\text{-}4)$$

The oxidation of sulphate iron in high temperature water is fast, thus reaction reaches equilibrium very quickly. Therefore, the ferrous to ferric iron oxidation rate is chosen as the rate determining step for modeling purposes.

The concentration gradient of ferrous iron within the pond "A" is modeled by the dispersion equation. By using the concentration of ferrous iron in the influent of the pond and using the dispersed flow model, the concentration gradient within the pond is predicted as shown in Figure 4.7. In order to compare the results from the dispersed flow model and CSTR, the concentration gradient within the pond using ideal CSTR is calculated and shown in Figure 4.7.

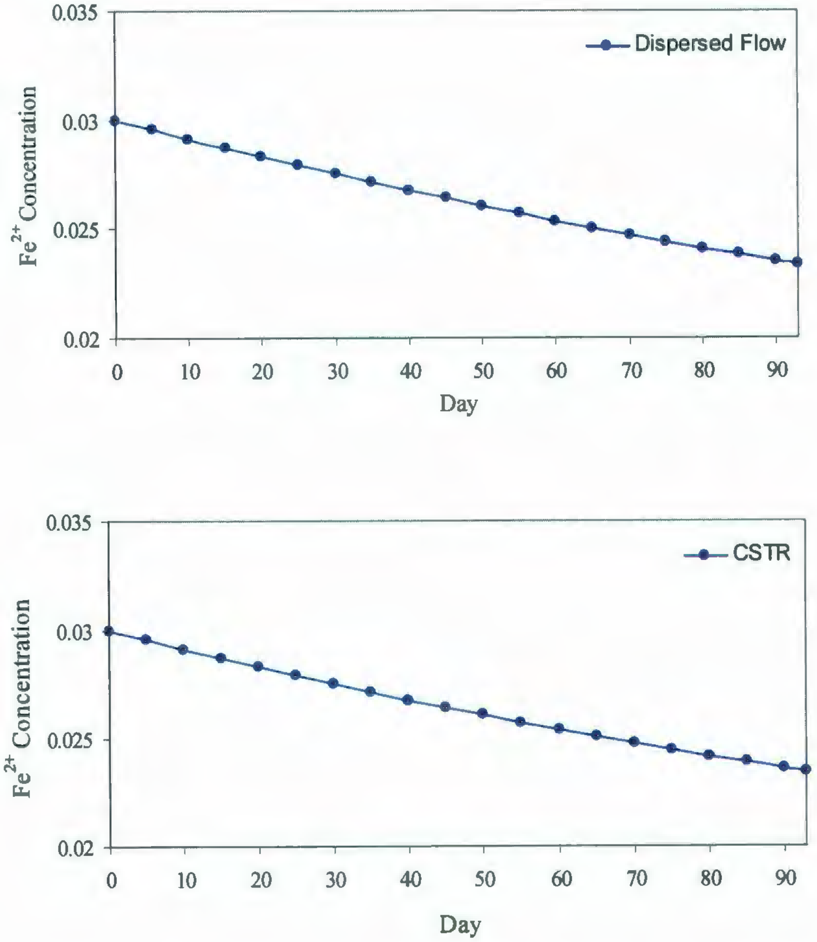

Figure 4.7. Ferrous iron concentration gradient within the pond "A" using dispersed flow and CSTR

Considering that the Peclet number is less than 1 (using Arcievala's equation) the fact that the pond is in CSTR condition was expected. Using both of these models for this case study, it may be said that the WSP acts approximately as a CSTR.

4.4.1.1 Evaluating the effect of Peclet number on dispersion model

The results of the empirical equations used in finding the Peclet numbers are compared in this section. Based on the hydraulic condition of Pond "A", the Peclet number may be calculated by different empirical equations (Table 4.8).

Table 4.8. Peclet numbers used in the dispersion model related to Pond "A"

Peclet number formula	Value
Fisher (1967)	1.06
Arceivala (1981)	0.7
Polprasert and Bhattarai (1985)	1.582

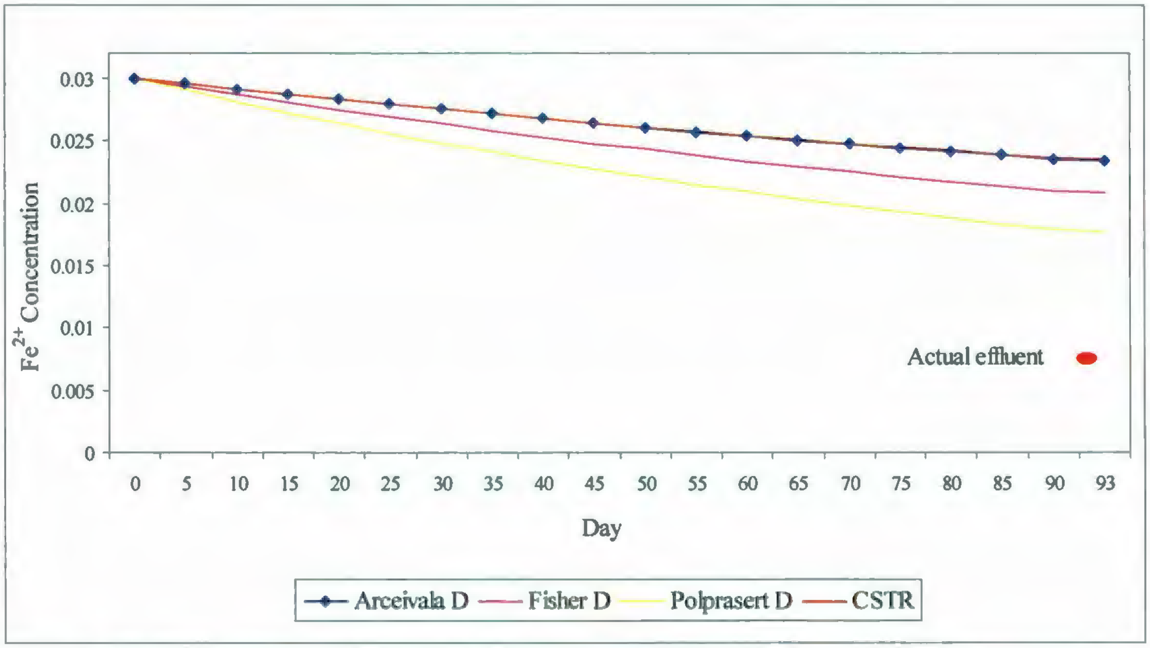

Figure 4.8. Comparison of the dispersed flow model using different dispersion coefficients with CSTR

All Peclet numbers calculated by these empirical equations show the condition of the system approximately as CSTR. Variations in the ferrous iron concentration within the pond are plotted in Figure 4.8. These values are developed using the dispersed flow model by applying the Peclet numbers obtained from empirical equations. The results of comparing the dispersed flow model with CSTR shows that using this model better predict the effluent of the pond than CSTR. Among the Peclet numbers developed using different empirical equations, integrating the one based on Polprasert et al. (1985) equation in the dispersed flow model will lead to a better prediction of ferrous iron concentration in the pond's effluent.

4.4.2 Nickel concentration gradient within pond "B"

Nickel concentration in the influent and effluent of the pond has been obtained from the field which may be seen in Table 4.9.

Table 4.9. Concentration of Nickel in the influent and effluent of pond "B"

Nickel	Concentration (ug/L)
Influent	82
Effluent	31

Considering the chemical concentrations at the influent of the pond "B", the following chemical components shown in Table 4.10 were predicted using MINTEQ.

Table 4.10. Nickel species at the influent of the pond "B"

Nickel species
$NiH(CN)^{-4}$
Ni^{+2}
NiF^{+}
$NiHCO_3^{+}$
$NiHPO_4$ (aq)
$NiNO_3^{+}$
$NiSO_4$ (aq)

For modeling purposes, the rate constant of Ni^{+2} oxidation is used because it is the slowest reaction rate constant (Njau et al., 2000) among the oxidation of nickel components in the influent of pond "B".

$$Ni^{2+} + OH^{-} \rightarrow NiOH^{+} \qquad (4\text{-}5)$$

The value of Peclet number was calculated according to the formulas mentioned by Fisher (1967), Liu (1977) and Polprasert et al., (1985). These values may be seen in Table 4.11.

Table 4.11. Peclet numbers used in the dispersion model related to Pond "B"

Peclet number formula	Value
Fisher (1967)	26.34
Liu (1977)	38.77
Polprasert and Bhattarai (1985)	41.7189

The Nickel concentration gradient within the pond "B" using the dispersion model is compared with the concentration gradient using the conventional CSTR. This comparison may be seen in Figure 4.9.

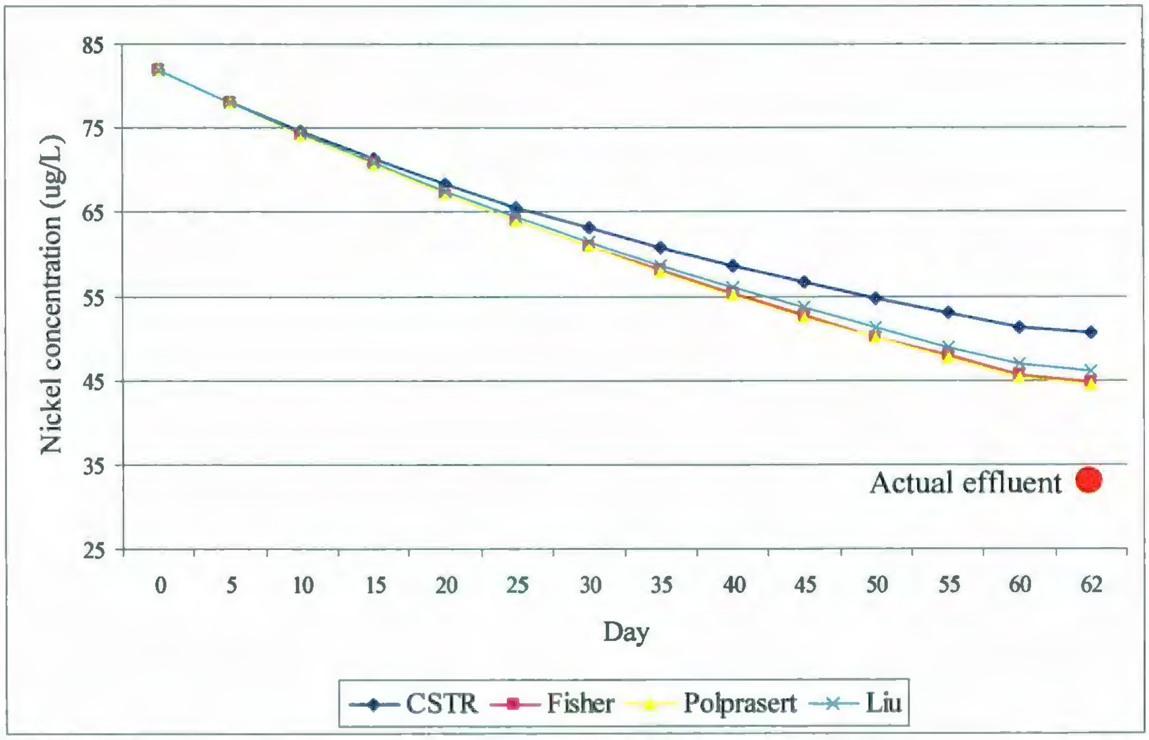

Figure 4.9. Nickel concentration gradient within the Pond "B" using dispersion model and ideal CSTR

This diagram shows that the Peclet number calculated with the empirical equation mentioned by Polprasert et al. (1985) gives a better prediction of the effluent of the pond. Besides, comparison of the dispersion model with CSTR in this case study also shows that using this model better predicts the effluent of the pond. It should be noted that in dispersed flow model, the Peclet number makes the model sensitive to small changes in any of the three parameters of Pe and therefore the dispersion model better predicts the non-idealities in the pond than the ideal CSTR or PFR.

Summary

The non-idealities within the ponds such as concentration and temperature gradient do not follow assumptions of ideal reactors. Different parameters such as geometry, inlet and outlet positions and inlet flow velocity affect hydraulic performance of the basin. Problems such as recirculation or reverse flow and short circuiting in the system are difficult to predict and can lead to a reduction in the theoretical retention time of the pond and, thus decreasing treatment efficiency.

Due to the non-idealities in the ponds, there are a number of different approaches available to model the non-idealities; among them the dispersion model may predict the effluent of the pond more reliably compared to ideal CSTR or PFR. Comparing the results of modeling the chemicals concentration gradient within the ponds is a validation of the advantages of using the dispersed flow model in comparison with ideal CSTR or PFR. For modeling the chemical concentration gradient within the pond, after finding different chemical components of the species using MINTEQ in the influent, the rate of the slowest reaction is chosen to be used in dispersion model. This is the rate determining step among the reactions that take place in the pond. It should be noted that by the time that this specific reaction is completed, the other oxidation reactions which are faster than this particular reaction have already been completed.

The dispersion model is highly dependent on dispersion coefficient which itself is based on hydraulic performance of the basin. The results of comparing CFD analysis with actual tracer test nominates the CFD models as a good option to determine the actual retention time and dispersion index for use in the dispersion model. Furthermore, instead of using costly and time dependent tracer studies and highly sensitive CFD analysis, empirical equations are another suitable option for finding the dispersion coefficient.

CHAPTER 5[4]

Ecological Risk Assessment

Abstract:

After modeling the chemical concentration gradient within the pond and obtaining chemical concentrations in the effluent, a methodology was developed to assess the effect on the environment. Ecological risk assessment is the process of defining and quantifying risks to ecological entities and determining the acceptability of the predicted risk. The USEPA (1998) has established a systematic framework for ecological risk assessment. The four steps of EPA framework are hazard identification, exposure assessment, dose-response modeling and risk characterization. These steps are used for identifying and quantifying the risk of the chemical contaminants to ecological entities. The estimated risk of the effluent of treatment systems can be used to assess the performance of the treatment process. Comparing the amount of risk for different chemical species with existing guidelines helps one to evaluate the efficiency of the treatment system. In case the risk of the effluent contaminants of the treatment system exceeds the existing guidelines, further or alternative treatment should be considered. The objective of this chapter is to assess the risk of effluent contaminants from the WSP to the ecosystem. A case study is considered in this chapter to demonstrate the use of ecological risk assessment methodology and to quantify the risk of the effluent contaminants of the tailing pond to the ecosystem.

---

[4] A part of this chapter is going to be published and cited as:
Abbassi, R., Khan , F., Hawboldt, K. 2009. Ecological risk assessment of a stabilization pond discharge. Environmental engineering and management journal, Submitted.

5.1 Ecological risk assessment of the tailing pond effluent

Ecological risk assessment is a method that defines the relationship between pollution and environmental effects (Gaudet, 1994). The general risk assessment model proposed by the USEPA (1998) is outlined in Figure 5.1.

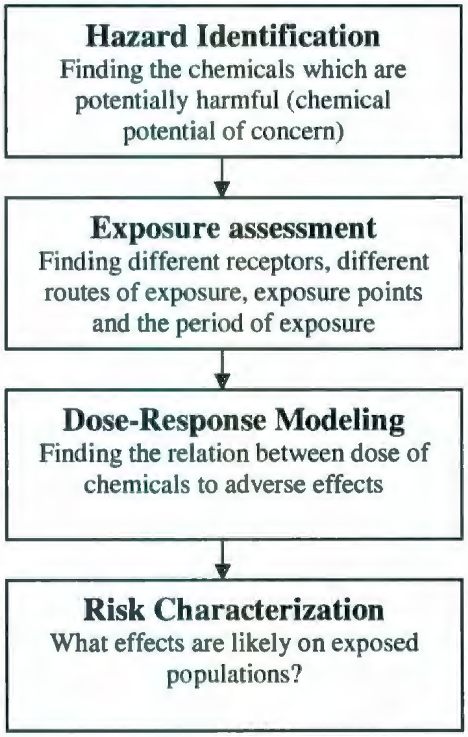

Figure 5.1. Procedure of risk assessment model (USEPA, 1998)

In present research, different processes of the ecological risk assessment as stated by the EPA framework will be used to assess the effect of the tailing pond discharge to ecological entities in the study region.

As the first step, determining the chemicals of concern is a part of hazard identification. The second step is exposure assessment which will identify different routes of exposure through different media. Finally, based on the dose-response assessment and risk characterization, the amount of risk for these chemicals will be demonstrated and these amounts will be compared with the well-known environmental guidelines such as EPA and CCME. Figure 5.2 provides the framework of the risk assessment process considering the risk assessment approach.

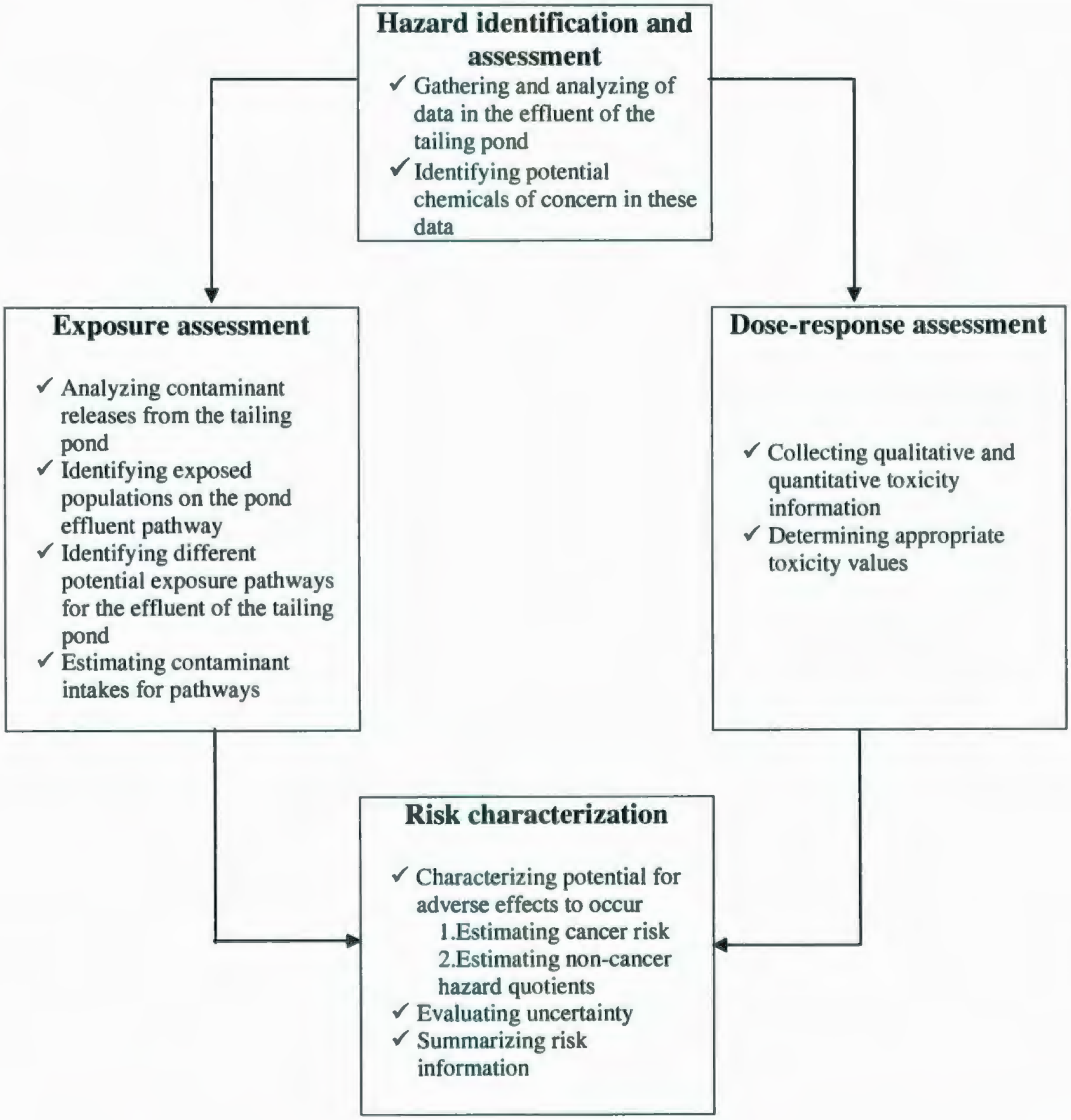

Figure 5.2. Different risk assessment processes as stated by EPA for the effluent contaminants of the tailing pond

It should be noted that the goal in most risk-based decision making processes is to reduce risk as much as possible. Sometimes higher levels of treatment are required to reduce the risk associated with the effluent concentration. To reduce the risk, attempts should be made to manage it. Considerations such as cost should be considered for managing risk. If the estimated risk exceeds acceptable criteria, alternative strategies to minimize and control risk will be developed.

5.2 Application of the ecological risk assessment to a case study

The EPA recommended framework for ecological risk assessment has been applied for a tailing pond discharge scenarios. This framework as mentioned previously is considered to estimate the risk of effluent contaminants to ecological entities in the study region. The name and the location of the WSP used as a case study in this part will not be disclosed herein, due to the confidentiality of the data.

5.2.1 Site specification

The tailing pond is located east of the mine mill and is used for co-disposal of tailings and mineralized mine rock during the open pit operations. The acid generating rock is placed under water in the tailing pond to reduce oxidation and acid generation. Moreover, this pond receives the process water from the mill. The effluent of the tailing pond goes directly through a marine embayment. In addition, there is a risk of seepage to groundwater and to freshwater ponds. Biological receptors include: aquatic animals (freshwater and marine water fish), aquatic plants, terrestrial animals and terrestrial plants.

5.2.2 Hazard identification

Metals considered in this modeling scenario include cadmium, cobalt, copper, lead, nickel, and zinc. These metals produce hazardous effects on ecological receptors and human health (Lee et al., 2006; Lim et al., 2008). In addition, these metals were selected for study as they are present in the tailing pond.

Three different transport scenarios are considered in the study. The treated effluent of the WSP migrates to the bay through the discharge pipeline. Seepage from the pond transports from the soil to groundwater that is flowing under the pond area. In the worse case scenario, it is assumed that approximately 10% overflow of the tailing pond would enter the surrounding soil. These pathways are illustrated in Figure 5.3.

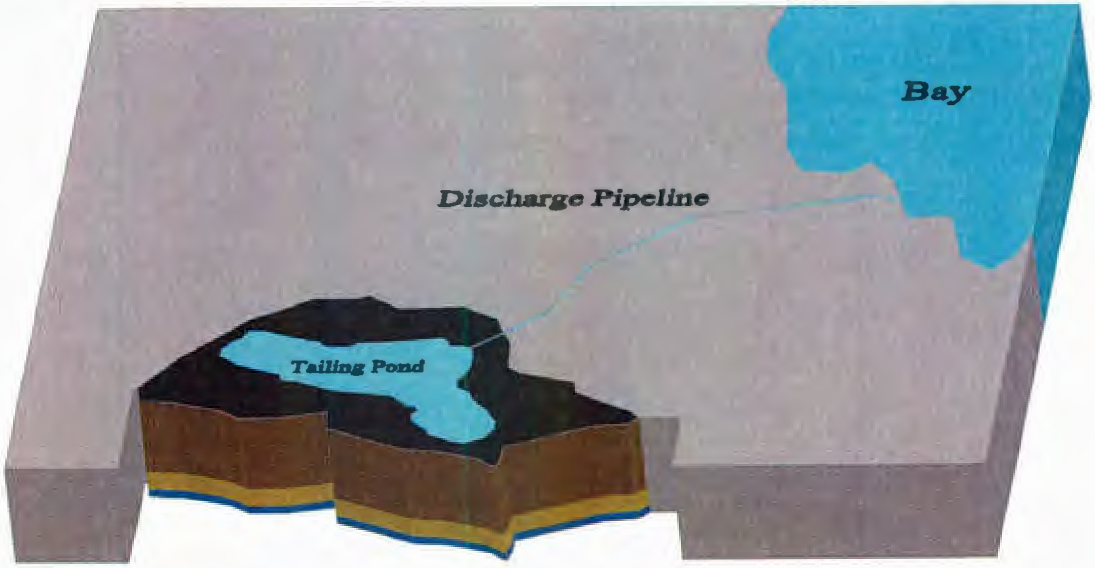

Figure 5.3. Schematic showing the transport pathways for the tailing pond's discharge

5.2.3 Fate and transport of the contaminants

The transport of contaminants within the soil and groundwater related to seepage from the tailing pond is modeled by SEVIEW 6.3 (Schnelker, 2006). It includes SESOIL and AT123D. SESOIL is a one-dimensional vertical transport model, simulating the contaminant transport and fate based on diffusion, adsorption, volatilization, biodegradation, and hydrolysis. Parameters calculated by SESOIL are passed to AT123D, a three dimensional groundwater transport model. Transport and fate processes simulated by AT123D include advection, dispersion, sorption and biological decay and show how far a contaminants plume will migrate in the groundwater. ATD123D can run about 450 scenarios which the combination of three contaminant types, eight source configurations, three source release types and four types of aquifer dimensions may define these run options (Khan et al., 2003).

For the simulation, the mean of seasonal variation of temperature, humidity, and precipitation were collected from 1997-2007 for the region (Environment Canada, 2007). The soil column considered in this simulation included approximately 0.3 m of peat moss and topsoil, 15.5 m of silty sand, following with 3.5 m of clay and do not reflect the actual condition of the study region. In this modeling scenario, the topsoil was not considered due to its narrow thickness and high permeability in comparison with the total depth of the soil column.

The maximum concentration of these chemicals in the groundwater is calculated using SEVIEW. Inputs for the model were included the climate condition of the study region, chemicals of concern, soil characteristics and groundwater specific factors.

The concentration of metals in the marine water is calculated according to Arceivala's equation (1981), considering the initial dilution which is the ratio of initial concentration of effluent discharge to marine water and the maximum concentration in the centerline of the plume. Pycnocline is a rapid change in water density with depth which is often caused by a combination of decreasing water temperature and increasing salinity in marine water. For this modeling, the pycnocline is considered at 9m depth from the surface.

$$D_{initial} = \frac{Uby}{Q} \qquad (5\text{-}1)$$

For finding the concentration of metals in the soil, contaminants are considered to be deposited on the soil surface and mixed uniformly with the underlying soil (the top soil with 0.3 m depth). The concentration in the soil is calculated by the total amount of contaminant on the soil surface divided by the mass of the soil (Fjeld et al., 2006).

$$C_{soil} = \frac{C_t}{\rho_s A Z_r} \tag{5-2}$$

5.2.4. Exposure pathways for different ecological entities in the study area

Due to the site specific conditions, three exposure pathways are considered in the modeling scenario.

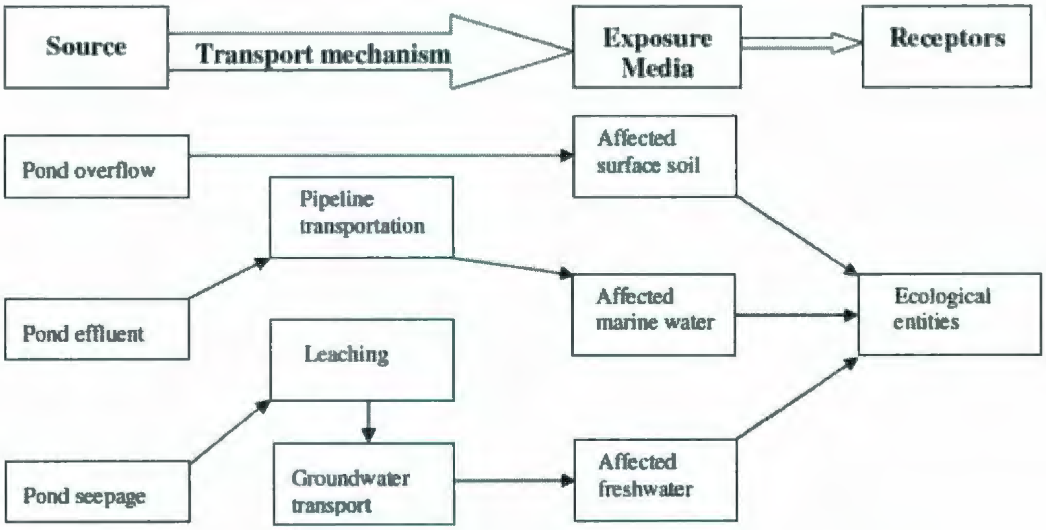

Figure 5.4. Simplified flowchart of exposure pathways

The effluent of the tailing pond discharge to the marine water is the primary pathway for marine fish and terrestrial animals. The seepage of the pond through to groundwater and into the freshwater pond in the vicinity of the tailing pond is also considered. The last exposure pathways considered in this modeling scenario is soil contamination due to the overflow of the pond.

The concentration of the metals in the tails water and discharge of the pond can be seen in Table 5.1. For confidentiality purposes, the actual data has been modified, thus the data in Table 5.1 are not the real data of the pond received from the field.

Table 5.1. Concentration of metals in the tailing water and treated effluent

Metals	Concentration in the tailing water (mg/l)	Concentration in the treated effluent (ug/l)
Nickel	0.11	34.1
Copper	0.022	BTL
Cobalt	0.022	BTL
Cadmium	0.0011	BTL
Zinc	0.055	BTL
Lead	0.011	BTL

*. BTL: Below the detection limit of ICP

The initial dilution of the wastewater discharge to the marine environment, the dilution factor is calculated, which is 1:27. The maximum metals concentration in the groundwater is obtained using SEVIEW (Table 5.2).

Table 5.2. Maximum concentration of CPC in the groundwater received from SEVIEW

Metals	Nickel	Copper	Cobalt	Zinc	Cadmium	Lead
Max. Concentrations (mg/l)	$4.9*10^{-2}$	$5.87*10^{-3}$	$5.87*10^{-3}$	$2.35*10^{-2}$	$4.6*10^{-4}$	$4.7*10^{-3}$

The last exposure pathways considered in this modeling scenario is contaminated soil. The metals concentration of the soil, calculated based on the pond's overflow, can be seen in Table 5.3.

Table 5.3. Concentration of metals in the soil according to 10% overflows from the pond

Metals	Nickel	Copper	Cobalt	Zinc	Cadmium	Lead
Concentrations (mg/Kg soil)	$1*10^{-2}$	$0.2*10^{-5}$	$0.2*10^{-5}$	$0.5*10^{-5}$	$0.1*10^{-6}$	$0.1*10^{-5}$

The terrestrial animals considered as receptors in this modeling scenario ingested food (plants, aquatic animals and other terrestrial animals), soil and water in the tailing pond region. The amount of food ingestion (FI) and water intake (WI) for 6 of mammals based on their body weight (BW) are found by following formulas (USEPA, 1993):

$$\text{FI (kg/day)} = 0.0687\,(\text{BW})^{0.822} \tag{5-3}$$

$$\text{WI (L/day)} = 0.099(\text{BW})^{0.9} \tag{5-4}$$

The amount of the soil ingestion is assumed to be 13% of the food ingestion for these species. Furthermore, for three bird species existed in the study region, the amount of food ingestion and water intake is calculated, by following formulas (USEPA, 1993):

$$\text{FI (g/day)} = 0.648(\text{BW})^{0.651} \tag{5-5}$$

$$\text{WI (L/day)} = 0.59(\text{BW})^{0.67} \tag{5-6}$$

The amount of the soil ingestion considered in this scenario is the same as the one that was considered for the mammals; 13% of the food ingestion. The diet of the nine terrestrial species available in the study region is shown in Table A1.1 of the Appendix I. Chemicals may be accumulated in the body burdens of these terrestrial animals and, these species can be a food source for the other animals. The rate of transfer of metals from the points of entry into body to muscle tissues is based on specific species and metal-specific transfer factor. This ingestion transfer factor for different terrestrial animals and different chemicals is available in Table A1.2 of the Appendix I.

Metals may be transferred to muscle tissue of terrestrial animals by exposure of metal bearing food, soil and drinking water. The tissue concentration (body burdens) based on concentration of the ingested food from different media and the ingested transfer factor for different metals is calculated according to following formula (Beak, 1997):

$$C_{animal} = F_{ing}[\sum C_w I_w K_w + \sum C_s I_s K_s + \sum C_{tp} I_{tp} K_{tp} + \sum C_{ta} I_{ta} K_{ta} + \sum C_{aa} I_{aa} K_{aa} + \sum C_{ap} I_{ap} K_{ap}] \quad (5\text{-}7)$$

In this modeling scenario, the potential exposure pathways of aquatic organisms to metal released due to the effluent of the tailing pond is considered; including exposure to the water column containing dissolved and particle metals. It should be noted that exposure to metal-bearing sediment is not considered in this modeling scenario. Two groups of freshwater and marine water fish are considered for the modeling purposes, including arctic charr and brook trout (freshwater species) along with arctic charr and sculpin (marine water species).

Bio-Concentration Factors (BCFs), which represent the ratio of the concentration of chemicals in aquatic animals tissue compared to concentration of the same chemicals in the surrounding water column, were obtained (CCME, 1997; USEPA, 1999), and outlined in Table A1.3 of the Appendix I.

The concentration of metals in the mussel tissue (Body Burdens) of aquatic animals can be calculated by having the BCFs (L/Kg) and concentration in the water according to following formula (Sanderson et al., 2009):

$$C_{aa} = C_w * BCF \tag{5-8}$$

The last organisms considered in this modeling scenario are terrestrial and aquatic plants, ingested by terrestrial animals. The abandoned terrestrial plants in the study area are Lichens, Bakeapples, Coniferous and Deciduous browse. While, Sedge is the aquatic plant common to the study area. The soil to plant transfer factor, which is the concentration of metal in the soil divided by the measured concentration of metals in the plant tissues according to terrestrial plants and chemicals of concern in the study region, is outlined in Table A1.4 of the Appendix I. For Sedge (aquatic plants), BCFs show the ratio of concentration of metals in comparison with the surrounding environment, as shown in Table A1.5 of the Appendix I. Available concentration in the plants tissues for terrestrial and aquatic plants can be found according to following equations, respectively:

$$C_{Plant} = C_{Soil} * B_v \tag{5-9}$$

$$C_{Plant} = C_{Water} * BCF \tag{5-10}$$

5.2.5. Toxicological benchmark doses for terrestrial animals

The benchmark doses typically represent the Non Observable Adverse Effect Level (NOAEL) where some sublethal effect (e.g. weight loss) has not been observed. Considering the existing NOAEL for mammalian test species ($NOAEL_t$), the equivalent NOAEL ($NOAEL_w$) for the mammalian wildlife species can be found by using the adjustment factor for differences in body size. Allometric equation used to adjust for weight differences between the test species (e.g. Rat) and mammalian wildlife species can be seen below (Sample et al., 1996):

$$\mathrm{NOAEL}_w = \mathrm{NOAEL}_t * \left(\frac{bw_t}{bw_w}\right)^{1/4} \tag{5-11}$$

The adjustment factor for the birds can be calculated by the following equation:

$$\mathrm{NOAEL}_w = \mathrm{NOAEL}_t \tag{5-12}$$

This NOAEL according to the data for rats (Sample et al., 1996) and body weight of terrestrial animals existed in the study region may be seen in Table A1.6 of Appendix I.

5.2.6. Risk characterization

From confirmed information concerning the amount of chemicals in the Bay (Table 5.1), the amount of chemicals existing in the tailing pond seepage entering the freshwater pond near the WSP and the amount of chemicals in the soil according to WSP watershed, the ecological risk assessment software (ERAS), developed at Memorial University of Newfoundland, to determine the risk. The code of the program was written in MATLAB, version 7.1. This software is capable of calculating the food ingestion, soil ingestion, water intake and toxicological benchmark according to body weight of the animals, as mentioned previously. Moreover, different routes of exposure to the chemicals such as food ingestion (e.g. eating plants or other terrestrial and aquatic animals), soil and water are considered in the software. Doses of metal received by terrestrial animals are calculated based on the chemical concentrations in the foods containing all ingested animal, vegetable matter, ingested soil and drinking water. The dose is further based on ingested rates of food, soil and water and the defined body weight of the animals.

The total exposure dose and the amount of HQ for terrestrial animals are calculated by the software as stated by following formulas:

$$D_{\exp} = (\sum C_i I_i) / BW \tag{5-13}$$

$$HQ = D_{\exp} / D_{bench} \tag{5-14}$$

Considering the assumption that HQ for each individual chemical of concerns are additive, the hazard index (HI) is calculated by ERAS, summing of all hazard quotients (Lim et al., 2008).

$$HI = \sum HQ \tag{5-15}$$

5.2.7. Uncertainty analysis

A less biased approach to risk assessment uses uncertainty analysis to estimate the degree of confidence that can be placed in the risk estimate (Hammonds et al., 1994). Two distinct categories based on the nature of uncertainties may be considered in the quantitative ecological risk assessment. First is the variability, which is the common source of uncertainty, and is caused by inherent fluctuations or differences in a quantity or process. The variability of hydrogeologic parameters across a site such as hydraulic gradient, hydraulic conductivity and aquifer thickness may be examples of this kind of uncertainty. Second is incertitude, which is the type of uncertainty arisen from limitations of the scientific knowledge or incomplete descriptions of a mechanism or process. For example, the lack of having the toxicological benchmark for different ecological entities in the study region can produce this kind of uncertainty (Fjeld et al., 2006).

Despite of the sources and types of uncertainty in the ecological risk assessment, these uncertainties are quantified and analyzed using the concepts of probability and statistics. For evaluating the uncertainty of calculating risk, @RISK seeks to determine the outcome of a decision situation as probability distribution. In an @RISK risk analysis, the output probability distributions give the decision maker a complete picture of all the possible outcomes. It uses advanced Monte Carlo simulation techniques to analyze risk in the Excel spreadsheet model. The first step in conducting the Monte-Carlo simulation is to specify the probability distribution for the uncertain variable. @RISK contains many different distributions, but the one which is chosen should reflect, as much as possible, the input variables actual uncertainty. Using the increasingly common Monte Carlo simulation in quantitative uncertainty analysis (Poulter, 1998), demonstrates the location of any particular risk estimate within the range of risk, leading to decrease uncertainties for risk estimation.

The variability is one of the categories of uncertainty consider in this research. It should be noted that incertitude uncertainty is not considered in present modeling scenario. The body weight of the animal is one of the variables that can produce uncertainties for estimating ecological risk assessment. The ecological entities have a range in body weight and using a specific value of this parameter to find the risk may produce uncertainty in the results. In this paper, the 90% confidence intervals for animal's body weight are calculated. Since, the body weight is affected on the other parameters included in HQs estimation, the range of this index, by using the lower and upper bonds of the 90% intervals for the body weight, is calculated for the ecological entities exposed to metal concentrations from the effluent of the tailing pond.

5.2.8 Risk parameters analysis

The results of finding HQs by ERAS considering different exposure roots (direct and indirect) are shown in Table 5.4. This software has the capability to calculate the concentration of chemicals in animals' body burden, and uses this calculation for finding the amount of HQ, as mentioned previously.

Table 5.4. HQ for different terrestrial animals in the study region

Hazard quotient	Nickel	Copper	Cobalt	Zinc	Cadmium	Lead
Snowshoe Hare	$8.72*10^{-5}$	$3.98*10^{-5}$	$6.56*10^{-5}$	$9.96*10^{-7}$	$6.23*10^{-6}$	$7.95*10^{-6}$
Ptarmigan	$3*10^{-4}$	$6.64*10^{-5}$	$3.4*10^{-4}$	$1.25*10^{-5}$	$1.6*10^{-5}$	$2.9*10^{-4}$
Caribou	$1.2*10^{-3}$	$9.5*10^{-3}$	$3.2*10^{-4}$	$2.4*10^{-4}$	$4*10^{-4}$	$3.9*10^{-4}$
Black Bear	$8*10^{-4}$	$6.9*10^{-4}$	$1.5*10^{-3}$	$2.7*10^{-4}$	$1*10^{-4}$	$1.9*10^{-4}$
Polar Bear	$5.8*10^{-3}$	$7.2*10^{-3}$	$1.9*10^{-2}$	$2.5*10^{-2}$	$6.1*10^{-3}$	$4*10^{-4}$
Harlequin Duck	$2*10^{-3}$	$3.8*10^{-3}$	$4.1*10^{-3}$	$7*10^{-3}$	$3.6*10^{-3}$	$1.9*10^{-3}$
Merganser	$2.2*10^{-3}$	$7.6*10^{-4}$	$5.7*10^{-3}$	$1.32*10^{-3}$	$1.84*10^{-4}$	$4.9*10^{-3}$
Beaver	$1.8*10^{-3}$	$1.63*10^{-2}$	$5.5*10^{-3}$	$4*10^{-4}$	$6.9*10^{-4}$	$6.6*10^{-4}$
Ringed Seal	$1*10^{-3}$	$6.79*10^{-5}$	$1.1*10^{-4}$	$1.7*10^{-6}$	$1.07*10^{-5}$	$1.36*10^{-5}$

The HI, which is the sum of HQ, is demonstrated in Figure 5.5.

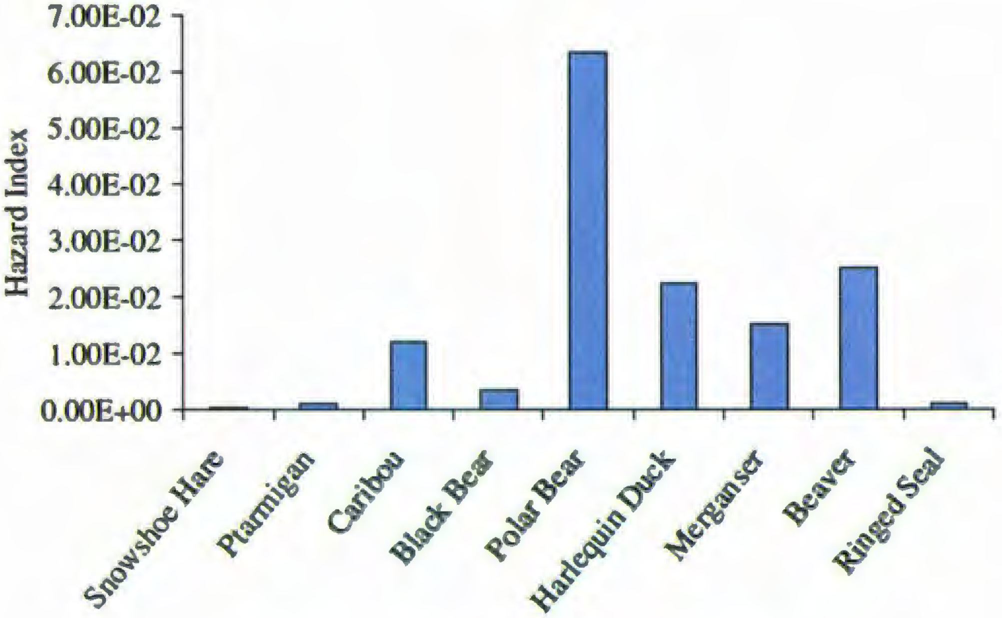

Figure 5.5. Hazard index for ecological entities

HQ of 1 or greater indicates that the level of predicted exposure is equal to or greater than the threshold level of exposure (Lee et al., 2006). Accordingly, if the HQ values are less than 1, no environmental effects of any form are expected. Predicted HQ values for each metal of concern and each animal within the study area were below 1, shown in Table 5.4. The maximum HI is for polar bear. The evaluation of HQs shows that these chemicals do not have major toxic effects on the ecological entities in the vicinity of the tailing pond. This shows that effluent of the tailing pond in the study area does not have any major effects on the surrounding environment and demonstrating the proper performance of this pond in the study region.

The uncertainty analysis is completed by finding the risk range according to different body weight of the animals in the study region. It should be noted that the parameters of the model for finding HQ such as food ingestion, soil ingestion, water intake and NOAEL are dependent on the body weight of the animals. Changes in body weight of different animals may produce an uncertainty within the risk estimates. Using @Risk for doing Monte Carlo simulation and the weight of polar bear (500 ± 150), demonstrates the range of risk estimate (with 90% confidence interval) as shown in Figure 5.6. The range of the HQs calculated for different animals according to the range of their body weights still does not show any risk of effluent metal concentration of the tailing pond to the ecological entities within the study area.

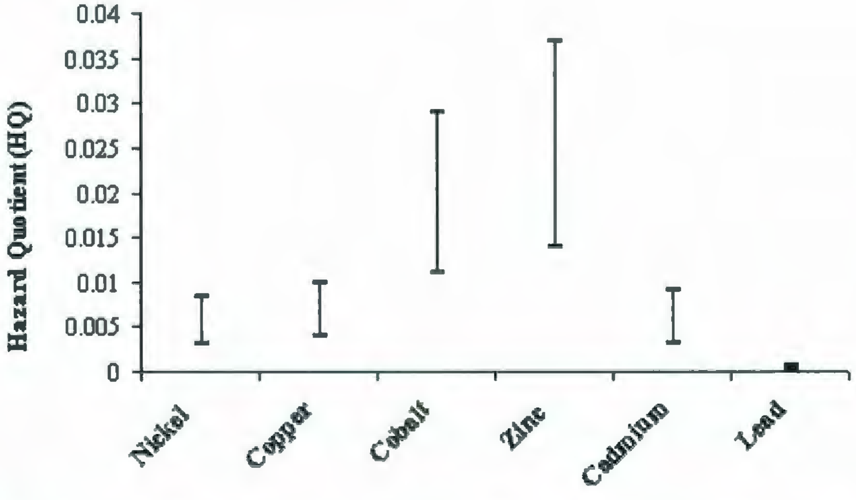

Figure 5.6. HQ intervals according to different chemicals for polar bear

Summary

The performance of the WSP as a treatment system for treating AMD is evaluated using a risk-based approach. The estimated risk to ecological entities for the chemical concentration in the pond's discharge and comparing the results with the existing environmental guidelines help to determine the treatment performance of the WSP. Four steps of environmental risk assessment according to EPA framework are used to estimate the amount of risk. For the studied WSP, the amount of HQs related to different chemicals and different animals existing in the study region shows that the risk of effluent contaminants is below the acceptable limits. Because the estimated risk is associated with uncertainties, the uncertainty analysis using the Monte Carlo simulation is conducted. The range of risk provided by uncertainty analysis again confirms acceptable risk according to guideline's criteria. Therefore, determining the risk of the effluent contaminants from this WSP to ecological entities in the study region reapproves the effective performance of this treatment system. The risk-based methodology may be used for the evaluation of any treatment system.

CHAPTER 6

Conclusions and Recommendations

Abstract:

The research conducted in the current study has introduced risk-based evaluation of AMD treatment system. This chapter presents a summary of the conclusions drawn from this work. Recommendations for future research are also provided.

6.1 Conclusions

AMD impacts surrounding ecosystems and therefore must be properly managed. Determining the likely chemical nature of AMD is critical in water management and treatment system design. Analytical methods to determine mineral content are time consuming and costly. A methodology is proposed to decrease the requisite number of analyses using predictive models to determine the possible presence of minerals. This methodology may assist in directing analysis of the wastewater, focusing attention on important or key components for analysis rather than a carte blanche approach. In addition, it could assist with the interpretation of the analytical output and thereby reduce analytical costs. From mine water analysis, metal and non-metal species, are used to generate Eh-pH diagrams. These diagrams help to identify the key metals and their oxidative state. This information is used to elucidate the chemical analyses of the AMD and determine the oxidative state of the metals measured. Next, chemical reaction equilibrium models are used to determine the possible minerals in the AMD, based on input from the previous steps. This is critical as it will identify major acid producing/consuming minerals present and thereby aid to determine the optimal water management and treatment system. This method must be used in conjunction with analytical methods.

The most common method for treating AMD is WSP. The methodology outlined above can be combined with WSP model to predict impacts on the environment. Different models exist to study the transportation and transformation of contaminants within the pond, most of which are based on assumptions of ideal reactors. The non-idealities within the ponds such as concentration and temperature gradient do not follow assumptions of ideal reactors. There are different approaches available to model non-idealities; among them the dispersion model may predict the effluent of the pond more reliably in comparison with ideal CSTR or PFR. Dispersed flow model may cover the gap of non-idealities between two ideal models, CSTR and PFR. The results of the case studies described in this research are a confirmation of this statement. The main parameters used in dispersed flow model, retention time and dispersion index, may vary extensively based on the hydraulic behavior of the pond. Therefore, sufficient knowledge about the actual hydraulic behavior of the system is required for accurate prediction of these parameters. Parameters, including geometry of the pond, inlet and outlet positions and inlet velocity affect the hydraulic performance of the basin. Problems, such as recirculation or reverse flow and short circuiting in the system exist and are difficult to predict. These problems lead to a reduction in the theoretical retention time and decreased treatment efficiency of the pond. Comparing the results of CFD analysis with actual tracer test shows that the CFD model may be used to determine the actual retention time and dispersion number. Moreover, using the empirical equations as an option for finding the dispersion number used in dispersed flow model is recommended.

After finding the actual concentration of the chemicals in the pond's discharge, Environmental Risk Assessment process may help to find the hazardous effect of chemical contaminants on humans and the ecosystem. Application of ERA framework helps to assess the impact of the effluent of the pond. Hazard identification is the first step in this process, done by deciding about chemicals of concern and site characteristics such as the site history, contaminant level in media, environmental characteristics affecting chemical fate and transport and potentially affected population and biota. The transport of contaminants within the media is calculated in exposure assessment. As a part of fate and transport modeling, SEVIEW is used to simulate the transport of chemical contaminants within the soil and the groundwater. SEVIEW has the ability to predict the accurate concentration of chemicals in soil and ground water conditional to the availability of environmental parameters (e.g. soil characteristics and weather conditions). To obtain the chemical concentrations in the marine water, the dilution of the contaminants reaching the marine water may be considered using Arceivala's equation. Determining the place of pycnocline and waste water flow rate may help to calculate the dilution factor. For finding the benchmark doses for mammalian wildlife species, finding the NOAEL for mammalian test species and changing doses according to the animals' body weights is useful. The last step in risk assessment process is risk characterization done by finding the amount of HQ. Using the data obtained from the ingestion of food by different animals, and the concentration accumulated in the animal's body burden integrated with toxicological benchmark for the specific animal leads to accurate determination of this index.

As the value of risk is combined with different uncertainties, the uncertainty analysis uses Monte Carlo simulation which demonstrates a range for risk based on the related parameters. Comparing this range with the well known guidelines such as CCME or USEPA may help to evaluate the performance of the treatment system. In the case that the value of risk exceeds the criteria, further treatment of AMD should be considered.

By applying three steps: characterization of AMD, modeling the WSPs based on their non-ideality and ecological risk assessment, this research lead to the conclusions as follows:

- ✓Eh-pH diagrams may be used to characterize the specific AMD. HSC chemistry which is a software designed for drawing Eh-pH diagram based on chemical species, is a useful tool to study AMD characteristics.
- ✓Computer-assisted thermodynamic chemical equilibrium models are useful tools for describing the reactions that occur in a chemical system. These models assist in predicting the behavior of chemical system. MINTEQ software based on these models may be used to predict different possible chemical components that exist in AMD.
- ✓The chemical oxidation of a mineral can be classified as acid producing or consuming (the reactions that generate or consume H^+) or non-acid producing or consuming. This will help put a variety of minerals producing AMD in different categories.

- ✓The flow in WSPs is rarely ideal and the assumptions of ideal CSTRs and PFRs often do not exist. Therefore, designing the treatment system such as WSPs based on ideal models may give misleading results.
- ✓Dispersed flow model is one of the non-ideal models that may cover the non-idealities that exist within the pond. The main parameters of this model may vary extensively based on the hydraulic behavior of the system.
- ✓CFD software may be useful to find the actual retention time and dispersion coefficient. However, these software are case sensitive and inaccurate interpretation of the hydraulic conditions of the pond may also lead to misleading results.
- ✓Using the empirical equations is another option to find the dispersion index. Most of these equations are based on the pond's geometry, which is the most important hydraulic parameter of ponds. The advantages of using these equations are reducing the cost of actual tracer studies and predicting the dispersion index required at the design stage of a WSP.
- ✓USEPA framework has been used to assess risk of the hazardous chemical components in the pond's discharge. Comparing the calculated risk with the guidelines will help to characterize the WSP efficiency and the level of treatment. Risk-based treatment provides a methodology to evaluate the treatment efficiency of the pond. In cases where estimated risk exceeds the acceptable criteria, methods to improve the treatment are also developed.
- ✓As a part of risk assessment process, the fate and transport of contaminants within the soil and the groundwater are calculated using SEVIEW. Parameters related to site

specific conditions such as soil characteristics and weather conditions should be considered in this simulation.

- ✓ The dilution factor should be considered to obtain the actual concentrations of the chemical species in the marine water. Flow rate of the wastewater discharged to the marine water and the specific condition of the bay such as the place of pycnocline are required to determine to reach this propose.
- ✓ A less biased approach to risk assessment uses uncertainty analysis to estimate the degree of confidence that can be placed in the risk estimate. Despite of the sources and types of uncertainty in the environmental risk assessment, these uncertainties should be quantified and analyzed using the concepts of probability and statistics.

6.2 Recommendations

Based on this research, the following recommendations are suggested for future research:

- ✓ In the reactions taking place in AMD, many secondary chemical components based on the specific conditions of AMD (e.g. pH and temperature) are produced. Investigations of secondary reactions taking place in AMD under different conditions and evaluations of the effect of existing chemical species on these reactions are recommended.
- ✓ WSP is one of the cost effective methods used for treating AMD. However, this method is not suitable for restricted areas. Researchers recommend many treatment methods for treating AMD. Comparing these methods and evaluating their

performance according to specific conditions (e.g. cold weather) is suggested for future research.

✓Different hydraulic parameters such as the pond geometry, the inlet/outlet configurations and positions, wind and the inlet jet affect the actual retention time and dispersion coefficient. The combination of these parameters may lead to change the hydraulic behavior of the basins. Finding the effect of different hydraulic parameters of the WSP on actual retention time and dispersion index and integrating equations that consider these behaviors may help to design the WSP easily with the optimum performance. Evaluating the effects of different hydraulic parameters and their combinations on the pond's retention time and dispersion index is recommended.

✓The depth of the WSP is one of the parameters of the pond's design that may not be neglected easily. Using three dimensional CFD modeling to determine the optimum conditions of pond performance according to different hydraulic parameters is suggested for future investigations.

✓Comparing the risk evaluation results with the existing guidelines may not always satisfy the regulations. Therefore, changing the treatment system in a way that reduces the risk of discharged contaminants is desired. Evaluating different methods to improve the performance of the WSP is recommended.

✓The variability and incertitude uncertainties are two types of uncertainties need to be considered in ERA processes. Uncertainty analysis should be done considering all types of uncertainties in different parameters.

CHAPTER 7

Statement of Originality

7.1. Novelty

The novelty of the present study by integrating three steps of mine waste management, characterization of AMD, modeling the WSPs considering non-idealities and ecological risk assessment can be viewed from the following perspectives:

- ✓The methodology proposed for AMD characterization is useful to determine the chemical components of the specific tail's water. Identifying the existing chemical components of AMD is required prior to choosing the specific treatment system.
- ✓ Methods such as optical microscopy, electron microscopy and X-ray diffraction are used to identify the minerals producing AMD. The methodology recommended in this study can be used in conjunction with these analytical tests, to decrease the number of these costly and complex tests.
- ✓The non-idealities within the tailing pond reduce the actual retention time, resulting in decreases of the treatment efficiencies. The dispersion model used in the present study bridges the gap of ideal models for modeling the concentration gradient within the pond. Applications of the dispersed flow model for different case studies confirm the validity of this non-ideal model in predicting the actual concentration of chemicals in the pond's discharge.
- ✓Determination of the actual values of dispersion coefficients used in dispersed flow model remains a great concern for researchers. Tracer studies used to find the dispersion coefficient are costly and do not allow the designer to estimate dispersion

index for the ponds which are not yet constructed. Application of the methodology presented in this research would help the researchers to obtain the actual retention time and dispersion index using CFD code.

✓ Different empirical equations exist to estimate the dispersion coefficient in the WSPs and lagoons. Testing and validation of these equations for real case studies provide more confidence on the sustainability of these equations used in tailing pond modeling.

✓ The risk-based methodology presented in this study characterizes the potential impact of chemical concentrations in the pond's discharge to human health and the ecosystem in the pond's vicinity. The risk amount produces the criteria to evaluate the treatment efficiency of the ponds. It also helps to determine if the treatment system should be improved or alternative treatment should be considered.

References

Abbas, H., Nasr, R., and Seif, H. 2006. Study of waste stabilization pond geometry for the wastewater treatment efficiency. Ecological engineering, 28: 25-34.

Abis, K.L., and Mara, D. 2006. Temperature measurement and stratification in facultative waste stabilization ponds in the UK climate. Environmental monitoring and assessment, 114: 35-47.

Agency for toxic substances & disease registry (ATSDR); Exposure Evaluation: Evaluating Exposure Pathways; Department of Health and Human Services, www.atsdr.cdc.gov.

Agunwamba, J., Egbuniwe, N., and Ademiluyi, J. 1992. Prediction of the dispersion number in waste stabilization ponds. Water research, 26(1): 85-89.

Agunwamba, J.C. 2006. Effect of the location of the inlet and outlet structures on short-circuiting: Experimental investigation. Water environment research, 78: 580-589.

Akcil, A., and Koldas, S. 2006. Acid Mine Drainage (AMD): causes, treatment and case studies. Journal of Cleaner Production, 14: 1139-1145.

Amiri, M.C. 2003. Principles in Mass Transfer. Arkan Publishing center, Iran, ISBN: 964-6227-34-1.

Aldana, G.j., Guganesharajah, K., and Bracho, N. 2005. The development and calibration of a physical model to assist in optimizing the hydraulic performance and design of maturation ponds. Water science and technology, 51(12): 173-181.

Arceivala, S.J. 1981. Waste water treatment and disposal. Marcel Dekker INC., New York and Basel.

Baleo, J.N., Humeau, P., and Cloirec P.L. 2001. Numerical and experimental hydrodynamics of lagoon pilot. Water research, 35(9): 2268-2276.

Ball, J.W, Runkel, R.L., and Nordstrom, D.K. 2006. Transport Modeling of Reactive and Non-Reactive Constituents from Summitville, Colorado: Preliminary Results from the Application of the OTIS/OTEQ Model to the Wightman Fork/Alamosa River System.

Banda, C.G. 2003. Modern design of waste stabilization ponds in warm climates: Comparison with traditional design methods. School of civil engineering, University of Leeds, Leeds, England.

Banda, C.G., Sleigh, P.A., and Mara, D.D. 2006. CFD-Based Design of Waste Stabilization Ponds: Significance of Wind Velocity. IWA specialist conference on waste stabilization ponds, Bangkok, Thailand.

Beak international incorporated. 1997. Assessment of trace metal effects Voisey's bay mine mill. Brampton, Ontario, Prepared for voisey's bay nickel company limited

Belzile, N., Chen, Y.W., Cai, M.F., and Li, Y. 2004. A review on pyrrhotite oxidation. Journal of geochemical exploration, 84: 65-76.

Bondad, MGR., Arthur, J.R. and Subasinghe, R.P. 2008. Understanding and applying risk analysis in aquaculture. Food and agriculture organization of the united nations, Rome, Italy.

Brissaud, F., Lazarova, V., Ducoup, C., Joseph, C., Levine, B., and Tournoud, M. G. 2000. Hydrodynamic behavior and faecal coliform removal in a maturation pond. Water science and technology, 42: 119-126.

Brookfield, A.E., Blowes, D.W., and Mayer, K.U. 2006. Integration of field measurements and reactive transport modeling to evaluate contaminant transport at a sulfide mine tailings impoundment. Journal of contaminant Hydrology, 88: 1-22.

Brunk, C. 1998. Risk management workshop.

http://cmte.parl.gc.ca/Content/HOC/committee/362/envi/reports/rp1031697/envi01/15-ch8-e.html

Byrd, D.M., and Cothern, C.R. 2000. Introduction to risk analysis: A systematic approach to science-based decision making. Government institutes, a division of ABS group Inc., ISBN: 0-86587-696-7.

Canadian council of ministers of the environment (CCME). 1996. A framework of ecological risk assessment: General guidance. The national contaminated sites remediation program, Winnipeg, Manitoba, Canada.

Canadian council of ministers of the environment (CCME). 2007. Canadian water quality guidelines for the protection of aquatic life.

Chien, Y.S., and Liou, C.T. 1995. Steady state Multiplicity for Autocatalytic reactors in a Nonideal Mixing of CSTR with two Unpremixed Feeds. Chemical Engineering Science, 50(22): 3645-3650.

Clark, M.M 1996. Transport modeling for environmental engineers and scientists. John Wiley and Sons, USA, ISBN 0-471-12348-X.

Chow, V.T., Eliassen, R., and Linsley, R.K. 1979. Waste water engineering: Treatment, Disposal, reuse, McGraw-Hill.

Costello, C. 2003. Acid Mine Drainage: Innovative Treatment Technologies. National network of environmental management of environmental management studies fellow for U.S.EPA, Washington, DC, USA.

Covello, V.T., and Merkhofer, M.W. 1993. Risk assessment methods, approaches for assessing health and environmental risks. Plenum Press, New York and London, ISBN: 0-306-44382-1.

Crites R.W., Middlebrooks E.J., and Reed S.C. 2005. Natural wastewater treatment systems. Taylor & Francis group, ISBN: 0-8493-3804-2.

Da Silva, G., Lastra, M.R., and Budden, J.R. 2003. Electrochemical passivation of Aphalerite during bacterial oxidation in the presence of Galena. Minerals engineering, 16: 199-203.

Diez, S., Noonan, G.O., MacFarlane, J.K., and Gschwend, P.M. 2007. Ferrous iron oxidation rates in the pycnocline of a permanently stratified lake. Chemosphere, 66: 1561-1570.

Dold, B. 2005. Basic conceps of environmental geochemistry of sulfide mine-waste. Centre d'Analyse Minérale, Université de Lausanne, Switzerland.

Edler, L., and Kopp-Schneider, A. 1998. Statistical models for low dose exposure. Mutation Research, 405: 227-236.

Egiebor, N.O., and Oni, B. 2007. Acid rock drainage formation and treatment: a review. Asia-Pacific Journal of chemical engineering, 2:47-62.

Elberling, B., Nicholson, R.V., and Scharer, J.M. 1994. A combined kinetic and diffusion model for pyrite oxidation in tailings: a change in controls with time. Journal of hydrology, 157: 47-60.

Environment Canada. 2007. National climate data and information achieve, Nain, NL, Canada.

Espana, J.S., Pamo, E.L., and Pastor, E.S. 2006. The oxidation of ferrous iron in acidic mine effluents from the Iberian pyrite belt (Odiel basin, Huelva, Spain): Field and laboratory rates. Journal of geochemical exploration, 92: 120-132.

Fares, Y. 1993. Circulation pattern in long narrow lakes based on shallow water equations. Advances in Hydro-Science and Engineering. Wang, S. (Ed). Volume 1: 1142-1147.

Fares, Y., and Lloyd, B. 1995. Wind effects on residence time in waste stabilization lagoons. HYDRA 2000, Thomas Telford, London.

Faustman, M.E. 1996. Review of Noncancer Risk assessment: Application of Benchmark Dose Methods. Department of environmental health, University of Washington, Seattle, WA, USA.

Ferrara, R.A., and Harleman, D.R.F. 1981. Hydraulic modeling for waste stabilization ponds. ASCE, 107, EE4.

Fjeld, R.A., Eisenberg, N.A, and Compton, K.L. 2006. Quantitative environmental risk analysis for human health. John Wiley & Sons, USA, ISBN-13: 978-0-471-72243-4.

Fisher, B. H. 1967. The mechanics of dispersion in natural streams. Journal of hydraulic Division ASCE, 93:187–216.

Fluent. 2003. User manual 6.2, Fluent Inc.

Food and drug administration (FDA). 2002. Initiation and conduct of all major risk assessments within a risk analysis framework. Center of food safety and applied nutrition, USA.

Frederick, G., and Lloyd, B. 1996. An evaluation of retention time and short-circuiting in waste stabilization ponds using Serratia marcescens bacteriophage as a tracer. Water Science and Technology, 33(7): 49-56.

Froment, G.F., and Bischoff, K.B. 1979. Chemical reactor analysis and design. John Wiley & sons, USA, ISBN: 0-471-02447-3.

Fyfe, J., Smalley, J., Hagara, D. and Sivakumar, M. 2007. Physical and hydrodynamic characteristics of a dairy shed waste stabilization pond system, Water science and technology, 55(11): 11-20.

Gancarski P. 2007. CFD modeling of an oxidation ditch, MSc thesis, Cranfield University, UK.

Garcia,C., Ballester, A., Gonzalez, F., and Blazquez, M.L. 2005. Pyrite behaviuor in a tailing pond. Hydrometallurgy, 76: 25-36.

Garrels, R. M., and Christ, C. L. 1965. Minerals, Solutions, and Equilibria. Harper & Rowe, N.Y. 450 pp.

Gaudet C. 1994. A framework for ecological risk assessment at contaminated sites in Canada: Review and recommendations. The national contaminated sites remediation program, Ottawa, Ontario, Canada.

Ginige, T.A. 2002. Mining Waste: The Aznalcóllar Tailings Pond Incident, Spanish Law (Part II). European Environmental Law Review, 11 (4): 102-113.

Gloyna, E.F., Malina, J.F., and Davis E.M. 1976. Facultative waste stabilization pond design. Water resources symposium, No, 9, Center for research in water resources, University of Texas, Austin.

Golder associates. 1997. Voisey's Bay mine-mill project. NL, Canada, Project number: 961-1832-7040.

Grunwald, S. 2008. Oxides and Hydroxides. Soil and water science, University of Florida.

Gu, R., and Stefan, H.G. 1995. Stratification dynamics in wastewater stabilization ponds. Water resource, 29(8): 1909-1923.

Gujer, W. 2008. Systems analysis for waste technology. Springer Berlin Heidelberg, 101:127, ISBN: 978-3-540-77277-4.

Haimes, Y.Y. 1998. Risk modeling, assessment, and management. John Wiley & Sons, USA, ISBN: 0-471-24005-2.

Hammonds, J.S., Hoffman, F.O., and Bartell, S.M. 1994. An introductory guide to uncertainty analysis in environmental and health risk assessment, Environmental restoration risk assessment council, Tennessee, USA.

Hayes, R.E. 2001. Introduction of chemical reactor analysis. Taylor & Francis group, ISBN: 978-1-56032-927-5.

Health Canada. 1995. Investigating human exposure to contaminants in the environment : A community handbook. Minister of National Health and Welfare, ISBN: 0-662-23543-6.

Hill, C.G. 1977. An introduction to chemical engineering kinetics & reactor design. John Wiley & Sons, USA, ISBN 0-471-39609-5.

International atomic energy agency (IAEA). 1994. Handbook of parameter values for the prediction of radionuclide transfer in temperature environments. IAEA technical report series, No. 364.

James, A. 1987. An alternative approach to the design of waste stabilization ponds. Water science technology, 19(12): 213-218.

Juanico, M. 1991. Should waste stabilization ponds be designed for perfect-mixing or plug-flow. Water science technology, 23: 1495-1502.

Karteris, A., Papadopoulos, A., and Balafoutas, G. 2005. Modeling the temperature pattern of a covered anaerobic pond with computational fluid dynamics. Water, Air and soil pollution, 162: 107-125.

Kellner, E., and Pires, E.C. 2002. The influence of thermal stratification on the hydraulic behavior of waste stabilization ponds. Water science and technology, 45(1): 41-48.

Khan, M.A., and Ahmad, S.I. 1992. Performance evaluation of pilot waste stabilization ponds in subtropical region. Water science and technology, 26(7): 1717-1728.

Khan F.I., and Husain, T. 2003. Evaluation of a petroleum hydrocarbon contaminated site for natural attenuation using 'RBMNA' mythology. Environemntal modeling and software, 18: 179-194.

Khan, F.I. 2008. Risk assessment: Class handout. Memorial university of Newfoundland, St. John's, NL, Canada.

Kirby C.S., and Brady J.A.E. 1998. Field determination of Fe^{2+} oxidation rates in acid mine drainage using a continuously-stirred tank reactor. Applied geochemistry, 13(4): 509-520.

Klopffer, W. 1994. Environmental hazard Assessment of chemicals and products Part II: Persistence and degradability of organic chemicals. Environmental science and pollution research, 1(2): 108–116.

Kock, D., and Schippers, A. 2006. Geomicrobiological investigation of two different mine waste tailings generating acid mine drainage. Hydrometallurgy, 83: 167-175.

Komnitsas, K., Xenidis, A., and Adam, K. 1995. Oxidation of pyrite and arsenopyrite in sulphidic spoils in Lavrion. Minerals Engineering, 8 (12): 1443-1454.

Kortenski, J. 1992. Carbonate minerals in Bulgarian coals with different degrees of coalification. International journal of coal geology, 20: 225-242.

Kortenski, J., and Kostova, I. 2006. Occurrence and morphology of pyrite in Bulgarian coals. International journal of coal geology, 29: 273-290.

Lee, S.W., Lee, B.T., Kim, J.Y., Kim, K.W., and Lee, J.S. 2006. Human risk assessment for heavy metals and As contamination in the abandoned metal mine areas, Korea. Environmental modeling and assessment, 119: 233-244.

Lee, Q.F. 2007. Unit operation laboratory non-ideal tubular reactors. Department of chemical and biological engineering, The University of British Columbia.

Levenspiel, O. 1972. Chemical Reaction Engineering. Department of Chemical Engineering, Oregon State University, USA, ISBN 0-471-53016-6.

Lim, H.S., Lee, J.S., Chon, H.T., and Sager, M. 2008. Heavy metal contamination and health risk assessment in the vicinity of the abandoned Songcheon Au-Ag mine in Korea. Journal of Geochemical Exploration, 96: 223-230.

Lin, H.K. 2006. Electrochemical behavior of Tennantite in chloride solutions. Journal of the electrochemical society, 153: 74-79.

Liu, H. 1977. Predicting dispersion coefficient of stream. Journal of environmental Engineering Division, ASCE. 103(1): 59-69.

Lorens, M., Saez, J., and Soler, A. 1992. Influence of thermal trifurcation on the behaviour of a deep wastewater stabilization pond. Water resource, 26: 569-577.

Lonesiy, T. 2006. Mining waste and wetlands. Master thesis, Lulea University of technology, Sweden.

Losordo, T.M., Ebeling, J.M., and Piedrahita, R.H. 1986. Stratification measurement techniques in aquaculture ponds. American Society of Agricultural Engineers, Paper Number: 86-5047.

Lottermroser, B. 2003. Mine wastes: Characterization, Treatment, and environmental impacts. Springer, Germany, ISBN 3540005269.

Louise, A.K., and Mara, D. 2006. Temperature measurement and stratification in facultative waste stabilization ponds in the UK climate. Environmental monitoring and assessment, 114: 35-47.

Lovanh, N.C., Loughrin, J.H., Cook, K., Rothrock, M., and Sistani, K. 2007. Effect of Stratification on the Profile of an Anaerobic Swine Waste Treatment Lagoon in Kentucky. International Symposium on Air Quality and Waste Management for Agriculture, Broomfield, Colorado, USA.

Lupankwa, K., Love, D., Mapani, B., Mseka, S., and Meck, M. 2006. Influence of the Trojan Nickel Mine on surface water quality, Mazowe valley, Zimbabwe:

Runoff chemistry and acid generation potential of waste rock. Physics and Chemistry of the Earth, 31: 789-796.

Marecos Do Monte, M.H.F., and Mara, D.D. 1987. The hydraulic performance of waste stabilization ponds in Portugal, Water science and technology, 19(12): 219-227.

Marshall, E.M. and Bakker, A. 2003. Computational fluid mixing; Fluent Inc, Lebanon, New Hampshire, USA, www.fluent.com.

Metcalf & Eddy. 1979. Wastewater Engineering: Treatment, Disposal, Reuse. McGraw-Hill, USA.

Molnar, A., Markos, J., and Jelemensky, L. 2005. Some considerations for safety analysis of chemical reactors. Chemical engineering research and design, 83, A2: 167-176.

Moreno, M.D. 1990. A tracer study of the hydraulics of facultative stabilization ponds, Water resource, 24(8): 1025-1030.

Moses, C.O., Nordstrom, D. K., Herman, J.S., and Mills, A.L. 1987. Aqueous pyrite oxidation by dissolved oxygen and by ferric iron. Geochimica et Cosmochimica Acta, 51(6):1561-1571.

Murphy, K.L., and Wilson, A.W. 1974. Characterization of mixing in aerated lagoons. ASCE Journal of environmental engineering, 100(5): 1105-1117.

Muttamara, S., and Puetpaiboon, U. 1997. Roles of baffles in waste stabilization ponds, Water science and technology, 35(8): 275-284.

Nameche, T., and Vasel, J.L. 1998. Hydrodynamic studies and modelization for aerated lagoons and waste stabilization ponds. Water resource. 32(10): 3039-3045.

Nelson, K.L., Cisneros, B.J., Tchobanoglous, G., and Darby, J.L. 2004. Sludge accumulation, characteristics, and pathogen inactivation in four primary stabilization ponds in central Mexico. Water research, 38: 111-127.

Nieto, J.M., Sarmiento, A.M, Olias, M., Canovas, C.R., Riba, I., Kalman, J., and Angel, D.T. 2007. Acid mine drainage pollution in the Tinto and Odiel rivers (Iberian pyrite Belt, SW Spain) and bioavailability of the transported metals to the Huelva Estuary. Environment international, 33: 445-455.

Njau, K.N., Woude, M., Visser, G.J., and Janssen, L.J.J. 2000. Electrochemical removal of nickel ions from industrial wastewater. Chemical Engineering Journal 79: 187–195.

Nordstrom, D.K. 1985. The rate of ferrous iron oxidation in a stream receiving acid mine effluent; Selected papers in the hydrologic sciences, US Geological Survey Water Supply, 113–119.

Paugatch, K., Martha, S., Gartshore, I., and Pagoria, P. 2007. Computational modeling of large aerated lagoon hydraulics. Water research, 41: 2109-2116.

Phua, S.T.G., Davey, K.R., Daughtry, B.J. 2007. A new risk framework for predicting chemical residue(s)—Preliminary research for PCBs and PCDD/Fs in farmed Australian Southern Bluefin Tuna (Thunnus maccoyii). Chemical enginnering and processing, 46(5): 491-496.

Pourbaix, M. 1974. Atlas of electrochemical equilibria in aqueous solutions. National association of corrosion engineers, Houston, Texas, USA.

Pedahzur, R., Nasser, A. M., Dor, I., Fattal, B., and Shuval, H. I. 1993. The effect of baffle installation on the performance of a single cell stabilization pond. Water science and technology, 27(7-8): 45-52.

Pearson, H.W., Mara, D.D., and Arridge, H.A. 1995. The influence of pond geometry and configuration on facultative and maturation waste stabilisation pond performance and efficiency. Water Science and Technology, 31(12): 129-139.

Persson, J. 2000. The hydraulic performance of ponds of various layouts. Urban water, 2: 243-250.

Persson, J., and Wittgren, H.B. 2003. How hydrological and hydraulic conditions affect performance of ponds. Ecological engineering, 21: 259-269.

Piondexter, M.E. and Perrier, E.R. 1981. Hydraulic efficiency of dredged material impoundments: A field evaluation, Symposium on surface water impoundments, 2: 1165-1174.

Pollack, S.S. 1979. Estimating mineral matter in coal from its major inorganic elements. Fuel, 58: 76-78.

Polprasert, C., and Bhattarai, K.K. 1985. Dispersion model for waste stabilization ponds. Journal of environmental engineering, 111(1): 45-59.

Poulter, S.R. 1998. Monte Carlo simulation in environmental risk assessment-science policy and legal issues. Risk: Health, Safety & Environment, 7.

Preul, H.C., and Wagner, R.A. 1987. Waste Stabilization pond prediction model. Water science technology, 19(12): 205-211.

Ramaswami, A., Milford, J.B., and Small, M.J. 2005. Integrated environmental modeling: Pollutant transport, fate, and risk in the environment. John Wiley and Son's, USA.

Ravengai, S., Owen, R., and Love, D. 2004. Evaluation of seepage and acid generation potential from evaporation ponds, Iron Duke Pyrite Mine, Mazowe Valley, Zimbabwe. Physics and Chemistry of the Earth, 29: 1129-1134.

Rawat, N.S., and Singh, G. 1982. The role of micro-organisms in the formation of acid mine drainage in the north eastern coal field of India. International journal of mine water, 2: 29-36.

Rinker, M.J., Nesbitt, H.W., and Pratt, A.R. 1997. Marcasite oxidation in low-temperature acidic (pH 3.0) solutions: Mechanism and rate laws. American mineralogist, 82: 900-912.

Risk Assessment-Exposure Model, Toxicity Analysis and Evaluation; Environment Canada, Ontario region, ON, Canada (http://www.on.ec.gc.ca/pollution/ecnpd/tabs/tab16-e.html).

Roine, A. 2002. Outokumpu HSC chemistry for windows, chemical reaction and equilibrium software with extensive thermochemical database, version 5.1. Outokumpu Research Oy, Pori.

Romano, C.G., Mayer, K.U., Jones, D.R., Ellerbroek, D.A., and Blowes, D.W. 2003. Effectiveness of various cover scenarios on the rate of sulfide oxidation of mine tailings. Journal of hydrology, 271: 171-187.

Romero, F.M., Armienta, M.A., and Hernandez, G.G. 2007. Solid-phase control on the mobility of potentially toxic elements in an abandoned lead/zinc mine tailings impoundment, Taxco, Mexico. Applied geochemistry, 22: 109-127.

Rose, P.D., Boshoff, G.A., Van Hille, R.P., Wallace, L.C.M., Dunn, K.M., and Duncan, J.R. 1998. An integrated algal sulphate reducing high rate ponding process for the treatment of acid mine drainage wastewaters. Biodegradation, 9: 247-257.

Ruochuan, G., Frederick, N., and Stefan, Heinz. 1996. Water quality stratification in shallow wastewater stabilization ponds. Water resources bulletin, Paper No. 95153.

Safieddine, T. 2007. Hydrodynamics of waste stabilization ponds and aerated lagoons, PhD thesis, Department of Bioresource Engineering, McGill University, Montreal, Canada.

Salter, H.E., Boyle, L., Ouki, S.K., Quarmby, J., and Williams, S.C. 1999. Tracer study and profiling of a tertiary lagoon in the United Kingdom. Water resource, 33(18): 3782-3788.

Sample, B.E., Opresko, D.M., and Suter, G.W. 1996. Toxicological benchmarks for wildlife, Office of environmental management, U.S. department of energy

Sanderson, H., Fauser, P., Thomsen, M., and Sorensen, P.B. 2009. Human health risk screening due to consumption of fish contaminated with chemical warfare agents in Baltic sea. Journal of hazardous materials, 162: 416-422.

Schnelker R. 2006. Seview: Integrated contaminant transport and fate modeling system, Environmental software consultants, Inc., Madison, Wisconsin, USA

Schippers, A. 2004. Biogeochemistry of metal sulfide oxidation in mining environments, sediments, and soils. Geological society of America special paper, 379: 49-62.

Sherriff, B.L., Sidenko, N.V., and Salzsaluar, K.A. 2007. Differential settling and geochemical evolution of tailings' surface water at the Central Manitoba Gold Mine. Applied Geochemistry, 22: 342-356.

Shields, F.D., Thackston, E.L., Schroeder, P.R. and Batch, D.P. 1987. Design and management of dredged material contaminant areas to improve hydraulic performance, Us Army crops of engineers, Technical report D-87-2, June.

Shilton, A. 2000. Potential application of computational fluid dynamics to pond design. Water science and technology, 42(10-11): 327-334.

Shilton, A. 2001. Studies into the hydraulics of waste stabilization ponds, PhD thesis, Massey University, New Zealand.

Shilton, A. and Harrison, J. 2003. Development of guidelines for improved hydraulic design of waste stabilization ponds, Water science and technology, 48(2): 173-180.

Shilton, A. and Bailey, D. 2006. Drouge tracking by image processing for the study of laboratory scale pond hydraulics, Flow measurement and instrumentation, 17: 69-74.

Smith, K.S., and Wildeman, T.R. 2003. Fundamentals of mine-drainage formation and chemistry. Billings symposium / ASMR annual meeting.

Soares, S.R.A., and Bernardes, R.S. 2001. Reaction coefficient (K) evaluation for full-scale facultative pond systems. Bioresource technology, 78: 99-102.

Sperling, M. 2002. Relationship between first-order decay coefficients in ponds, for plug flow, CSTR and dispersed flow. Water science and technology, 45(1): 17-24.

Suter G.W. 2007. Ecological risk assessment, Taylor and Francis group, United States, ISBN-13: 978-156670-634-3.

Swayze, A.G., Smith, K.S., Clark, R.N., Sutley, S.J., Pearson, R.M., Vance, J.S., Hageman, P.L., Briggs, P.U., Meier, A.L., Singleton, M.J., and Roth, S. 2000. Using Imaging Spectroscopy to Map Acidic Mine Waste. Environmental Science and Technology, 34: 47-54.

Sweeney, D.G., Cromar, N.J., Nixon, J.B., Ta, C.T., and Fallowfield, H.J. 2003. The spatial significance of water quality indicators in waste stabilization ponds - Limitations of residence time distribution analysis in predicting treatment efficiency. Water science and technology, 48(2): 211-218.

Sweeney, D.G., Nixon, J.B., Cromar, N.J., and Fallowfield, H.J. 2005. Profiling and modeling of thermal changes in a large waste stabilization pond. Water science & Technology, 51(12): 163-172.

Thackston, E.L., Shields, F. D., and Schroeder, P.R. 1987. Residence time distributions of shallow basins. ASCE J. Environmental Engineering, 113(6): 1319–1332.

Thompson S.E., Burton C.A., Quinn D.J., and Ng, Y.C. 1972. Concentration factors of chemical elements in edible aquatic organisms, Prepared for U.S. atomic energy commission, Bio-medical division, University of California, U.S.A.

Torres, J.J., Soler, A., Saaez, J., and LLorensm, M. 2000. Hydraulic performance of a deep stabilization pond fed at 3.5M depth. Water research, 34(3): 1042-1049.

Torres, J.J., Soler, A., Saez, J., Leal, L. M., and Aguilar, M. I. 1999. Study of the internal hydrodynamics in three facultative ponds of two municipal WSPs in Spain, Water resource, 33(5): 1133-1140.

Torres, J.J., Soler, A., Saez, J., and Ortuno, J.F. 1997. Hydraulic performance of a deep wastewater stabilization pond. Water research, 31(4): 679-688.

Uluatam, S.S, and Kurum, Z. 1992. Evaluation of the wastewater stabilization pond at the METU treatment plant. International Journal of Environmental Studies, 41(1-2): 71-80.

U.S. Environmental Protection Agency (USEPA). 1991. Risk Assessment for Toxic Air Pollutants: A Citizen's Guide - EPA 450/3-90-024.

U.S. Environmental Protection Agency (USEPA). 1993.Wildelife exposure factors handbook. Volumes 1, EPA/600/R-93/187.

U.S. Environmental Protection Agency (USEPA). 1994. Technical document of acid mine drainage prediction. Office of solid waste. Washington, USA, 48.

U.S. Environmental Protection Agency (USEPA). 1997. *Exposure Factors Handbook.* Office of Health and Environmental Assessment. Volumes 1 and 2. EPA/600/P-95/002Fa and EPA/600/P-95/002Fb.

U.S. Environmental Protection Agency (USEPA). 1998. Guidelines for ecological risk assessment, Risk assessment forum. EPA-630-R-98-002F. Washington, USA.

U.S. Environmental Protection Agency (USEPA). 1999. Office of solid waste, Media to receptor bio-concentration factors (BCFs)

Valsaraj, K.T. 1995. Elements of environmental engineering: thermodynamics and kinetics. Lewis Publishers, ISBN 1566700892.

Van Buren, M.A., Watt, W.E., Marsalek, J., and Anderson, B.C. 2000. Thermal Balance of On-Stream Storm-Water Management Pond. Journal of Environmental Engineering, 126: 509-517.

Vassilev, S.V., and Tascon, JMD. 2003. Methods for characterization of inorganic and mineral matter in coal: a critical overview. Energy & fuels, 17:271-281.

Vorkas, C. A. and Lioyd, B. J. 2000. The application of a diagnostic methodology for the identification of hydraulic design deficiencies affecting pathogen removal, Water science and technology, 42(10): 99-109.

Walker, D.J. 1998. Modeling residence time in storm water ponds, Ecological engineering: 247-262.

Wehner, J.F., and Wilhelm, R.H. 1956. Boundary conditions of flow reactor. Chemistry engineering science, 6: 89-93.

Wilson, B.N, and Barfield, B.J 1984. A Sediment Detention Pond Model Using CSTRS Mixing Theory. American society of Agricultural Engineers, 27(5): 1339-1344.

Wood, M.G., Greenfield, P., Howes, T., Johns, M., and Keller, J. 1995. Computational fluid dynamic modeling of wastewater ponds to improve design. Water science and technology, 31(12): 111- 118.

Wood, M.G. 1997. Development of computational fluid dynamic models for the design of waste stabilization ponds. Doctorate Thesis. Department of chemical engineering, University of Queensland, Brisbane, Australia.

Wood, M.G., Howes, T., Keller, J., and Johns, M.R. 1998. Two-dimensional computational fluid dynamic models for waste stabilization ponds. Water research, 32(3): 958-963.

Yaman, S., Yavuz, R., Kucukbayrak, S., and Taptik, Y. 2001. Stepwise demineralization and chemical isolation of the mineral matter of Goynuk lignite. Energy conservation and management, 42: 2119-2127.

Yukon zinc corporation. 2005. Wolverine project environmental assessment report: 2-105.

Appendix I:

Table A1.1. Terrestrial animal's diet and duration of stay in the study area (Beak, 1997)

Animal	*Total intake*	*Duration of stay in the study area*
Snowshoe Hare	Deciduous browse (75%) Coniferous browse (25%)	1 year
Ptarmigan	Deciduous browse (70%) Bakeapples (20%) Coniferous browse (10%)	1 year
Caribou	Lichens (75%) Scrubs, grasses & sedges (25%)	4 months
Black Bear	70% vegetation consumption (Including 75% Bakeapples & 25% deciduous browse) 15% terrestrial animals (Including snowshoe Hare (80%) & caribou (20%)) 15% of aquatic animals (charr)	1 year
Polar Bear	Seals (80%) Marine charr (10%) Mergansers (5%) Harlequin duck (5%)	10% of the year
Harlequin Duck	Freshwater invertables (50%) Marine mussels (50%)	Six months
Merganser	Marine water charr (50%) Freshwater charr (50%)	Six months
Beaver	Terrestrial vegetation (50%) (Including deciduous browse (50%) & coniferous browse (%50)) Aquatic plant (50%)	1 year
Ringed Seal	Marine water Charr (50%) Sculpin (50%)	1 year

Table A1.2. Ingestion transfer factors for terrestrial animals (IAEA, 1994)

Animal	*Nickel*	*Copper*	*Cobalt*	*Zinc*	*Cadmium*	*Lead*
Snowshoe Hare	0.005	0.039	0.062	4.1	0.0075	0.0004
Ptarmigan	1	0.5	2	7	0.8	0.4
Caribou	0.005	0.039	0.062	4.1	0.0075	0.0004
Black Bear	0.005	0.022	0.025	0.14	0.0075	0.0004
Polar Bear	0.005	0.022	0.025	0.14	0.0075	0.0004
Harlequin Duck	1	0.5	2	7	0.8	0.4
Merganser	1	0.5	2	7	0.8	0.4
Beaver	0.005	0.039	0.062	4.1	0.0075	0.0004
Ringed Seal	0.005	0.022	0.025	0.14	0.0075	0.0004

Table A1.3. BCFs (Kg/L) for different aquatic species in the study region (Thompson et al., 1972)

Freshwater species	*Nickel*	*Copper*	*Cobalt*	*Zinc*	*Cadmium*	*Lead*
Arctic charr	100	200	300	2000	200	300
Brook trout	100	200	300	2000	200	300
Marine water species						
Arctic charr	500	667	1000	3300	3000	300
Sculpin	500	667	1000	3300	3000	300

Table A1.4. Soil to plant transfer factor, B_v (Kg/Kg) (Beak, 1997; IAEA, 1994)

Chemical component	*Lichens*	*Bakeapples*	*Coniferous browse*	*Deciduous browse*
Nickel	0.45	0.41	0.24	0.24
Copper	1.58	2.54	0.8	0.8
Cobalt	0.41	0.41	0.211	0.211
Zinc	7.48	1.32	1.266	1.266
Cadmium	0.08	0.08	0.0053	0.0053
Lead	1.55	0.02	0.0053	0.0053

Table A1.5. Bio-concentration factor for Sedge (Unitless) (Thompson et al., 1972)

Plant	*Nickel*	*Copper*	*Cobalt*	*Zinc*	*Cadmium*	*Lead*
Sedge	50	1000	200	1000	270	200

Table A1.6. Toxicological benchmark doses for terrestrial animals within the study area (Sample et al., 1996)

Animal	*Nickel*	*Copper*	*Cobalt*	*Zinc*	*Cadmium*	*Lead*
Snowshoe Hare	56.56	14.15	8.56	226.27	7.07	56.57
Ptarmigan	107	61.7	12	131	20	11.3
Caribou	17.76	4.44	2.69	71.05	2.22	17.76
Black Bear	17.58	4.4	2.63	70.33	2.19	17.58
Polar Bear	13.01	3.25	2	52.05	1.62	13.01
Harlequin Duck	107	61.7	12	131	20	11.3
Merganser	107	61.7	12	131	20	11.3
Beaver	29.09	7.28	4.41	116.38	3.63	29.09
Ringed Seal	23.14	5.79	3.5	92.56	2.89	23.14

Table A1.7. Body weight of terrestrial animals within the study area

Animal	*Body Weight (kg)*
Snowshoe Hare	1.4
Ptarmigan	0.6
Caribou	144
Black Bear	150
Polar Bear	500
Harlequin Duck	0.6
Merganser	0.7
Beaver	20
Ringed Seal	50